Institut für Theoretische Physik
Universität zu Köln

Quantum Criticality of Crystals

Master Thesis
Supervisor PD Markus Garst

by
Christopher Max
Matrikelnr. 4760808

January 2015, Köln

Contents

Chapter 1

Introduction

1.1 Motivation

The physics of metals at very low temperatures has attracted much attention over the last decades. Since the discovery of superconductivity in mercury by H. K.Onnes in 1911, [1], it has been a constant challenge for physicists to understand the properties of metals in full detail.

In this thesis we will consider a special phase of metals which is called the 'nematic phase'. It is characterized by a hybridization between the conduction electrons and the localized electrons that effectively leads to a quadrupolar distribution of the conduction electrons w.r.t. the ions. Meanwhile the translational symmetries of the system are preserved. Here we will describe this phase in an effective Ginzburg-Landau theory which was introduced in [2].

The first experimental evidences for nematic phases in metals were provided in 1999 by [3]. They observed an anisotropic restistance tensor in an electronic configuration in the first Landau level of a two-dimensional electron system. These measurements were interpreted in [4] as the occurence of special kind of nematic phase which is called the "stripe nematic phase".

The central question we want to answer in this thesis is what happens if we couple the electrons to strain fields of the underlying lattice. At low temperatures this coupling can have a large effects for the system. The most popular phenomenum is the occurence of a superconducting phase. In our system the anisotropy of the nematic phase leads to hybridization effects between the density fluctuations of the Fermi liquid and the strain fields of the lattice. The quantum fluctuations in the Fermi liquid only become relevant in the vicinity of a quantum critical point where the thermal fluctuations are weak. Hence it is necessary to calculate the properties of the uncoupled Fermi liquid at the isotropic-to-nematic qunatum critcal point. This has been done in two dimensions [5], [6] via a Hertz-Millis theory. Here we will adopt these calculations to derive the properties of the three dimensional Fermi liquid. In contrast to the two dimensional case, it turns out that the Hertz-Millis theory in three dimensions always converges.

1.2 Outline

We start with an introduction to the basic principles of elasticity in crystals. Thereby we follow the historical route and first build up the elasticity theory for homogeneous macroscopic objects. The basic quantities will then be modified for the correct treatment of deformations in crystals. Strain in crystals can be seperated into static and dynamic strain. On the one side the physics of static strain lead to criterions for the macroscopic stability of the crystal. On the other side the dynamic strains, which are nothing else than acoustic phonons, determine the thermodynamic properties of the lattice. After the basic principles of lattice transformations are explained, we compare the specific heat of stable crystals with the specific heat at a lattice transition point.

The next chapter describes a Fermi liquid with quadrupolar interaction. The Fermi liquid model is the standard model for electrons in metals at low temperatures. A detailed discussion of the Fermi liquid and the interaction with phonons can be found in [7]. We will not repeat the basic definitions but focus on the effects of the quadrupolar interaction. Via a Hubbard-Stratonovich transformation we can describe the interaction effects by bosons which resemble quadrupolar strain fluctuations of the Fermi sphere. The result of this chapter is an effective action for these bosons. It predicts large fluctuations of the bosons when the Fermi liquid is close to the quantum critical point.

With the knowledge about the two systems we are then ready to analyse the coupled system of phonons and electrons. The interaction is thereby mediated by the quadrupolar bosonic excitations. The symmetries of the strain and the bosons lead to important enhancement effects in the coupling. In the action this is resembled by a bilinear interaction term between the critical bosons and the lattice degrees of freedom. These will be analysed in detail. For that we calculate the free energy and the specific heat of the full system. We end up with two terms corresponding to the Fermi liquid and the lattice with renormalized parameters. One of the central results is the identification of the boson mass r as a tuning parameter of the coupled system. At the critical value r_0, which is completely defined by the crystal, the electrons induce a symmetry transformation of the lattice for low temperatures. Meanwhile the criticality of the Fermi liquid is suppressed for $T \to 0$. Finally we analyse the fermionic self energy correction for the coupled system and the effective electron-phonon vertex.

Chapter 2

Crystal Elasticity Theory

In this chapter the description of deformations of crystals via the elasticity theory is presented. The analysis of deformations is a long studied topic in physics. Originally it was developed for macroscopic homogeneous objects, e.g. steel beams in buildings.
In the end we want to describe the strains and stresses inside crystals. The idea is to do this by using the formalisms of the elasticity theory. For that we have to consider the effects of the lattice symmetries of the crystals.
In the following we start with an introduction into the classical elasticity theory. The basic definitions are based on the books [8] and [9]. Thereby we focus ourselves on the most important quantities which are relevant for the description of crystals. These will then be used to develop the crystal elasticity theory. Finally we end up with a description of the dynamics of strain, i.e. of phonons.

2.1 Elasticity

Elasticity here means the response of a solid to strains or stresses which are induced from outside. The deformations can be described by a displacement field $\boldsymbol{u}(\boldsymbol{r}, t)$. It describes the displacement of the solid at the place $\boldsymbol{r}$ and time t. In crystals this would describe the difference between the new position of the atoms at place $\boldsymbol{r}'(\boldsymbol{r}, t)$ and its original position $\boldsymbol{r}$. From here on it will be assumed that the differences of the displacement between two neighbouring atoms is small, i.e. $\partial_x u \ll 1$.

2.1.1 The Strain Tensor

We start with the consideration of a general strain field $\boldsymbol{u}(\boldsymbol{r}, t)$. All informations about the strain are contained in this field. So in general it is possible to use it as the central quantity. But in practice it turned out that it is better to use the so called strain tensor. The advantage of this quantity is that it only measures the local change of distances in the solid. All homogeneous displacements, which don't change the properties of the solid, are not contained.
So we consider now two places $\boldsymbol{r}_1$ and $\boldsymbol{r}_2$ in the undeformed material with distance $d\boldsymbol{r} = \boldsymbol{r}_1 - \boldsymbol{r}_2$. The solid shall now be deformed according to the strain filed $\boldsymbol{u}$. The square of the

new distance is given by

$$\begin{aligned} dl^2 =&\big(d\boldsymbol{r} + \boldsymbol{u}(\boldsymbol{r}_1) - \boldsymbol{u}(\boldsymbol{r}_2)\big)^2 \\ \approx& dx_i dx_i + 2\frac{\partial u_i}{\partial x_j} dx_i dx_j + \frac{\partial u_i}{\partial x_j}\frac{\partial u_i}{\partial x_k} dx_j dx_k \\ =& d\boldsymbol{r}^2 + \Big(\frac{\partial u_i}{\partial x_j} + \frac{\partial u_j}{\partial x_i} + \frac{1}{2}\frac{\partial u_k}{\partial x_i}\frac{\partial u_k}{\partial x_j}\Big) dx_i dx_j \end{aligned} \tag{2.1.1}$$

For the approximation the formula $\boldsymbol{u}(\boldsymbol{r}_1) - \boldsymbol{u}(\boldsymbol{r}_2) = \frac{\partial \boldsymbol{u}}{\partial \boldsymbol{r}}(\boldsymbol{r}_1 - \boldsymbol{r}_2)$ was used which is valid for infinitesimal distances.

One can see now that the new distance is completely given by the matrix

$$\frac{\partial u_i}{\partial x_j} + \frac{\partial u_j}{\partial x_i} + \frac{1}{2}\frac{\partial u_k}{\partial x_i}\frac{\partial u_k}{\partial x_j}$$

and the initial distance $d\boldsymbol{r}$. The matrix can be further simplified by neglecting the term of order $\boldsymbol{u}^2$. This leads to the definition of the **strain tensor**

$$u_{ij}(\boldsymbol{r}, t) = \frac{1}{2}\Big(\frac{\partial u_i}{\partial x_j} + \frac{\partial u_j}{\partial x_i}\Big)$$

The strain tensor is symmetric and thus has 6 degrees of freedom. Furthermore the tensor is now invariant under translations of the whole crystal. Hence this is a much more natural basis for the description of crystals than the original field $\boldsymbol{u}$.

2.1.2 The Stress Tensor

To describe forces on the crystal one uses the strain tensor $\sigma_{ij}(\boldsymbol{r}, t)$. This tensor is a symmetric 3x3 matrix and determines completely the stress in the body by the following relation:

For a given unit-vector $\boldsymbol{n}$ the product

$$\boldsymbol{F}_j = \sigma_{ij}\boldsymbol{n}_i$$

gives the forces acting on the plane perpendicular to $\boldsymbol{n}$ in direction $\boldsymbol{e}_j$. So the diagonal elements of the stress tensor σ_{ii} determine the pressure along the axes. The off-diagonal parts determine the shear components of the stress. In other words one can say that the first index denotes the direction in which the force acts and the second one denotes the direction of the outer normal of the plane on which the force is applied.

In experiments one often considers samples with an uni-axial outer pressure p. The stress tensor in the sample then has the form

$$\sigma = \begin{pmatrix} -p & 0 & 0 \\ 0 & -p & 0 \\ 0 & 0 & -p \end{pmatrix}$$

In general one has also forces, such as gravity, which act on the whole volume and not only on the surface. But these forces can be considered as homogeneous on our length scales. Thus they only lead to constant energy shift in the free energy and do not influence the thermodynamic properties of the system.

2.1.3 Hooke's Law

Up to now the stress and strain of solids has been treated as separate objects. In reality, strain of course also leads to stress in the solid and vice versa. The relationship between these two quantities depends on the microscopic properties of the solid. Later these will be discussed in more detail. Here we take a more phenomenological point of view. The lowest order interaction one can consider is **Hooke's Law**

$$\sigma_{ij} = C_{ijkl} u_{kl} \tag{2.1.2}$$

with a 4-tensor C_{ijkl}. This tensor is called **Elastic Modulus Tensor**. By its definition and the symmetries of σ_{ij} and u_{kl} one can derive the following symmetries

$$\begin{aligned} C_{ijkl} &= C_{klij} \\ C_{ijkl} &= C_{jikl} = C_{ijlk} \end{aligned}$$

By these symmetries the elastic modulus tensor possesses only 21 components. In crystals there are always certain symmetries of the lattice which further reduces the number of independent components.

In the following the tensors will represented in the Voigt notation. The idea behind this notation is to use the symmetries of tensors to represent them as tensors of lower order. In three dimensions this is done by the bijection

$$\begin{aligned} \rho(i,j) &= i \text{ for } i = j \\ \rho(i,j) &= 9 - i - j \text{ for } i \neq j \end{aligned}$$

One can see that this mapping is only well defined, if the original tensor components are invariant under index exchanges $i \leftrightarrow j$.

The stress tensor $\left(\sigma_{ij}\right) = \begin{pmatrix} \sigma_{11} & \sigma_{12} & \sigma_{13} \\ \sigma_{12} & \sigma_{22} & \sigma_{23} \\ \sigma_{13} & \sigma_{23} & \sigma_{33} \end{pmatrix}$ becomes a vector in the Voigt notation of the form

$$\left(\sigma_\alpha\right) = \left(\sigma_1, \sigma_2, \sigma_3, \sigma_4, \sigma_5, \sigma_6\right)^T = \left(\sigma_{11}, \sigma_{22}, \sigma_{33}, \sigma_{23}, \sigma_{13}, \sigma_{12}\right)^T$$

The strain tensor $\left(u_{ij}\right) = \begin{pmatrix} u_{11} & u_{12} & u_{13} \\ u_{12} & u_{22} & u_{23} \\ u_{13} & u_{23} & u_{33} \end{pmatrix}$ is mapped to

$$\left(u_\alpha\right) = \left(u_1, u_2, u_3, u_4, u_5, u_6\right)^T = \left(u_{11}, u_{22}, u_{33}, 2u_{23}, 2u_{13}, 2u_{12}\right)^T$$

The factor 2 in the last three entries comes from the double counting of the terms with $i \neq j$, $k \neq l$ in the free energy $F = \frac{1}{2} u_{ij} C_{ijkl} u_{kl}$. It ensures that in the new notation the free energy can be written as

$$F = \frac{1}{2} u_\alpha C_{\alpha\beta} u_\beta$$

For the elastic modulus tensor one can apply the mapping on the first two indices and on the last two indices separately. This maps then the 4-tensor to a 2-tensor of the ordering

$$(C_{\alpha\beta}) = \begin{pmatrix} C_{1111} & C_{1122} & C_{1133} & C_{1123} & C_{1113} & C_{1112} \\ C_{2211} & C_{2222} & C_{2233} & C_{2223} & C_{2213} & C_{2212} \\ C_{3311} & C_{3322} & C_{3333} & C_{3323} & C_{3313} & C_{3312} \\ C_{2311} & C_{2322} & C_{2333} & C_{2323} & C_{2313} & C_{2312} \\ C_{1311} & C_{1322} & C_{1333} & C_{1323} & C_{1313} & C_{1312} \\ C_{1211} & C_{1222} & C_{1233} & C_{1223} & C_{1213} & C_{1212} \end{pmatrix}$$

With the symmetry $C_{ijkl} = C_{klij}$ this can be reduced to

$$(C_{\alpha\beta}) = \begin{pmatrix} C_{11} & C_{12} & C_{13} & C_{14} & C_{15} & C_{16} \\ C_{12} & C_{22} & C_{23} & C_{24} & C_{25} & C_{26} \\ C_{13} & C_{23} & C_{33} & C_{34} & C_{35} & C_{36} \\ C_{14} & C_{24} & C_{34} & C_{44} & C_{45} & C_{46} \\ C_{15} & C_{25} & C_{35} & C_{45} & C_{55} & C_{56} \\ C_{16} & C_{26} & C_{36} & C_{46} & C_{56} & C_{66} \end{pmatrix}$$

This form resembles the 21 degrees of freedom of in the elastic modulus tensor. The Hooke's law in Voigt notation is now given by a simple matrix-vector product

$$\sigma_\alpha = C_{\alpha\beta} u_\beta$$

2.1.4 Equation of Motion for Strain

The forces in the body have to add up to zero since we are not interested in the total motion of the body. So for the i-th component the equation

$$\frac{1}{2} \int_V d^3 r \rho \partial_t^2 u_i = \int_{\partial V} ds\, \sigma_{ij} n_j$$

has to be fulfilled. On the right hand side we can apply Gauss' theorem

$$\int_{\partial V} ds\, \sigma_{ij} n_j = \int_V d^3 r \frac{\partial \sigma_{ij}}{\partial x_j}$$

This leads then to the equation of motion for strain without body forces:

$$\int_V d^3 r \left[\rho \partial_t^2 u_i - \frac{\partial \sigma_{ij}}{\partial x_j} \right] = 0 \tag{2.1.3}$$

With Hooke's law we can write this in the equivalent form

$$\int_V d^3 r \left[\rho \partial_t^2 u_i - \frac{\partial}{\partial x_j} \left(C_{ijkl} u_{kl} \right) \right] = 0 \tag{2.1.4}$$

2.1.5 Free Energy

In general, the free energy F is given by

$$F = E - TS$$

where E denotes the internal energy, T the temperature and S the entropy of the body. We define E to be zero when there is no strain. The internal energy of a given strain field $\boldsymbol{u}(\boldsymbol{r}, t)$ can be calculated by considering the process of deforming an initially undeformed body. The forces which act on the body in this process are applied on the surface.
For these surface forces the rate at which work is done is given by

$$\int_{\partial V} \sigma_{ij} n_j \partial_t u_i ds = \int_{\partial V} \big(\sigma_{ij} \partial_t u_i\big) n_j ds$$

Again one can use Gauss' theorem to write this as

$$\int_V d^3r \frac{\partial}{\partial x_j} \big(\sigma_{ij} \partial_t u_i\big) = \int_V d^3r \Big(\frac{\partial \sigma_{ij}}{\partial x_j} \partial_t u_i + \sigma_{ij} \partial_t u_{ij}\Big) \tag{2.1.5}$$

With the equation of motion the first term on the right hand side can be written as

$$\int_V d^3r \rho \Big(\partial_t^2 u_i \partial_t u_i\Big) = \partial_t \Big(\frac{1}{2} \int_V d^3r \rho \big(\partial_t \boldsymbol{u}\big)^2\Big)$$

The integral on the right hand side is the kinetic energy in the system. Hence the first term of eq. 2.1.5 corresponds to the change of the kinetic energy.
Finally, the second term can be identified with the change of the intrinsic energy

$$U = \int_V d^3r\, \sigma_{ij} u_{ij} = \frac{1}{2} \int_V d^3r\, u_{ij} C_{ijkl} u_{kl}$$

Hence the free energy is given by

$$F = F_0 + \frac{1}{2} \int_V d^3r\, u_{ij} C_{ijkl} u_{kl}$$

where F_0 contains the thermal contributions which do not depend on the strain.
With the free energy and the equation of motion we now have the two central formulas which are needed in the thermodynamic description of crystals. But before these can be applied one has to clarify its meanings in the non-homogeneous crystals.

2.2 Elasticity in Crystals

In the previous section the basic concepts of the elasticity theory were introduced. Now we want to apply these on crystals. The most important difference in crystals compared to homogeneous bodies is that the atoms or molecules are distributed in a lattice structure. Hence fields in the crystals such as strain fields can only be defined on discrete points, too. Furthermore the symmetries of the lattice lead to the restriction that all physical quantities of the crystal also have to satisfy these symmetries. Before going into more detail, the basic definitions and properties of fields in crystals will be repeated in the following section.

2.2.1 Definition of Strain Fields in Crystals

The crystal lattice is given by

$$\mathcal{R} = \left\{ \boldsymbol{R_n} = n_1\boldsymbol{a}_1 + n_2\boldsymbol{a}_2 + n_3\boldsymbol{a}_3 \middle| \boldsymbol{n} = \left(n_1, n_2, n_3\right) \in \mathbb{Z}^3 \right\}$$

where $\boldsymbol{a}_1, \boldsymbol{a}_2, \boldsymbol{a}_3$ are the basis vectors of the lattice. The structure of the atoms or molecules which lie on the lattice points will not be considered here. We will treat them as point masses. This is sufficient for our purposes because we are only interested in the low energy properties of the crystal.

So the crystal is a lattice which is invariant under translations $\boldsymbol{r} \to \boldsymbol{R_n} + \boldsymbol{r}$. This implies that any physical quantity $\psi(\boldsymbol{r})$ of the crystal also has to be invariant under these translations, i.e.

$$\psi(\boldsymbol{r}) = \psi(\boldsymbol{r} + \boldsymbol{R_n}) \tag{2.2.1}$$

The Fourier transformed version of this field is

$$\psi(\boldsymbol{r}) = \sum_{\boldsymbol{q}} \psi_{\boldsymbol{q}} e^{-i\boldsymbol{q}\cdot\boldsymbol{r}}$$

Now the equation 2.2.1 implies

$$e^{i\boldsymbol{q}\cdot\boldsymbol{R_n}} = 1 \Leftrightarrow \boldsymbol{q} \cdot \boldsymbol{R_n} = 2\pi m \text{ for } m \in \mathbb{Z}$$

This condition for $\boldsymbol{q}$ implies that the momentum has to be an element of the **reciprocal lattice $\mathcal{G}$** defined by

$$\mathcal{G} = \left\{ \boldsymbol{G_m} = m_1\boldsymbol{b}_1 + m_2\boldsymbol{b}_2 + m_3\boldsymbol{b}_3 \middle| \boldsymbol{m} = \left(m_1, m_2, m_3\right)^T \in \mathbb{Z}^3 \right\}$$

The basis vectors are defined by

$$\boldsymbol{b}_1 = 2\pi \frac{\boldsymbol{a}_2 \times \boldsymbol{a}_3}{\det\left(\boldsymbol{a}_1, \boldsymbol{a}_2, \boldsymbol{a}_3\right)}, \quad \boldsymbol{b}_2 = 2\pi \frac{\boldsymbol{a}_3 \times \boldsymbol{a}_1}{\det\left(\boldsymbol{a}_1, \boldsymbol{a}_2, \boldsymbol{a}_3\right)}, \quad \boldsymbol{b}_3 = 2\pi \frac{\boldsymbol{a}_1 \times \boldsymbol{a}_2}{\det\left(\boldsymbol{a}_1, \boldsymbol{a}_2, \boldsymbol{a}_3\right)}$$

Hence the spacial dependence is given by

$$\psi(\boldsymbol{r}) = \sum_{\boldsymbol{q}\in\mathcal{G}} \psi_{\boldsymbol{q}} e^{-i\boldsymbol{q}\cdot\boldsymbol{r}}$$

The natural next step is to consider the dynamics of such a field. For this one has to know the forces which are acting in the crystal. In general these can have multiple forms and origins. Here we will from now on only consider the strain fields.

We start again with the expansion of the internal energy w.r.t. the strain $\boldsymbol{u}(\boldsymbol{r})$:

$$U = U_0 + \sum_{\boldsymbol{n}} \frac{\partial U_{\boldsymbol{n}}(0)}{\partial u_{\boldsymbol{n},i}} u_{\boldsymbol{n},i} + \frac{1}{2} \sum_{\boldsymbol{n},\boldsymbol{m}} \frac{\partial^2 U_{\boldsymbol{n},\boldsymbol{m}}(0)}{\partial u_{\boldsymbol{n},i} \partial u_{\boldsymbol{m},j}} u_{\boldsymbol{n},i} u_{\boldsymbol{m},j} + \mathcal{O}(u^3) \tag{2.2.2}$$

The sum is taken over all atoms $\boldsymbol{R_n}$, $\boldsymbol{R_m}$. The static term U_0 can be set to zero. The first derivative of the energy w.r.t. the strain has to vanish at the equilibrium position. Otherwise there would be a state with lower energy which is in contradiction to the definition of the equilibrium position. So the internal energy to second order in the strain is given by

$$U = \frac{1}{2} \sum_{\boldsymbol{n},\boldsymbol{m}} \frac{\partial^2 U_{\boldsymbol{n},\boldsymbol{m}}(0)}{\partial u_{\boldsymbol{n},i} \partial u_{\boldsymbol{m},j}} u_{\boldsymbol{n},i} u_{\boldsymbol{m},j}$$

This looks quite similar to the internal energy we obtained in the elasticity theory. The differences come from the discrete lattice points we are dealing with.

2.2.2 Continuum Limit

As mentioned before we are only interested in the low energy properties of the crystal. In terms of phonons this means that we are in the long wavelength limit. There, the short distances between the atoms become irrelevant. In term of fields in the crystal this means that we can consider them as continuously defined for all values of $\boldsymbol{r}$.
The internal energy is then given by

$$U = \frac{1}{2}\int d^3r_1\, d^3r_2\, u_i(\boldsymbol{r}_1)\frac{\partial^2 U_0(\boldsymbol{r}_1,\boldsymbol{r}_2)}{\partial u_i(\boldsymbol{r}_1)\partial u_j(\boldsymbol{r}_2)}u_j(\boldsymbol{r}_2)$$

where $U_0(\boldsymbol{r}_1,\boldsymbol{r}_2)$ is the continuum version of $U_{\boldsymbol{n},\boldsymbol{m}}(0)$. The forces do not depend on the microscopic structure of the molecules but only act at the center of mass. Hence we can write $\frac{\partial^2 U_0(\boldsymbol{r})}{\partial u_i(\boldsymbol{R}+\boldsymbol{r})\partial u_j(\boldsymbol{R}-\boldsymbol{r})} = U_{ij}(\boldsymbol{r}_1-\boldsymbol{r}_2)$. In the internal energy we can then introduce new coordinates $\boldsymbol{R}=\frac{1}{2}(\boldsymbol{r}_1+\boldsymbol{r}_2)$ and $\boldsymbol{r}=\frac{1}{2}(\boldsymbol{r}_1-\boldsymbol{r}_2)$ and get

$$U = \frac{1}{2}\int d^3R\, d^3r\, u_i(\boldsymbol{R}+\boldsymbol{r})U_{ij}(\boldsymbol{r}_1-\boldsymbol{r}_2)u_j(\boldsymbol{R}-\boldsymbol{r})$$

The interaction becomes irrelevant for large distances. So we can expand the strain fields in $\boldsymbol{r}$:

$$\begin{aligned} U =& \frac{1}{2}\int d^3R\, d^3r\left[u_i(\boldsymbol{R})+\frac{\partial u_i(\boldsymbol{R})}{\partial r_k}r_k\right]U_{ij}(\boldsymbol{r}_1-\boldsymbol{r}_2)\left[u_j(\boldsymbol{R})-\frac{\partial u_j(\boldsymbol{R})}{\partial r_l}r_l\right] \\ =& \frac{1}{2}\int d^3R\, d^3r\left\{u_i(\boldsymbol{R})U_{ij}(\boldsymbol{r}_1-\boldsymbol{r}_2)u_j(\boldsymbol{R})-\frac{\partial u_i(\boldsymbol{R})}{\partial r_k}\left[r_kU_{ij}(\boldsymbol{r}_1-\boldsymbol{r}_2)r_l\right]\frac{\partial u_j(\boldsymbol{R})}{\partial r_l}\right\} \end{aligned}$$

The integral over $\boldsymbol{r}$ in the first term vanishes, i.e. this term is zero. Physically this term resembles the internal energy from a constant strain which is just a translation of the crystal. With the definition

$$C_{ijkl} = -\frac{1}{2}\int d^3r\, r_kU_{ij}(\boldsymbol{r}_1-\boldsymbol{r}_2)r_l$$

The internal energy can finally be written in the form we already know from the elasticity theory

$$U = \frac{1}{2}\int d^3R\, u_{ij}(\boldsymbol{R})C_{ijkl}u_{kl}(\boldsymbol{R})$$

From the definition of the elastic modulus tensor one can recover the symmetries in the indices which were used in the elasticity theory. The special feature here is that we still have lattice symmetries. These imply some features for this tensor which will be discussed in the following section. Moreover one can see that the C_{ijkl} are space independent.

2.2.3 Elastic Modulus Tensor in Crystals

If a crystal has a certain symmetry, all quantities of the crystal also have to satisfy this symmetry. Thus the free energy

$$F = \frac{1}{2}\int_V d^3r\, u_{ij} C_{ijkl} u_{kl} = \frac{1}{2}\int_V d^3r\, u_\alpha C_{\alpha\beta} u_\beta$$

has to be invariant under all symmetry transformation and for all possible values of the u_{ij}. The corresponding equations lead to restrictions for the elastic modulus tensor. For example, in a cubic lattice, it has to be of the form

$$C^{\text{cubic}}_{\alpha\beta} = \begin{pmatrix} C_{11} & C_{12} & C_{12} & 0 & 0 & 0 \\ C_{12} & C_{11} & C_{12} & 0 & 0 & 0 \\ C_{12} & C_{12} & C_{11} & 0 & 0 & 0 \\ 0 & 0 & 0 & C_{44} & 0 & 0 \\ 0 & 0 & 0 & 0 & C_{44} & 0 \\ 0 & 0 & 0 & 0 & 0 & C_{44} \end{pmatrix}$$

For a tetragonal lattice one has less symmetries, i.e. there are more degrees of freedom in the elastic modulus tensor

$$C^{\text{tetra}}_{\alpha\beta} = \begin{pmatrix} C_{11} & C_{12} & C_{13} & 0 & 0 & 0 \\ C_{12} & C_{11} & C_{13} & 0 & 0 & 0 \\ C_{13} & C_{13} & C_{33} & 0 & 0 & 0 \\ 0 & 0 & 0 & C_{44} & 0 & 0 \\ 0 & 0 & 0 & 0 & C_{44} & 0 \\ 0 & 0 & 0 & 0 & 0 & C_{66} \end{pmatrix} \tag{2.2.3}$$

The equation of motion 2.1.4 then simplifies to

$$\int_V d^3r \left[\rho \partial_t^2 u_i - C_{ijkl}\frac{\partial u_{kl}}{\partial x_j}\right] = 0 \tag{2.2.4}$$

for $i = 1, 2, 3$. A complete list of the strain tensors in the different lattices can be found in appendix A of [10].

2.3 Acoustic Phonons

Later we will analyse the thermodynamics of acoustic phonons at a phase transition of the underlying lattice. For that we have to understand their treatment within the elasticity theory. This will be introduced in the following.

Phonons can be considered as strain fields of the form

$$\boldsymbol{u}(\boldsymbol{r}, t) = \boldsymbol{e}_{\hat{q}} \exp\left[i\big(\boldsymbol{q}\cdot\boldsymbol{r} - \omega(\boldsymbol{q})t\big)\right]$$

where $\boldsymbol{e}_{\hat{q}}$ denotes the polarization vector. It direction depends on the direction of the momentum $\boldsymbol{q}$. In the following we will drop the index $\hat{q}$.

A very detailed introduction of phonons as strain fields can be found in [9]. The strain tensor for this field becomes

$$u_{ij} = i(q_i e_j + q_j e_i) \exp \Big[i\big(\boldsymbol{q} \cdot \boldsymbol{r} - \omega(\boldsymbol{q})t\big) \Big]$$

The corresponding equation of motion

$$\rho \partial_t^2 u_i(\boldsymbol{r}, t) = C_{ijkl} \partial_j \partial_i u_l(\boldsymbol{r}, t)$$

then reads in the Fourier transformed way

$$\boxed{\rho \omega^2(\boldsymbol{q}) u_i(\boldsymbol{q}, \omega) = D_{il}(\boldsymbol{q}) u_l(\boldsymbol{q}, \omega)} \tag{2.3.1}$$

where $D_{il}(\boldsymbol{q}) = C_{ijkl} q_j q_k$.

We see that the solutions of these equations are given by the eigenvectors and eigenvalues of the **dynamical matrix** D_{ij}. This matrix is symmetric and positive definite. Hence there are always three real eigenvalues and eigenvectors. These correspond to three different dispersion relations $\omega_i(\boldsymbol{q})$ with its polarization directions $\boldsymbol{u}_i$.

Form the definition of D_{ij} one can conclude that the relation

$$\omega(\boldsymbol{q}) = q v(\hat{q})$$

has to be valid where $\boldsymbol{q} = q\hat{q}$, $||\hat{q}|| = 1$. This means that we have a dispersion proportional to q. The function $v(\hat{q})$ resembles the sound velocity in the direction $\hat{q}$.

The direction dependence of the dispersion is in general hard to calculate. One has to find the roots of a polynomial of order three. In principle this can be done analytically, see appendix A, but leads to very complicated results. They are only used to determine the general structure for the dispersions.

In practice we only use local approximations for the dispersion. This means that we consider the dispersion in small neighborhoods around the directions we are interested in. In these neighborhoods we can then approximate the dispersion by perturbative solution of the eigenvalue equation 2.3.1. These will have much simpler forms. In the following section the local approximations for some lattices and directions are presented.

2.3.1 Cubic Lattice Symmetry

For a cubic lattice the elastic modulus tensor in Voigt notation reads as

$$C = \begin{pmatrix} C_{11} & C_{12} & C_{12} & 0 & 0 & 0 \\ C_{12} & C_{11} & C_{12} & 0 & 0 & 0 \\ C_{12} & C_{12} & C_{11} & 0 & 0 & 0 \\ 0 & 0 & 0 & C_{44} & 0 & 0 \\ 0 & 0 & 0 & 0 & C_{44} & 0 \\ 0 & 0 & 0 & 0 & 0 & C_{44} \end{pmatrix}$$

This is one of the most simplest forms for the elastic modulus tensor in lattices. It is given here as a basic example. Its corresponding dynamical matrix is

$$D(\boldsymbol{q}) = \begin{pmatrix} C_{11}q_1^2 + C_{44}q_2^2 + C_{44}q_3^2 & (C_{12} + C_{44})q_1 q_2 & (C_{12} + C_{44})q_1 q_3 \\ (C_{12} + C_{44})q_1 q_2 & C_{44}q_1^2 + C_{11}q_2^2 + C_{44}q_3^2 & (C_{12} + C_{44})q_2 q_3 \\ (C_{12} + C_{44})q_1 q_3 & (C_{12} + C_{44})q_2 q_3 & C_{44}q_1^2 + C_{44}q_2^2 + C_{11}q_3^2 \end{pmatrix}$$

which can be written in index notation as

$$D_{ij} = (C_{12} + C_{44})q_i q_j + \delta_{ij}\left[C_{44}q^2 + (C_{11} - C_{12} - 2C_{44})q_i^2\right]$$

Along the symmetry axes this matrix assumes a much simpler form:

1. $\boldsymbol{q} \perp [1, 0, 0]$

$$D = \begin{pmatrix} C_{44}(q_2^2 + q_3^2) & 0 & 0 \\ 0 & C_{11}q_2^2 + C_{44}q_3^2 & (C_{12} + C_{44})q_2 q_3 \\ 0 & (C_{12} + C_{44})q_2 q_3 & C_{44}q_2^2 + C_{11}q_3^2 \end{pmatrix}$$

2. $\boldsymbol{q}||[1, 1, 0]$

$$D = \begin{pmatrix} C_{11}q_1^2 + C_{44}q_1^2 & (C_{12} + C_{44})q_1 q_2 & 0 \\ (C_{12} + C_{44})q_1^2 & C_{44}q_1^2 + C_{11}q_1^2 & 0 \\ 0 & 0 & C_{44}q_1^2 + C_{44}q_1^2 \end{pmatrix}$$

This fact can be used in the local description of the dispersion relations.

2.3.2 Tetragonal Lattice Symmetry

For a tetragonal lattice the elastic modulus tensor in Voigt notation reads as

$$C = \begin{pmatrix} C_{11} & C_{12} & C_{13} & 0 & 0 & 0 \\ C_{12} & C_{11} & C_{13} & 0 & 0 & 0 \\ C_{13} & C_{13} & C_{33} & 0 & 0 & 0 \\ 0 & 0 & 0 & C_{44} & 0 & 0 \\ 0 & 0 & 0 & 0 & C_{44} & 0 \\ 0 & 0 & 0 & 0 & 0 & C_{66} \end{pmatrix}$$

In comparison with the elastic modulus tensor for the cubic lattice we now have more independent components, namely C_{66} and C_{13}. The dynamical matrix then becomes

$$D(\boldsymbol{q}) = \begin{pmatrix} C_{11}q_1^2 + C_{66}q_2^2 + C_{44}q_3^2 & (C_{12} + C_{66})q_1 q_2 & (C_{13} + C_{44})q_1 q_3 \\ (C_{12} + C_{66})q_1 q_2 & C_{66}q_1^2 + C_{11}q_2^2 + C_{44}q_3^2 & (C_{13} + C_{44})q_2 q_3 \\ (C_{13} + C_{44})q_1 q_3 & (C_{13} + C_{44})q_2 q_3 & C_{44}q_1^2 + C_{44}q_2^2 + C_{33}q_3^2 \end{pmatrix}$$

Its form for $\boldsymbol{q}||[1, 1, 0]$ is given by

$$D(\boldsymbol{q}) = q^2 \begin{pmatrix} C_{11} + C_{66} & C_{12} + C_{66} & 0 \\ C_{12} + C_{66} & C_{66} + C_{11} & 0 \\ 0 & 0 & 2C_{44} \end{pmatrix}$$

The eigenvectors are then given by

$$\boldsymbol{v}_1 = \frac{1}{\sqrt{2}}\big(1, 1, 0\big)^T,\ \boldsymbol{v}_2 = \frac{1}{\sqrt{2}}\big(1, -1, 0\big)^T,\ \boldsymbol{v}_3 = \big(0, 0, 1\big)^T$$

with eigenvalues

$$\omega_1 = \big(C_{11} + C_{12} + 2C_{66}\big)q^2,\ \omega_2 = \big(C_{11} - C_{12}\big)q^2,\ \omega_3 = 2C_{44}q^2 \tag{2.3.2}$$

This direction will later play an important role. Although we can determine the eigensystem for $D(\boldsymbol{q})$ is general, it will turn out that it is sufficient in many cases to consider only its local form.

2.3.3 Phonons within Quantum Field Theory

In quantum field theory the strain field is treated as an operator field. The field operator form of the strain is

$$\boldsymbol{u}(\boldsymbol{r},t)=\frac{1}{\sqrt{V}}\sum_{\boldsymbol{q}}\sum_{\alpha=1}^{3}\boldsymbol{e}_\alpha(\boldsymbol{q})\Big(u_\alpha^\dagger(\boldsymbol{q})e^{i\big(\boldsymbol{q}\cdot\boldsymbol{r}-\omega_\alpha(\boldsymbol{q})t\big)}+u_\alpha(\boldsymbol{q})e^{-i\big(\boldsymbol{q}\cdot\boldsymbol{r}-\omega_\alpha(\boldsymbol{q})t\big)}\Big) \tag{2.3.3}$$

where the $\boldsymbol{e}_\alpha(\boldsymbol{q})$ denote the eigenvectors of the matrix $D(\boldsymbol{q})$. $\boldsymbol{p}(\boldsymbol{r},t) := \rho\dot{\boldsymbol{u}}(\boldsymbol{r},t)$ can be considered as the momentum at the position $\boldsymbol{r}$ and time t. In accordance with quantum mechanics the quantization of the field is defined to obey the commutation relation

$$\big[p_i(\boldsymbol{r},t),u_j(\boldsymbol{r}',t)\big]=-i\delta(\boldsymbol{r}-\boldsymbol{r}')\delta_{ij} \tag{2.3.4}$$

From this relation we can now derive the commutation relations for the operators $\boldsymbol{u}(\boldsymbol{q})$ and $\boldsymbol{u}^\dagger(\boldsymbol{q})$ in momentum space by inserting 2.3.3 into 2.3.4. This leads to

$$\begin{aligned}
&\sum_{\boldsymbol{q},\boldsymbol{q}',\alpha,\alpha'} e_{\alpha,i}(\boldsymbol{q})e_{\alpha',j}(\boldsymbol{q}')\big(i\omega_\alpha(\boldsymbol{q})\big)\times\\
&\times\Big\{\Big[u_\alpha(\boldsymbol{q}),u_{\alpha'}(\boldsymbol{q}')\Big]\exp\Big(i\big(\boldsymbol{q}\cdot\boldsymbol{r}+\boldsymbol{q}'\cdot\boldsymbol{r}'-t(\omega_\alpha(\boldsymbol{q})+\omega_{\alpha'}(\boldsymbol{q}'))\big)\Big)\\
&\quad+\Big[u_\alpha(\boldsymbol{q}),u_{\alpha'}^\dagger(\boldsymbol{q}')\Big]\exp\Big(i\big(\boldsymbol{q}\cdot\boldsymbol{r}-\boldsymbol{q}'\cdot\boldsymbol{r}'-t(\omega_\alpha(\boldsymbol{q})-\omega_{\alpha'}(\boldsymbol{q}'))\big)\Big)\\
&\quad-\Big[u_\alpha^\dagger(\boldsymbol{q}),u_{\alpha'}(\boldsymbol{q}')\Big]\exp\Big(-i\big(\boldsymbol{q}\cdot\boldsymbol{r}-\boldsymbol{q}'\cdot\boldsymbol{r}'-t(\omega_\alpha(\boldsymbol{q})-\omega_{\alpha'}(\boldsymbol{q}'))\big)\Big)\\
&\quad-\Big[u_\alpha^\dagger(\boldsymbol{q}),u_{\alpha'}^\dagger(\boldsymbol{q}')\Big]\exp\Big(-i\big(\boldsymbol{q}\cdot\boldsymbol{r}+\boldsymbol{q}'\cdot\boldsymbol{r}'-t(\omega_\alpha(\boldsymbol{q})+\omega_{\alpha'}(\boldsymbol{q}'))\big)\Big)\Big\}\\
&=\frac{i}{\rho}\delta(\boldsymbol{r}-\boldsymbol{r}')\delta_{ij}
\end{aligned}$$

Here one can read of the commutation commutation relations

$$\big[u_\alpha(\boldsymbol{q}),u_{\alpha'}(\boldsymbol{q}')\big]=\big[u_\alpha^\dagger(\boldsymbol{q}),u_{\alpha'}^\dagger(\boldsymbol{q}')\big]=0 \tag{2.3.5}$$

$$\big[u_\alpha(\boldsymbol{q}),u_{\alpha'}^\dagger(\boldsymbol{q}')\big]=\big[u_\alpha^\dagger(\boldsymbol{q}),u_\alpha'(\boldsymbol{q}')\big]=\frac{1}{2\rho\omega_\alpha(\boldsymbol{q})}\delta_{\boldsymbol{q},\boldsymbol{q}'}\delta_{\alpha,\alpha'} \tag{2.3.6}$$

With this set of equations for the quantum field version of the acoustic phonons, we can now apply the standard machinery of quantum field theory. A detailed derivation of the phonon propagator **in a general basis for $\boldsymbol{u}$**

$$G_{\mathrm{ph}}^{-1}(\boldsymbol{q},\Omega_m)_{ij}=\rho\Omega_m^2\delta_{ij}+q_kC_{iklj}q_l$$

is given in [10]. Later we will use the representation of the **propagator in the eigenbasis of $D(\boldsymbol{q})$**

$$G_{\mathrm{ph}}^{-1}(\boldsymbol{q},\Omega_m)_{ij}=\rho\Big(\Omega_m^2+\omega_\alpha^2(\boldsymbol{q})\Big)\delta_{ij}$$

This propagator has a slightly different form compared to the common phonon propagator $G_{\text{ph, alt}}^{-1}(\boldsymbol{q},\omega)=\frac{\omega_\alpha^2(\boldsymbol{q})}{\omega^2-\omega_\alpha^2(\boldsymbol{q})}\delta_{ij}$ which can be found in textbooks,e.g. [7]. The reason lies in

the field $\boldsymbol{u}$ we are considering. Normally one normalizes the fields such that they satisfy the canoncial commutation relations. Here this makes no sense because later we want to describe the three acoustic modes as strain fields. A normalization would lead to different units for the dynamic and the static parts of the strain.
The resulting action for bare phonons is

$$S[\boldsymbol{u}^\dagger, \boldsymbol{u}] = \sum_{\boldsymbol{q}, \Omega_m} u_\alpha^\dagger(\boldsymbol{q}, \Omega_m) \rho \Big(\Omega_m^2 + \omega_\alpha^2(\boldsymbol{q}) \Big) u_\alpha(\boldsymbol{q}, \Omega_m) \tag{2.3.7}$$

2.3.4 Thermodynamics of Acoustic Phonons

2.3.4.1 Free Energy

The free energy density of a quantum mechanical system is defined as

$$F = -\frac{T}{V} \ln Z$$

where Z is the partition sum. We already know the action of the acoustic phonons, see eq. 2.3.7. The partition sum can then be calculated via the field integral

$$Z = \int \mathcal{D}[\boldsymbol{u}^\dagger, \boldsymbol{u}] \, \exp \Big(- S[\boldsymbol{u}^\dagger, \boldsymbol{u}] \Big)$$

The action is quadratic in the bosonic strain field. Hence the partition sum is just a Gaussian integral which yields

$$Z = \det G_{\text{ph}} = \prod_{\boldsymbol{q}, \Omega_m, \alpha} g_{\text{ph},\alpha}(\boldsymbol{q}, \Omega_m)$$

where $g_{\text{ph},\alpha}(\boldsymbol{q}, i\Omega_m) = \rho \Omega_m^2 + \rho \omega_\alpha^2(\boldsymbol{q})$ is the propagator of the phonon mode α. In the free energy this product converts into a sum

$$F = -\frac{T}{V} \sum_{\alpha=1}^{3} \Big\{ \sum_{\boldsymbol{q}, \Omega_m} \ln \big[\rho \Omega_m^2 + \rho \omega_\alpha^2(\boldsymbol{q}) \big] \Big\}$$

So the free energy can be split into three contributions from the different acoustic phonon modes and each term can be considered separately.
The sum over the bosonic Matsubara frequencies Ω_m is evaluated in appendix B. The result is

$$F = \sum_{\alpha=1}^{3} F_\alpha(0) + \frac{2}{(2\pi)^3} \int d^3q \Big(T \ln \big[2 \sinh \big(\frac{\omega_\alpha(\boldsymbol{q})}{2T} \big) \big] - \frac{\omega_\alpha(\boldsymbol{q})}{2} \Big)$$

2.3.4.2 Specific Heat

With the free energy we can calculate the specific heat via the formula

$$C(T) = -T \frac{\partial^2 F}{\partial T^2}$$

Insertion of the free energy of the phonons leads to

$$C(T) = \frac{2}{(2\pi)^3} \sum_{\alpha=1}^{3} \int d^3q \frac{\omega_\alpha^2(\boldsymbol{q})}{4T^2} \sinh^{-2} \big(\frac{\omega_\alpha(\boldsymbol{q})}{2T}\big)$$

The dispersions are in general linear in the momentum $\omega_i(\boldsymbol{q}) \propto q$. After the substitution $\boldsymbol{q} \to 2T\boldsymbol{q}$ the specific heat reduces to

$$C(T) = \frac{2T^3}{\pi^3} \sum_{\alpha=1}^{3} \int d^3q\, \omega_\alpha^2(\boldsymbol{q}) \sinh^{-2} \big(\omega_\alpha(\boldsymbol{q})\big)$$

This integral can be written in spherical coordinates. The integral over the momentum can be evaluated analytically using $\omega_\alpha(\boldsymbol{q}) = v_\alpha(\hat{q})q$:

$$C(T) = \frac{2T^3}{\pi^3} \sum_{\alpha=1}^{3} \int d\Omega \frac{\pi^4}{30 v_\alpha^3(\hat{q})} = \frac{\pi}{15} T^3 \sum_{\alpha=1}^{3} \int d\Omega \frac{1}{v_\alpha^3(\hat{q})}$$

The remaining integral over the direction of $\hat{q}$ leads to a constant which only depends on the elastic modulus tensor. An important feature of this formula is that the main contributions come from the directions where the velocities are small.

For a dispersion of the form $\omega^2(\boldsymbol{q}) = v_i^2 q_i^2$ the specific heat becomes

$$C(T) = T^3 \frac{4\pi^2}{15 v_x v_y v_z} \tag{2.3.8}$$

In this section we recovered the common result

$$C(T) \propto T^3$$

for the specific heat of phonons. We used that the dispersion is proportional to q which is true in most situation. Nevertheless there are also cases where this is wrong. Namely close to a lattice transformation one has a modified dispersion. In the following section the specific heat at the transition point from a tetragonal to a orthorhombic lattice will be discussed.

2.4 Lattice Transformations

Symmetry breaking phase transitions occur in a large variety of physical systems. In this section we want to describe a very important class of phase transitions which are the lattice transformations. Such a transformation can be viewed as the deformation of the unit cell of the lattice in a certain direction. Hence a good candidate for an order parameter are the homogeneous strain fields. Our aim is to build up an effective Ginzburg-Landau theory for these transformations in terms of strain.

We have seen that the symmetries of a lattice are closely related to the form of its elastic modulus tensor. Moreover we will show that the stability of a crystal is determined by the eigenvalues of this tensor. To see this we consider again the free energy of a strain field $\boldsymbol{u}$:

$$F = \frac{1}{2}\int d^3r\, u_\alpha(\boldsymbol{r}) C_{\alpha\beta} u_\beta(\boldsymbol{r})$$

$C_{\alpha\beta}$ is a symmetric, positive definite 6x6 matrix. Hence there is always an orthogonal matrix U such that

$$U^T C U = \begin{pmatrix} C_1 & 0 & 0 & 0 & 0 & 0 \\ 0 & C_2 & 0 & 0 & 0 & 0 \\ 0 & 0 & C_3 & 0 & 0 & 0 \\ 0 & 0 & 0 & C_4 & 0 & 0 \\ 0 & 0 & 0 & 0 & C_5 & 0 \\ 0 & 0 & 0 & 0 & 0 & C_6 \end{pmatrix}$$

So the free energy becomes

$$F = \int d^3r\, \big(\underbrace{U^T \boldsymbol{u} U}_{=:\boldsymbol{\varepsilon}}\big)_\alpha \big(U^T C U\big)_{\alpha\beta} \big(U^T \boldsymbol{u} U\big)_\beta = \int d^3r\, \varepsilon_\alpha^2 C_\alpha$$

The strain components ε_α denote the strain into the directions of the eigenvectors of $C_{\alpha\beta}$. The corresponding eigenvalues are commonly called stability parameters. In equilibrium, the strain vanishes by definition. Now when a crystal is stable under small deformations, this is equivalent to the fact that strain costs energy. This implies that all eigenvalues of the elastic modulus tensor have to be positve. Large eigenvalues correspond to a crystal which is more stable.

Thus a lattice transformation is possible only if at least one of the stability parameters is going to zero. A detailed classification of all kinds of lattice transformations which can be described in this way has been made by Cowley [11].

There are transition of first and of second order. The specific type for a given stability parameter can be derived by considering the effective Landau potential of the associated

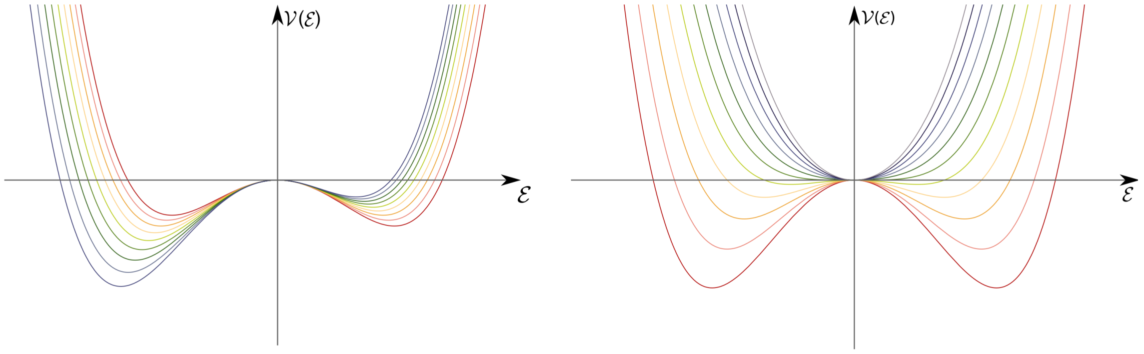

Figure 2.1: The Landau potential for the strain with cubic term (left) and without cubic term (right) for different potential parameters. One can see that the cubic terms leads to a jump of the minimal strain ε.

strains. Here we only consider the cases where there is only one eigenvector to the given eigenvalue. We denote this strain direction by ε:

$$\mathcal{V}(\varepsilon) = \frac{r}{2}\varepsilon^2 + \frac{v}{3!}\varepsilon^3 + \frac{u}{4!}\varepsilon^4$$

The Landau parameter r quantifies the stability of the crystal: it is stable for $r > 0$ while it is unstable for $r < 0$. The key point is now that this potential must be invariant under symmetry transformations of the lattice. This is in general not true for the cubic term. For example, the strain term $\left(u_{xx} - u_{yy}\right)^3$ in the tetragonal lattice is not invariant under the exchange $x \leftrightarrow y$. Hence the cubic term is forbidden for this direction. Whether this term is allowed for other lattice symmetries and strain directions can be read off in Cowley's tabular on page 4 of [11] in the last column.

When this term is forbidden we have the following minima of the potential

$$\varepsilon_{\min} = \begin{cases} 0 \text{ for } r \geq 0 \\ \pm\sqrt{-\frac{6r}{u}} \text{ for } r < 0 \end{cases}$$

Hence we observe a continuous change of the strain at $r = 0$, i.e. the phase transformation is of second order. Furthermore the Landau potential becomes very flat around the minimum for $r \to 0$. This leads to strong fluctuations of ε which are characteristic for second order transitions.

Now if the cubic term is present we can write the potential in terms of the shifted variable $\tilde{\varepsilon} = \varepsilon + \frac{u}{v}$ as

$$\mathcal{V}(\tilde{\varepsilon}) = \frac{\tilde{r}}{2}\tilde{\varepsilon}^2 + \frac{u}{4!}\tilde{\varepsilon}^4 - h\tilde{\varepsilon}$$

where we skipped the constant term and $\tilde{r} = \frac{r}{2} - \frac{v^2}{4u}$, $h = \frac{rv}{u} - \frac{v^3}{3u^2}$. Now the tuning of r leads to a variation of the local minimas. A phase transition occurs when the potential has the same value at the local minimas. The resulting change of the strain is discontinuous. Hence we have here a phase transition of first order.

In this thesis we are interested in the second order phase transitions because they obtain critical strain fluctuations near the transition point. Later we will investigate the case when the fluctuations are excited by a coupled order parameter. The table 2.2 from [12] contains all possible second order lattice transformations.

Besides being continuous or discontinuous, there is one more important attribute in the classification of lattice transitions for which a cubic term doesn't exist. This is the appearance of soft phonons in the vicinity of the transition point. Soft phonons denote phonon modes whose velocity vanishes in some directions. These directions can be either discrete points or planes. Cowley classifies the possible cases as follows:

- **Type 0:** There are no soft phonons at the transition point.
- **Type I:** There are soft phonons whose velocity vanishes in discrete directions.
- **Type II:** There are soft phonons whose velocity vanishes if the direction lies in a given plane.

elastic transition	constant	strain	type
orthorhombic → monoclinic	c_{44}	ε_{23}	I
orthorhombic → monoclinic	c_{55}	ε_{13}	I
orthorhombic → monoclinic	c_{66}	ε_{12}	I
tetragonal → orthorhombic	$c_{11} - c_{12}$	$\varepsilon_{11} - \varepsilon_{22}$	I
tetragonal → orthorhombic	c_{66}	ε_{12}	I
tetragonal → mono- or triclinic	c_{44}	$(\varepsilon_{23}, \varepsilon_{13})$	I+II
hexagonal → mono- or triclinic	c_{44}	$(\varepsilon_{23}, \varepsilon_{13})$	I+II

Figure 2.2: List of all second order lattice transformations from [12]. The first column denotes the initial and final symmetries. In the second and third column the strain directions with the corresponding stability conditions are given. The meaning of the last column is explained in the main text.

In the following we consider the second order phase transition from a tetragonal lattice to an orthorhombic lattice in more detail. In preparation for this, in the next section we introduce the critical exponents. These exponents describe the behaviour of the relevant physical quantities in the vicinity of the critical point.

2.4.1 Critical Exponents

In this section we introduce the one of the most important concepts in the description of second order phase transitions, namely the critical exponents. These numbers describe the scaling of the physical quantities of the system w.r.t. to the reduced distance $\tau = 1 - \frac{T}{T_C}$ from the critical temperature T_C. For example the specific heat satisfies the relation

$$C(T) \propto |\tau|^{-\alpha}$$

The number α then denotes the critical exponent of the specific heat. A notation list for the most important quantities is given in the following table:

Physical quantity	Notation	Critical Exponent
Specific heat	C	α
Correlation length	ξ	ν
Susceptibility	χ	γ

Another very important scaling relation is given by the critical values of the tuning parameter r and the critical temperature T_C. It can be written in the form

$$T_C \propto r^{z\nu} \tag{2.4.1}$$

z is the dynamical critical exponent. It can be considered as the critical exponent for the relation between the energy and the momenta

$$E \propto q^z$$

For acoustic phonons with a linear dispersion we have $\omega(\boldsymbol{q}) \propto q$ we have

$$E(\boldsymbol{q}) \propto \omega(\boldsymbol{q}) \propto q$$

, i.e. $z = 1$. In the next section we will see, that there are lattice transformations,such as the tetragonal to orthorhombic lattice transformation, where we get a dispersion relation proportional to q^2 in some directions. This means that have $z = 2$ at the transition point for these special momentum directions.

2.4.2 Lattice Transformation: Tetragonal to Orthorhombic

We consider a crystal with a tetragonal lattice symmetry. A lattice transformation can be induced by an order parameter which breaks the lattice symmetry. Physically this can be done for example by applying external pressure to the sample or, as considered in the fourth chapter, by internal mechanisms. Here we will study the properties of the strain in the transition to an orthorhombic lattice. The elastic modulus tensor is now given in the form 2.2.3. The eigenvectors are given by

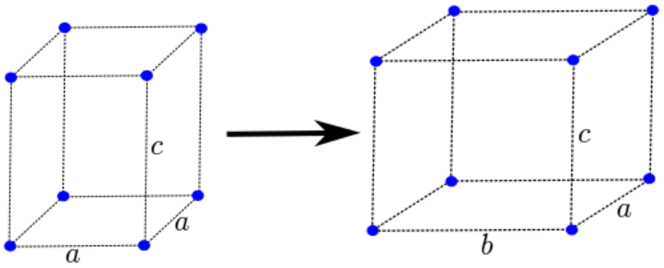

Figure 2.3: The tetragonal lattice (left) is deformed into an orthorhombic lattice (right).

$$\begin{aligned}
\boldsymbol{e}_1 =&\frac{1}{\sqrt{2}}\left(1,-1,0,0,0,0\right)^T,\\
\boldsymbol{e}_2 =&\sqrt{\frac{4C_{13}}{(C_+ + C_-)^2+4}}\left(\frac{C_+ + C_-}{2C_{13}},\frac{C_+ + C_-}{2C_{13}},1,0,0,0\right)^T,\\
\boldsymbol{e}_3 =&\sqrt{\frac{4C_{13}}{(C_+ + C_-)^2+4}}\left(\frac{C_+ - C_-}{2C_{13}},\frac{C_+ - C_-}{2C_{13}},1,0,0,0\right)^T,\\
\boldsymbol{e}_4 =&\left(0,0,0,1,0,0\right)^T,\\
\boldsymbol{e}_5 =&\left(0,0,0,0,1,0\right)^T,\\
\boldsymbol{e}_6 =&\left(0,0,0,0,0,1\right)^T
\end{aligned}$$

with eigenvalues

$$\begin{aligned}
&C_1 = C_{11} - C_{12},\ C_2 = \frac{C_+ - C_- + 2C_{33}}{2},\ C_3 = \frac{C_+ + C_- + 2C_{33}}{2}\\
&C_4 = C_{44},\ C_5 = C_{44},\ C_6 = C_{66}
\end{aligned}$$

where $C_+ = C_{11} + C_{12} - C_{33}$, $C_- = \sqrt{8C_{13}^2 + \big(C_{11} + C_{12} - C_{33}\big)^2}$.
In the tetragonal to orthorhombic lattice transformation the symmetry in the x-y-plane will be broken. Thus the displacement is directed in $\boldsymbol{e}_1$-direction. The energy cost for this strain $\varepsilon_1 \boldsymbol{e}_1$ is given by

$$\varepsilon_1^2 \big(C_{11} - C_{12}\big)$$

We see that this transition happens for

$$C_1 = C_{11} - C_{12} \to 0$$

By setting $C_{11} - C_{12}$ to zero, one of the three phonon branches of obtain roots for $\boldsymbol{q} \in <1, 1, 0>$. The dispersion of this mode in this direction

$$\omega(\boldsymbol{q}) = \big(C_{11} - C_{12}\big) q^2$$

has been calculated in 2.3.2. This is in perfect agreement with the prediction from Cowley's tabular of a soft phonons in the limit $C_{11} - C_{12} \to 0$ and $|q_1| = |q_2|, q_3 = 0$.
Later the behaviour of the dispersion around these roots will play an important role. It can be calculated by the following perturbative approach.
Let $\hat{q}_{||}$ a unit vector which lies in $<1, 1, 0>$. For this direction we can now choose a vector $\hat{q}_\perp$ in the x-y-plane and $\hat{q}_z$ parallel to the z-axis, such that the set $\{\boldsymbol{q}_{||}, \boldsymbol{q}_\perp, \boldsymbol{q}_z\}$ denotes a right-handed basis of the three dimensional vector space of momenta. A general momentum $\boldsymbol{q}$ can then be written as $\boldsymbol{q} = q_{||}\hat{q}_{||} + q_\perp \hat{q}_\perp + q_z \hat{q}_z$. The perturbative solution of the eigenvalue equation 2.3.1 for the expansion parameters $q_\perp$ and q_z around $q_\perp = 0, q_z = 0$ leads in second order to

$$\omega^2(\boldsymbol{q}) = \frac{C_{11} - C_{12}}{2\rho} q_{||}^2 + \Big(\frac{C_{11} + C_{12}}{2\rho} + \frac{C_{66}}{\rho}\Big) q_\perp^2 + \frac{C_{44}}{\rho} q_z^2 \tag{2.4.2}$$

For $C_{11} - C_{12} = 0$ the term proportional to $q_{||}^2$ vanishes. This means that we have to go back to the derivation of the effective potential 2.2.2 and take higher order terms into account. Doing this effectively leads to correction terms in 2.4.2 that are in lowest order proportional to q^4. The dispersion for $|q_{||}| \gg |q_\perp|, |q_z|$ and $C_{11} - C_{12} = 0$ is thus given by

$$\omega^2(\boldsymbol{q}) = \frac{C_{||}^{(4)}}{\rho} q_{||}^4 + \Big(\frac{C_{11}}{\rho} + \frac{C_{66}}{\rho}\Big) q_\perp^2 + \frac{C_{44}}{\rho} q_z^2 \tag{2.4.3}$$

where the first term now contains the higher order contributions.

2.4.2.1 Specific Heat

Now we want to derive the behaviour of the specific heat when our lattice obtains a phase transition.
We have seen in the previous section that smaller velocities are more relevant in the specific heat. To calculate the influence of the soft phonons we consider again the formula for the specific heat from the previous section

$$C(T) = \frac{2}{(2\pi)^3} \sum_{\alpha=1}^{3} \int d^3q \frac{\omega_\alpha^2(\boldsymbol{q})}{4T^2} \sinh^{-2}\Big(\frac{\omega_\alpha(\boldsymbol{q})}{2T}\Big)$$

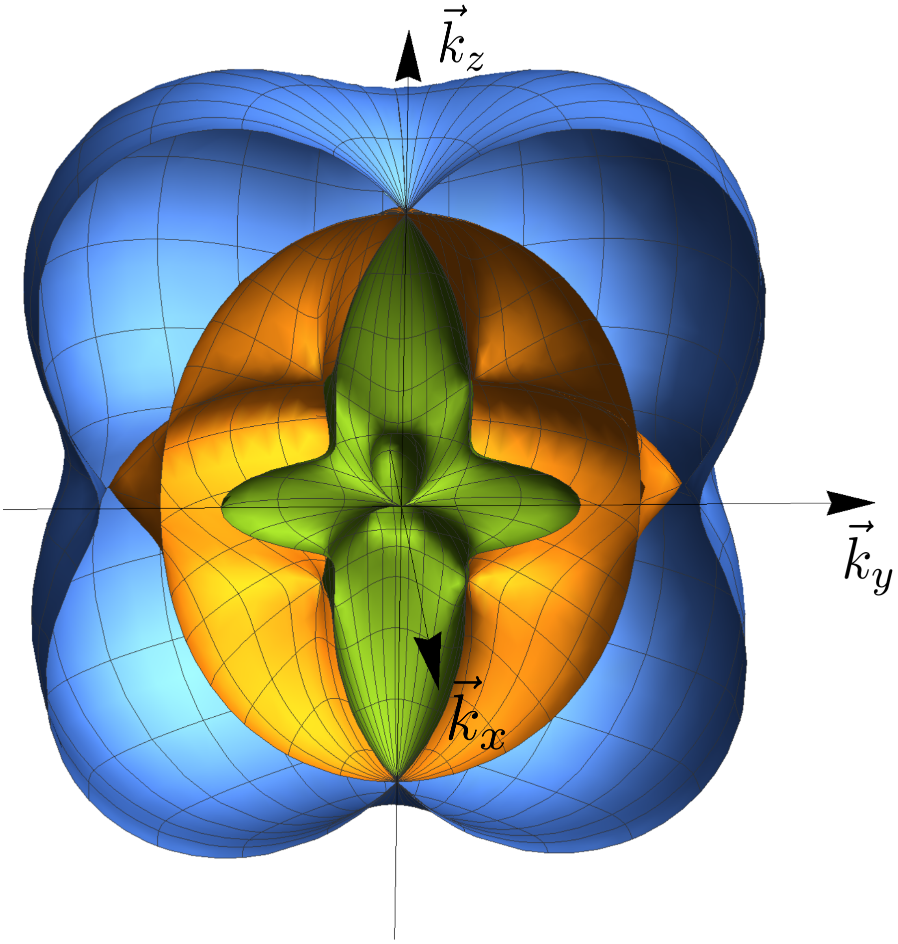

Figure 2.4: Plot of the sound velocities $v_\alpha(\hat{q})$ of the three different phonon modes for $C_{11} - C_{12} = 0$ and $\phi \in (\pi/2, 3\pi/2)$, $\theta \in (0, \pi)$. The dispersion modes have been calculated analytically via the methods described in app. A. The green dispersion has a roots for $\phi \in \{\pi/4, 3\pi/4, 5\pi/4, 7\pi/4\}$, $\theta = \pi/2$

For two of the phonon modes the relation $\omega_\alpha \propto q$ is still valid. For these modes the old result for the specific heat remains unchanged.

For the third mode which is soft in the $<1,1,0>$ directions we don't have this proportionality. There we can use the approximation 2.4.3 for the dispersion. Although this is only valid in the vicinity of the soft direction, it is sufficient since the small velocities dominate the specific heat. In general one can state that this approximation is sufficient for the specific heat as long as we only have one small eigenvalue of the elastic modulus tensor.

Now we do the substitutions $q_\perp \to 2Tq_\perp$, $q_z \to 2Tq_z$, $q_\parallel \to \sqrt{2T}q_\parallel$. The soft dispersion then obtains a prefactor $2T$ which leads again to a temperature independent integrand:

$$C_{\text{soft}}(T) = \frac{\sqrt{2}T^{2.5}}{\pi^3} \int d^3q\, \omega^2(\boldsymbol{q}) \sinh^{-2} \omega(\boldsymbol{q})$$

The remaining integral can be calculated analytically and yields

$$C_{\text{soft}}(T) = T^{2.5}\frac{7}{2}\frac{\Gamma\left(\frac{7}{2}\right)\zeta\left(\frac{7}{2}\right)}{\pi^2}\frac{\rho^{3/2}}{\sqrt{\left(\frac{C_{11}+C_{12}}{2}+C_{66}\right)C_{44}\sqrt{C_{\parallel}^{(4)}}}} \tag{2.4.4}$$

Instead of the T^3 we get here a specific heat which is proportional to $T^{2.5}$ when the crystal is close to the transition point, i.e. when the order parameter $r = C_{11} - C_{12}$ is very small. A comparison of the normal 2.3.8 and critical form of the specific heat 2.4.4 yields the **crossover temperature**

$$T_* = \left(\frac{105}{8}\frac{\Gamma(7/2)\zeta(7/2)}{\pi^4}\right)^2\frac{2r}{\sqrt{C_{\parallel}^{(4)}}}$$

So the crossover temperature is proportional to the tuning parameter r. We know that here we have the dynamical critical exponent $z = 2$. With relation 2.4.1 we thus get $\nu = \frac{1}{2}$ for the critical exponent of the correlation length.

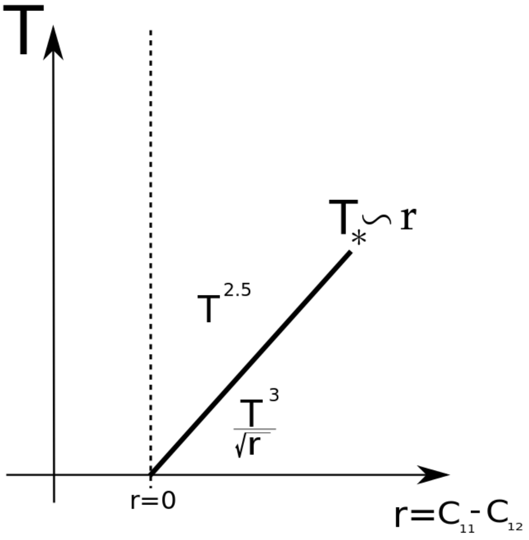

Figure 2.5: Phase diagram of the tetragonal to orthorhombic lattice transition.

Chapter 3

Fermi Liquid with Quadrupolar Interaction

In this chapter we will derive an effective model for the electronic part of the crystal. In metals there are the bounded electrons around the ions and the nearly free conduction electrons. For an isotropic metal we would have an isotropic distribution of the electrons around the ions. The effective action of this system would be $S[\Psi^\dagger, \Psi] = \int d^3x d\tau \left\{ \Psi^\dagger g_\mathrm{f}^{-1} \Psi \right\}$ where g_f is the free fermion propagator. This model is called the free electron gas. From this model we can derive the Fermi statistics that describe the distribution of the electrons in momentum space.

Taking also collisions between the electrons into account, we end up with the Fermi liquid model. This model was developed in 1956 by L.D.Landau, see [8], to describe the low temperature behavior of the electrons. He recognized that interaction between the electrons lead to important effects in the thermodynamic properties of the electronic system. Especially at low temperatures there are large discrepancies between the naive Fermi gas model and the experimental results, that are resolved by the Fermi liquid model.

Here we now construct a Fermi liquid model for a special class of metals, where the distribution of the electrons is **not isotropic** around the ions. The exact structure can be explained as follows.

In some materials we have a groundstate degeneracy of the $4f$ orbitals of the bounded electrons, [13]. These orbitals are associated with quadrupolar electric fields. In the unordered phase at high temperatures we would have equally occupied orbitals. Now in the ordered phase, where the electrons occupies a fixed orbital, rotation symmetry is broken. A special property of the compounds we are considering here is, that this leads to a nematic order. Hence we call this phase, where the rotation symmetry is broken, the nematic phase. In the literature this phase is also called the ferroquadrupolar phase.

The central aspect of this phase which makes physically interesting is that the bounded electrons interact with the conduction electrons. Effectively this leads to an anisotropy in the electronic density. Experiments have already measured some effect of this feature, such as an anisotropic restistance, seeresistance.

To date, nematic phases have been observed in ruthenates [14],[15], pnictides [16],[17],[18],[19] and Fe-based superconductors [20].

Here we now want to derive the thermodynamic properties of these systems at the transition point. Therefore we will construct an effective action that suitably describes the interaction effects of the electrons. This already has been done in two dimensional systems by [5], [6], [21]. In there dimensions we adopt the basic setup that has been made in these papers. There are some peculiarities in the perturbative description of these phase transition in two dimensions, see [5], that don't occur in three dimensions. The reason will be that the higher critical dimension provides the convergence of the effective theory in the vicinity of the critical point.

We start with the action for electrons in metals with a quadrupolar interaction as used in [6]:

$$S[\Psi^\dagger,\Psi] = \int d^3x d\tau \Big\{ \Psi^\dagger g_{\mathrm{f}}^{-1}\Psi + \frac{F_2}{2}\big(\Psi^\dagger \hat{Q}_{ij}\Psi\big)\big(\Psi^\dagger \hat{Q}_{ji}\Psi\big)\Big\} \tag{3.0.1}$$

g_{f}^{-1} denotes the free fermion propagator and F_2 is an interaction constant. The quadrupolar interaction operator is defined by its representation in momentum space

$$Q_{ij}(\boldsymbol{k}^{(m)}) = 3\frac{k_i^{(m)}k_j^{(m)}}{|\boldsymbol{k}^{(m)}|^2} - \delta_{ij}$$

where $\boldsymbol{k}^{(m)} = \frac{\boldsymbol{k}+\boldsymbol{k}'}{2}$ denotes the center of mass momentum of $\Psi_n^\dagger(\boldsymbol{k})$ and $\Psi_m(\boldsymbol{k}')$. The quadrupolar density in momentum space is thus given by

$$\Psi_{\boldsymbol{k}}^\dagger Q_{ij}\big[(\boldsymbol{k}+\boldsymbol{k}')/2\big]\Psi_{\boldsymbol{k}'} \tag{3.0.2}$$

The expectation values $\langle Q_{ij}\rangle$ of the different quadrupolar modes 3.0.2 give us a set of order parameters for the nematic phase. In three dimensional space there are five linear independent quadrupolar modes. As stated before, the non-vanishing quadrupolar density is a consequence of the anisotropies induced by the groundstate orbits of the bounded electrons. Hence in the unordered phase we have $\langle Q_{ij}\rangle = 0$. In the nematic phase we have $\langle Q_i j\rangle \neq 0$ for some, not necessarily all, of the quadrupolar modes. The specific form of the anisotropy in the nematic phase depends on the properties of the compound. In practice there are always modes which are energetically preferred. A detailed analysis of the interplay between two modes can be found in [22].

In the end we want to consider the effect of the anisotropies of the nematic Fermi liquid for a coupled tetragonal lattice. In the previous chapter we have seen that the second order tetragonal to orthorhombic lattice transformation is associated with the critical strain fluctuations $\varepsilon_{xx} - \varepsilon_{yy}$. The relevant coupling between the electrons and the lattice will be the coupling of these strain fluctuations to the quadrupolar electron-density fluctuations of the same symmetry. Therefore, it is sufficient to consider the case where we have the single mode

$$Q(\boldsymbol{k}) = \frac{1}{\sqrt{3}}Q_{xx}(\boldsymbol{k}) - \frac{2}{\sqrt{3}}Q_{yy}(\boldsymbol{k}) = \sqrt{3}\big(\hat{k}_x^2 - \hat{k}_y^2\big)$$

which has the same symmetries as $\varepsilon_{xx} - \varepsilon_{yy}$. Of course the linear combination of quadrupolar tensors is again a quadrupolar tensor. The nematic phase is then described by the order parameter $\langle Q\rangle$. It vanishes in the unordered phase whereas it is finite in the nematic phase.

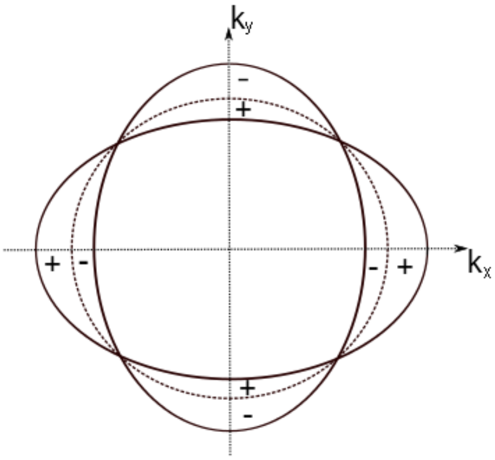

Figure 3.1: Deformation of the Fermi sphere in the k_x-k_y-plane due to the quadrupolar interaction Q. The plus and minus signs denote the sign of Q in the different momentum regimes. One can see that the points on the diagonals are fixed.

3.1 Effective Action for Quadrupolar Fluctuations

We start with the action 3.0.1. To calculate the thermodynamics for this action we would have to integrate of the fermionic field Ψ, which is not possible for in an exact analytical manner, because of the interaction terms proportional to Ψ^4. A classical perturbative approach for such an action is to perform a Hubbard-Stratonovich transformation. The idea is to introduce a new bosonic field as a free parameter to get rid of the quartic terms in Ψ. For that one uses the general identity

$$\exp\Big[-\lambda \boldsymbol{v}^\dagger v\Big] = \int \mathcal{D}w \exp\Big[-\frac{1}{4\lambda}w^2 + vw\Big]$$

where v and w denote arbitrary real fields. A more detailed description of this transformation can be found in [23],page 243ff. In our problem we identify $v \leftrightarrow \Psi^\dagger Q_{ij}\Psi$ and get for each mode the equation

$$\exp\Big(\frac{F_2}{2}\big(\Psi_n^\dagger \hat{Q}_{ij}\Psi_m\big)\big(\Psi_n^\dagger \hat{Q}_{ji}\Psi_m\big)\Big) = \int \mathcal{D}\phi_{ij} \exp\Big[-\frac{1}{2F_2}\big(\phi_{ij}\phi_{ij}\big) + \phi_{ij}\big(\Psi_n^\dagger \hat{Q}_{ij}\Psi_m\big)\Big]$$

So we defined for each quadrupolar mode of the fermionic fields an associated real bosonic field with the same symmetry. These new bosons will play a central role in the coupling of the electrons to the lattice. Physically they can be understood as volume preserving deformations of the Fermi sphere of quadrupolar symmetry.

With these steps we can rewrite the initial partition sum as follows

$$\begin{aligned} Z &= \int \mathcal{D}[\Psi^\dagger,\Psi] \exp\big[-S[\Psi^\dagger,\Psi]\big] \\ &= \int \mathcal{D}[\Psi^\dagger,\Psi] \exp\Big[\int d^3x d\tau \Big\{\Psi^\dagger g_{\mathrm{f}}^{-1}\Psi + \frac{F_2}{2}\big(\Psi^\dagger \hat{Q}_{ij}\Psi\big)\big(\Psi^\dagger \hat{Q}_{ji}\Psi\big)\Big\}\Big] \\ &= \int \mathcal{D}[\Psi^\dagger,\Psi]\mathcal{D}\Phi \exp\big(-S[\Psi^\dagger,\Psi,\Phi]\big) \end{aligned}$$

where the mixed action has the form

$$S[\Psi^\dagger,\Psi,\Phi]=\int d^3x d\tau\left\{\Psi^\dagger g_{\mathrm{f}}^{-1}\Psi-\frac{1}{2F_2}\phi_{ij}\phi_{ij}-\phi_{ij}\big(\Psi^\dagger\hat{Q}_{ji}\Psi\big)\right\}$$

and Φ denotes the set of all bosons ϕ_{ij}. This action contains now the bosonic fields as new degrees of freedom. To get back to the initial action we would have to integrate out these fields. Here we take another route and formulate a theory in terms of Φ. For that we evaluate the integral over the fermionic fields $\Psi^\dagger$, Ψ. The final action for Φ then contains all informations about the full system.

$$\begin{aligned}Z&=\int\mathcal{D}\Phi\det\Big(g_{\mathrm{f}}^{-1}+\phi_{ij}Q_{ij}\Big)\exp\Big[\int d^3x d\tau\frac{-1}{2F_2}\phi_{ij}\phi_{ij}\Big]\\&=\int\mathcal{D}\Phi\exp\Big[\int d^3x d\tau\,\frac{-1}{2F_2}\phi_{ij}\phi_{ij}+\mathrm{tr}\big\{\ln(g_{\mathrm{f}}^{-1}+\phi_{ij}Q_{ij})\big\}\Big]\end{aligned}$$

An expansion of the logarithm in the field ϕ via the sum

$$\log(1+x)=\sum_{k=1}^{\infty}(-1)^{k+1}\frac{x^k}{k}=x-\frac{x^2}{2}+\mathcal{O}(x^3)$$

leads to

$$Z=\int\mathcal{D}\Phi\exp\Big[\int d^3x d\tau\,\frac{-1}{2F_2}\phi_{ij}\phi_{ij}+\mathrm{tr}\big\{\ln(g_{\mathrm{f}}^{-1})\big\}+\mathrm{tr}\big\{g_{\mathrm{f}}\phi_{ij}Q_{ij}\big\}-\frac{1}{2}\mathrm{tr}\big\{(g_{\mathrm{f}}\phi_{ij}Q_{ij})^2\big\}\Big]$$

The first term $\mathrm{tr}\big\{\ln(g_{\mathrm{f}}^{-1})\big\}$ gives a constant contribution to the effective action. It is not necessary to calculate it in detail because it will not influence the dynamics of the field Φ. The next term is $\mathrm{tr}\big\{g_{\mathrm{f}}\phi_{ij}Q_{ij}\big\}$ which, because of energy and momentum conservation, is given by

$$\sum_{\boldsymbol{k},\omega_n}g_{\mathrm{f}}(\boldsymbol{k},i\omega_n)\phi_{ij}(0,0)Q(\boldsymbol{k})$$

The fermionic propagator does not depend on the direction of $\boldsymbol{k}$. When replacing the sum over the momentum by an integral in spherical coordinates one gets a result proportional to

$$\int d\Omega Q_{ij}(\hat{k})=\int_{-1}^{1}d(\cos\theta)\int_0^{2\pi}d\varphi\big(3\hat{k}_i\hat{k}_j-\delta_{ij}\big)=0$$

Hence this term vanishes. This is in accordance with the quadrupolar form of Q.
So the first relevant term is the term quadratic in the bosonic fields

$$\begin{aligned}&-\frac{1}{2}\mathrm{tr}\big\{(g_{\mathrm{f}}\phi_{ij}Q_{ij})^2\big\}\\=&\frac{-1}{2}\sum_{\boldsymbol{k},\boldsymbol{q},\omega_n,\Omega_m}g_{\mathrm{f}}(\boldsymbol{k}+\boldsymbol{q},i\omega_n+i\Omega_m)\phi_{ij}(q,i\Omega_m)Q_{ij}(\boldsymbol{k}+\boldsymbol{q})\,g_{\mathrm{f}}(\boldsymbol{k},i\omega_n)\phi_{kl}(-q,-i\Omega_m)Q_{kl}(\boldsymbol{k})\\=&\frac{-1}{2}\sum_{\boldsymbol{q},\Omega_m}\phi_{ij}(q,i\Omega_m)\phi_{kl}(-q,-i\Omega_m)\sum_{\boldsymbol{k},\omega_n}g_{\mathrm{f}}(\boldsymbol{k}+\boldsymbol{q},i\omega_n+i\Omega_m)Q_{ij}(\boldsymbol{k}+\boldsymbol{q})g_{\mathrm{f}}(\boldsymbol{k},i\omega_n)Q_{kl}(\boldsymbol{k})\\=&\frac{-1}{2}\sum_{\boldsymbol{q},\Omega_m}\phi_{ij}(q,i\Omega_m)\phi_{kl}(-q,-i\Omega_m)\Pi_{ijkl}(\boldsymbol{q},i\Omega_m)\end{aligned}$$

The quantity $\Pi_{ijkl}(\boldsymbol{q}, i\Omega_m)$ is called the **quadrupolar polarization**. It resembles the first non-vanishing correction to the effective propagator of the bosons ϕ.

3.2 Effective Action for ϕ

The polarization for the interaction mode Q is to first order in $\frac{\Omega_m}{v_F q}$ given by

$$\Pi(\boldsymbol{q}, \Omega_m) = -\frac{2mk_F}{45\pi^2} + E(\boldsymbol{q}) + \gamma(\hat{q})\frac{|\Omega_m|}{q}$$

The derivation of this quantity is presented in appendix C.
The second term

$$E(\boldsymbol{q}) := A^2\big(q_x^2 + q_y^2\big) + B^2 q_z^2$$

is the kinetic energy. It is symmetric under rotations in the x-y-plane. The anisotropy is a consequence of the anisotropic Q.
The last term is the **Landau damping term**. Its direction dependence is contained in the function

$$\gamma(\varphi_q, \Theta_q) = \frac{3}{1024\pi}\big(41 + 9\cos(4\varphi_q) + 4(5 - 3\cos(4\varphi_q))\cos(2\Theta_q) + 6\cos^2(2\varphi_q)\cos(4\Theta_q)\big) \tag{3.2.1}$$

The crucial point about this prefactor is, that it vanishes in the directions $\big(\pm 1, \pm 1, 0\big)^T$, $\big(\pm 1, \mp 1, 0\big)^T$.
In the common abbreviation we can say that the Landau damping vanishes for $\boldsymbol{q} \in <1\,1\,0>$.
$<1\,1\,0>$ denotes the set of all vectors which can be mapped to the direction $\big(\frac{1}{\sqrt{2}}, \frac{1}{\sqrt{2}}, 0\big)^T$ via symmetry transformations of the lattice.

The partition sum for the fluctuations now has the form

$$Z = \int \mathcal{D}\phi \, \exp\bigg(-\sum_{\boldsymbol{q},\Omega_m}\Big\{\phi(\boldsymbol{q}, \Omega_m)\Big(\frac{1}{2F_2} - \frac{2mk_F}{45\pi^2} + E(\boldsymbol{q}) + \gamma(\hat{q})\frac{|\Omega_m|}{q}\Big)\phi(-\boldsymbol{q}, \Omega_m)\Big\}\bigg)$$

So the propagator for the bosons ϕ is given by

$$g_\mathrm{b}^{-1}(\boldsymbol{q}, \Omega_m) = r + A^2\big(q_x^2 + q_y^2\big) + B^2 q_z^2 + \frac{\gamma(\hat{q})}{q}|\Omega_m|$$

where $r = \frac{1}{2F_2} - \frac{2mk_F}{45\pi^2}$ is the effective mass of these bosons. We see that the mass vanishes for

$$F_2 = \frac{45\pi^2}{4}\frac{1}{mk_F}$$

This point resembles the quantum critical point of the Fermi liquid. There the fluctutations of the Fermi sphere become critical, i.e. they are strongly enhanced. So in the vicinity of this point we expect modifications of the ordinary properties of the Fermi liquid. These are called non-Fermi liquid behaviour.
In the following we will consider the thermodynamic properties close to the critical point.

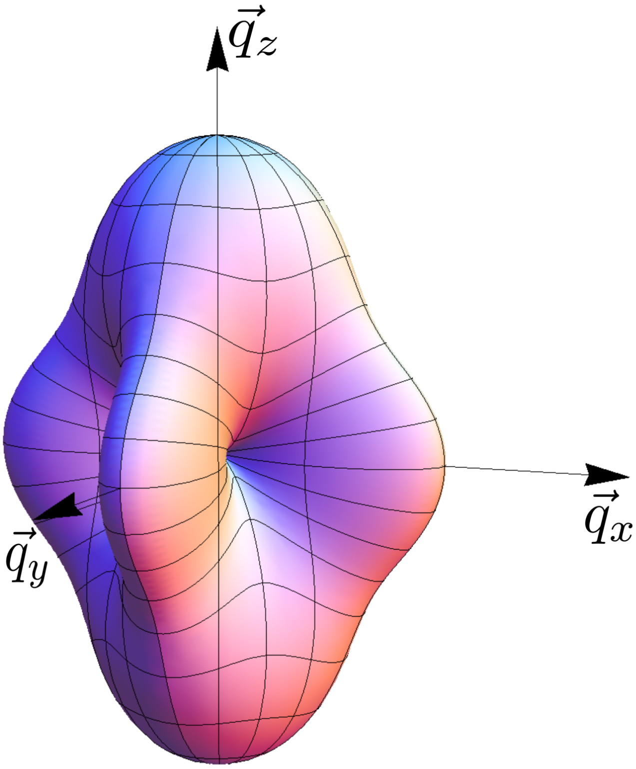

Figure 3.2: Plot of the Landau damping prefactor $\gamma(\hat{q})$. The prefactor strongly decreases close to its roots in the <1,1,0> directions. In the other regimes there is only a small variation of its values.

3.3 Quantum Phase Transitions

In classical continuous phase transitions we have a certain type of thermal fluctuations that become stronger while approaching the critical transition point. This point can be reached by tuning the tuning parameter r and the temperature T to its critical values $r = 0$ and $T = T_c$. An example is the lattice transformation that have seen in the previous chapter. Thereby the thermal fluctuations have been the strain fluctuations of the lattice.

Now a quantum phase transition is a phase transition whose critical temperature is zero. This implies that the critical point, now called quantum critical point (QCP), can only be reached asymptotically. It indicates the boundary between two different quantum phases at zero temperature. The fundamental difference now lies in the critical fluctuations. The thermal fluctuations of classical phase transitions are absent at zero temperature. Hence the critical fluctuations at a quantum phase transition have to be quantum fluctuations in the sense that they are a consequence of the Heisenberg uncertainty principle.

Although the QCP lies at $T = 0$ it can influence the physical properties at finite temperatures. The reason is that the quantum fluctuations are not instantly suppressed by the thermal fluctuations when going to finite temperatures. The ratio between these two types of fluctuations depends on the tuning parameter r and the temperature T. A comparison of the typical orders of the fluctuations leads to the inequality

$$k_B T > \hbar\omega_c \sim |r|^{\nu z}$$

It determines the temperatures where the thermal fluctuations dominate the system. The resulting quantum phase diagram is plotted in 3.3. We will see in the next section that

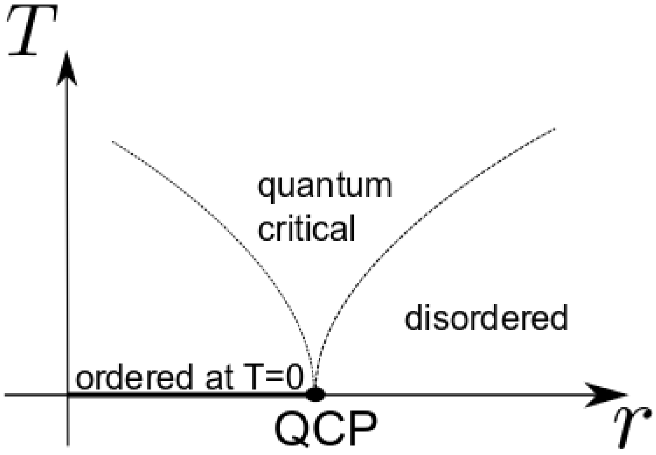

Figure 3.3: Quantum phase diagram for a isolated quantum critical point

.

the nematic Fermi liquid is one example of a system which obtains an isolated QCP.
Up to now we assumed that we an ordered phase that only exists for $r < 0$ and $T = 0$. In practice one is often interested in systems where the QCP is the endpoint of a classical phase transition. This means that we have transition line $r_C(T)$ in the phase diagram that distinguishes two classical phases and reaches the QCP at $T = 0$. Close to this line the thermal fluctuations are dominating. This leads to the quantum phase diagram plotted in 3.4. The tetragonal to orthorhombic lattice transition is one example where such a quantum critical endpoint is present. There we had the temperature-independent critical value $r_C = 0$ for the tuning parameter. More details about the theory of quantum phase transitions can be found in [24],[25]. In the next chapter will calculate the quantum phase diagram of the nematic Fermi liquid. The Fermi liquid is one of the major examples where the quantum criticality can drastically change the physical properties of the system. These effects are commonly called 'non-Fermi liquid' behaviour. A detailed derivation of non-Fermi liquid behaviour can be found in [7].

3.4 Critical Thermodynamics

One way to understand the characteristics of a phase transition is to calculate the thermodynamic quantities of the system. Here we will calculate the specific heat $C(T) = -T\frac{\partial^2 F}{\partial T^2}$ of the bosons close to the quantum critical point $r = 0$.

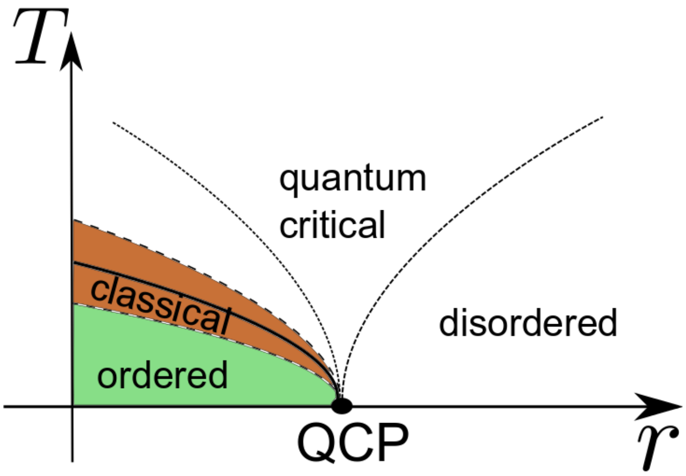

Figure 3.4: Quantum phase diagram for an quantum critical point endpoint. The straight line denotes at phase transition. Around this line we have a classical regime in the sense that there the quantum fluctuations are suppressed by the thermal fluctuations.

3.4.1 Free Energy

For the free energy we have to evaluate the integral

$$\begin{aligned} F &= -\frac{T}{V}\ln Z = -\frac{T}{V}\ln\left[\int d\phi \exp\big(-S[\phi]\big)\right] \\ &= -\frac{T}{V}\ln\left[\int d\phi \exp\Big(-\sum_{\boldsymbol{q},\Omega_m}\phi(\boldsymbol{q},\Omega_m)g_{\mathrm{b}}^{-1}(\boldsymbol{q},\Omega_m)\phi(-\boldsymbol{q},-\Omega_m)\Big)\right] \end{aligned}$$

The effective action of the bosons is quadratic in ϕ. Therefore we can use the formula for Gaussian integrals and get

$$F = \frac{T}{V}\sum_{\boldsymbol{q},\Omega_m}\ln\Big(g_{\mathrm{b}}(\boldsymbol{q},\Omega_m)\Big) \approx T\int\frac{d^3q}{(2\pi)^3}\sum_{\Omega_m}\ln\left[r+E(\boldsymbol{q})+\gamma(\hat{q})\frac{|\Omega_m|}{q}\right]$$

To transform the frequency sum into a complex integral one has to take care of the absolute value which is not holomorphic over the complex plane. Here we circumvent this problem by splitting the sum into positive and negative frequencies. This leads to

$$F = T\int\frac{d^3q}{(2\pi)^3}\ln\big[r+E(\boldsymbol{q})\big]+T\int\frac{d^3q}{(2\pi)^3}\left\{\sum_{\Omega_m>0}\ln\left[r+E(\boldsymbol{q})+\gamma(\hat{q})\frac{\Omega_m}{q}\right]+\sum_{\Omega_m<0}\ln\left[r+E(\boldsymbol{q})-\gamma(\hat{q})\frac{\Omega_m}{q}\right]\right\}$$

The first term is the $\Omega_m = 0$ term. The sums can be written as complex integrals

$$\oint_{\mathcal{C}_+}\frac{dz}{2\pi i}g(z)\ln\left[r+E(\boldsymbol{q})-\gamma(\hat{q})\frac{iz}{q}\right]+\oint_{\mathcal{C}_-}\frac{dz}{2\pi i}g(z)\ln\left[r+E(\boldsymbol{q})+\gamma(\hat{q})\frac{iz}{q}\right]$$

where $g(z) = \beta n_B(z)$ and $\mathcal{C}_\pm$ are the paths plotted in fig. 3.5.

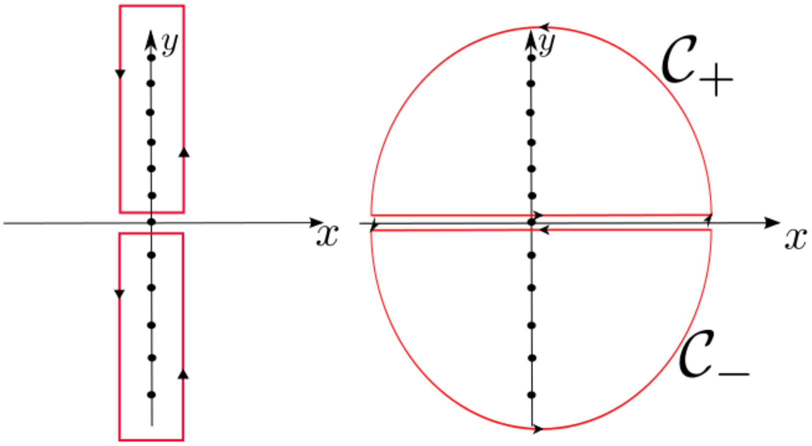

Figure 3.5: The deformation of the initial integration paths (left) to the new paths (right) doesn't change the integral.

The contribution from the half circles vanish for infinitely large radius. The integration along the real axis can be written as

$$\int_{-\infty}^{\infty} \frac{dx}{2\pi i} \beta \Big(n_B(x^+) \ln \Big[r + E(\boldsymbol{q}) - \gamma(\hat{q}) \frac{ix^+}{q} \Big] - n_B(x^-) \ln \Big[r + E(\boldsymbol{q}) + \gamma(\hat{q}) \frac{ix^-}{q} \Big] \Big)$$

for $x^{\pm} = x + i0^{\pm}$. The integrands are continuous around the real axis for $x \neq 0$. On the real axis we have $\ln \big[r + E(\boldsymbol{q}) - \gamma(\hat{q}) \frac{ix}{q} \big] = \overline{\ln \big[r + E(\boldsymbol{q}) + \gamma(\hat{q}) \frac{ix}{q} \big]}$. Thus the difference just gives the imaginary part of the logarithm $\mathrm{Im} \Big[\ln(x + iy) \Big] = \arctan \Big(\frac{y}{x} \Big)$.

$$- \int_{-\infty}^{\infty} \frac{dx}{2\pi i} \beta n_B(x) \arctan \Big(\frac{\gamma(\hat{q}) \frac{x}{q}}{r + E(\boldsymbol{q})} \Big)$$

The free energy now has the form

$$F = T \int \frac{d^3q}{(2\pi)^3} \frac{1}{r + E(\boldsymbol{q})} - \int_{-\infty}^{\infty} \frac{d\omega}{\pi} n_B(\omega) \arctan \Big(\frac{\gamma(\hat{q}) \frac{\omega}{q}}{r + E(\boldsymbol{q})} \Big) \tag{3.4.1}$$

Performing a partial integration in the second term simplifies the free energy to

$$F = T \int \frac{d^3q}{(2\pi)^3} \ln \big[r + E(\boldsymbol{q}) \big] + \int_{-\infty}^{\infty} \frac{d\omega}{\pi} T \Big[\ln \big(2 \sinh \frac{\omega}{2T} \big) - \frac{\omega}{2T} \Big] \frac{\frac{\gamma(\hat{q})}{q} \big(r + E(\boldsymbol{q}) \big)}{\big(r + E(\boldsymbol{q}) \big)^2 + \big(\frac{\gamma(\hat{q})}{q} \omega \big)^2} \tag{3.4.2}$$

3.5 Specific Heat

We are interested in the second derivate of the free energy w.r.t. T. Hence we can ignore the term linear and T and focus on the second term. The first derivative of the free energy in the form 3.4.1 is given by

$$\frac{\partial F}{\partial T} = -\int \frac{d^3q}{(2\pi)^3}\int_{-\infty}^{\infty}\frac{d\omega}{\pi}\frac{\omega}{2T^2}\mathrm{csch}^2\Big(\frac{\omega}{2T}\Big)\arctan\Big(\frac{\gamma(\hat{q})\frac{\omega}{q}}{r+E(\boldsymbol{q})}\Big)$$

Before calculating the second derivative we perform the substitution $\omega \to 2T\omega$

$$\frac{\partial F}{\partial T} = -\int \frac{d^3q}{(2\pi)^3}\int_{-\infty}^{\infty}\frac{d\omega}{\pi}2\omega\mathrm{csch}^2(\omega)\arctan\Big(\frac{\gamma(\hat{q})\frac{2T\omega}{q}}{r+E(\boldsymbol{q})}\Big)$$

The second derivative of the free energy w.r.t. T is

$$\frac{\partial^2 F}{\partial T^2} = -\int_{q\leq\Lambda}\frac{d^3q}{(2\pi)^3}\int_{-\infty}^{\infty}\frac{d\omega}{\pi}2\omega\mathrm{csch}^2(\omega)\frac{\gamma(\hat{q})\frac{2\omega}{q}\big(r+E(\boldsymbol{q})\big)}{\big(r+E(\boldsymbol{q})\big)^2+\big(\gamma(\hat{q})\frac{2T\omega}{q}\big)^2}$$

Rescaling $\boldsymbol{q} \to (2T)^{1/3}\boldsymbol{q}$ gives

$$\frac{\partial^2 F}{\partial T^2} = -2\int_{q\leq\frac{\Lambda}{(2T)^{1/3}}}\frac{d^3q}{(2\pi)^3}\int_{-\infty}^{\infty}\frac{d\omega}{\pi}\omega\mathrm{csch}^2(\omega)\frac{\gamma(\hat{q})\frac{2\omega}{q}\big(\frac{r}{(2T)^{2/3}}+E(\boldsymbol{q})\big)}{\big(\frac{r}{(2T)^{2/3}}+E(\boldsymbol{q})\big)^2+\big(\gamma(\hat{q})\frac{\omega}{q}\big)^2}$$

Here one can read of the scaling relation

$$T \sim r^{3/2}$$

between the order parameter r and the temperature. The exponent $\frac{3}{2} = \nu z$ can be identified with the product of the critical exponents $\nu = \frac{1}{2}$ and $z = 3$.
In the limit $r \to 0$, i.e. at the quantum critical point, the integration over q gives

$$\begin{aligned}\frac{\partial^2 F}{\partial T^2} =& -2\int\frac{d\Omega}{(2\pi)^3}\int_{-\infty}^{\infty}\frac{d\omega}{\pi}\omega^2\mathrm{csch}^2(\omega)\frac{\gamma(\hat{q})}{3e^2(\hat{q})}\ln\Big(\frac{e(\hat{q})\Lambda^3}{2T\gamma(\hat{q})\omega}\Big)\\ =& -\alpha\ln\Big(\frac{\Lambda^3}{2T}\Big)-\beta\end{aligned}$$

where $E(\boldsymbol{q}) = e(\hat{q})q^2$ and

$$\begin{aligned}\alpha =& \frac{2}{9}\int\frac{d\Omega}{(2\pi)^3}\frac{\gamma(\hat{q})}{e^2(\hat{q})}\\ \beta =& 2\int\frac{d\Omega}{(2\pi)^3}\int_{-\infty}^{\infty}\frac{d\omega}{\pi}\omega^2\mathrm{csch}^2(\omega)\frac{\gamma(\hat{q})}{3e^2(\hat{q})}\ln\Big(\frac{e(\hat{q})}{\gamma(\hat{q})\omega}\Big)\end{aligned}$$

Thus the specific heat has the form for $r = 0$:

$$C(T) = T\Big(\alpha\ln\Big(\frac{\Lambda^3}{2T}\Big)+\beta\Big)$$

3.6 Summary

The quadrupolar interaction of the electrons can effectively be described by strain of the Fermi sphere. We considered the dynamics of the strain excitations $\phi_{x^2-y^2}$. The propagator for this mode is

$$g_{\mathrm{b}}^{-1}(\boldsymbol{q}, i\Omega_m) = r + E(\boldsymbol{q}) + \gamma(\hat{q})\frac{|\Omega_m|}{q}$$

The prefactor $\gamma(\hat{q})$ of the Landau damping term only depends on the direction of $\boldsymbol{q}$. The most important feature is that it is positive everywhere except for the directions $<1\,1\,0>$. There the Landau damping vanishes. For the properties of the bare Fermi liquid we have calculated here, these roots played no important role. In the next chapter we will couple these bosons to the underlying lattice. There we will see that the roots of $\gamma(\hat{q})$ lead to important effects for the coupled system

After we have derived the effective action for the excitation modes we calculated the thermodynamics in the vicinity of the Pomeranschuk instability $r = 0$. We observed a non-Fermi liquid behaviour in the specific heat. The original law $C(T) \propto T$ is modified to $C(T) \propto T \ln T$. Severeal other properties of this quantum critical point are presented e.g. in [6].

Chapter 4

Quantum Critical Fermi Liquid on a Lattice

We are now ready to consider the full system of critical electrons with quadrupolar interaction which are coupled to the underlying lattice. We construct a perturbative action by constructing an effective coupling between the strain in the lattice and the bosons ϕ_{ij}. Thereby we have to take care of the lattice symmetries. Here we consider again a tetragonal lattice.
In the end our aim is to calculate the behaviour of the coupled system at low temperatures. Especially we want to know whether the coupling can induce a symmetry transformation into an orthorhombic lattice. As we have seen in chapter two, this transition corresponds the strain $\boldsymbol{e}_1 = \boldsymbol{u}_{xx} - \boldsymbol{u}_{yy}$. Intuitively it is clear that the best candidate for the excitation of this strain is the quadrupolar mode $\phi_{x^2-y^2}$ in the Fermi liquid, which is parallel to the strain. Quantitatively this can be seen in the construction of an effective coupling term in the action.
The lowest order terms correspond to a linear coupling of the strain to the quadrupolar modes of the form

$$S_{\text{int,lin}} \propto \sum_{\boldsymbol{q},\Omega_m} \sum_{\alpha} \big(u_{xx}(\boldsymbol{q},\Omega_m) - u_{yy}(\boldsymbol{q},\Omega_m) \big) \phi_\alpha(\boldsymbol{q},\Omega_m)$$

This term has to satisfy the symmetries of the crystal, e.g. $x \leftrightarrow y$. For the linear coupling terms this implies that the ϕ_{ij} must have the same symmetries as the strain direction. Thus here the only linear coupling term is

$$S_{\text{int,lin}} \propto \sum_{\boldsymbol{q},\Omega_m} \big(u_{xx}(\boldsymbol{q},\Omega_m) - u_{yy}(\boldsymbol{q},\Omega_m) \big) \phi_{x^2-y^2}(\boldsymbol{q},\Omega_m)$$

In the following we again leave the index of $\phi_{x^2-y^2}$ away. The coupling to the other modes only occur in higher order terms and is therefore subleading.

4.1 Action of the Full System

We are primarily interested in the effects of the boson coupling to the phonons, i.e. the dynamical strain. The effective action of the bare bosons is given by

$$S[\phi] = \sum_{\boldsymbol{q},\Omega_m} \phi(\boldsymbol{q},\Omega_m) g_{\mathrm{b}}^{-1}(\boldsymbol{q},i\Omega_m)\phi(-\boldsymbol{q},\Omega_m)$$

The form of the propagator $g_{\mathrm{b}}^{-1}(\boldsymbol{q},i\Omega_m) = r_0 + A^2(q_x^2+q_y^2) + B^2q_z^2 + \gamma(\hat{q})\frac{|\Omega_m|}{q}$ was calculated in the previous chapter.
The action of the phonons with $\boldsymbol{q} \neq 0$ is again given by

$$S[\boldsymbol{u}^\dagger,\boldsymbol{u}] = \sum_{\boldsymbol{q},\Omega_m} \boldsymbol{u}^\dagger(\boldsymbol{q},\Omega_m) G_{\mathrm{ph}}^{-1}(\boldsymbol{q},i\Omega_m)\boldsymbol{u}(\boldsymbol{q},\Omega_m)$$

where $\left(G_{\mathrm{ph}}^{-1}\right)_{ij}(\boldsymbol{q},i\Omega_m) = \rho\Omega_m^2\delta_{ij} + C_{ikjl}q_kq_l$.
Because of symmetry considerations, the general action of this system with linear coupling must have the form

$$S[\phi,\boldsymbol{u}^\dagger,\boldsymbol{u}] = \sum_{\boldsymbol{q},\Omega_m} \begin{pmatrix}\phi\\ \boldsymbol{u}\end{pmatrix}^\dagger \underbrace{\left(\begin{array}{c|ccc} g_{\mathrm{b}}^{-1}(\boldsymbol{q},i\Omega_m) & i\lambda q_x & -i\lambda q_y & 0 \\ \hline -i\lambda q_x & & & \\ i\lambda q_y & & G_{\mathrm{ph}}^{-1}(\boldsymbol{q},i\Omega_m) & \\ 0 & & & \end{array}\right)}_{=:H^{-1}(\boldsymbol{q},i\Omega_m)} \begin{pmatrix}\phi\\ \boldsymbol{u}\end{pmatrix}$$

Later on we will denote the coupling components by $\boldsymbol{v} = \big(-i\lambda q_x, i\lambda q_y, 0\big)^T$. The inverse propagator of the coupled system then has the form

$$H^{-1}(\boldsymbol{q},i\Omega_m) = \begin{pmatrix} g_{\mathrm{b}}^{-1}(\boldsymbol{q},i\Omega_m) & \boldsymbol{v}^\dagger \\ \boldsymbol{v} & G_{\mathrm{ph}}^{-1}(\boldsymbol{q},i\Omega_m) \end{pmatrix}$$

Of special interest for us is the coupling of the bosons to the soft mode. This can be read of by diagonalizing the action.
Let U be the orthogonal matrix which diagonalizes G_{ph}^{-1} at finite momentum, i.e. $U^TG_{\mathrm{ph}}^{-1}U = \mathrm{diag}\big(\rho\Omega_m^2+\rho\omega_1^2(\boldsymbol{q}), \rho\Omega_m^2+\rho\omega_2^2(\boldsymbol{q}), \rho\Omega_m^2+\rho\omega_3^2(\boldsymbol{q})\big)$. The inverse propagator in terms of the phonon modes is then

$$\tilde{H}^{-1} = \left(\begin{array}{c|ccc} g_{\mathrm{b}}^{-1}(\boldsymbol{q},i\Omega_m) & & \boldsymbol{v}^TU & \\ \hline & \rho\Omega_m^2+\rho\omega_1^2(\boldsymbol{q}) & 0 & 0 \\ U^T\boldsymbol{v} & 0 & \rho\Omega_m^2+\rho\omega_2^2(\boldsymbol{q}) & 0 \\ & 0 & 0 & \rho\Omega_m^2+\rho\omega_3^2(\boldsymbol{q}) \end{array}\right)$$

The three components of the vector $U^T\boldsymbol{v}$ denote the coupling strength between the bosons and the three phonon modes.

4.2 The Reduced System

For the bare phonons we have seen that the thermodynamics in the low energy regime are dominated by the small velocity phonons. For the sake of simplicity we ignore the coupling of the boson to the other two modes. This is possible because at the the soft mode is critically enhanced in the vicinity of the transition point. The remaining component of the coupling vector $U^T\boldsymbol{v}$ can be written in the form $-i\lambda C(\boldsymbol{q})$ where $C(\boldsymbol{q})$ is a real function that only depends on the lattice constants $C_{\alpha\beta}$ and the momentum $\boldsymbol{q}$. The effective action of this reduced system then has the form

$$S_{\text{eff}}[\phi, u^\dagger, u] = \sum_{\boldsymbol{q},\Omega_m} \left(\phi(-\boldsymbol{q},\Omega_m), u^\dagger(\boldsymbol{q},\Omega_m)\right) \underbrace{\begin{pmatrix} g_\phi^{-1}(\boldsymbol{q}, i\Omega_m) & i\lambda C(\boldsymbol{q}) \\ -i\lambda C(\boldsymbol{q}) & \rho\Omega_m^2 + \rho\omega^2(\boldsymbol{q}) \end{pmatrix}}_{=:G^{-1}(\boldsymbol{q},i\Omega_m)} \begin{pmatrix} \phi(\boldsymbol{q},\Omega_m) \\ u(\boldsymbol{q},\Omega_m) \end{pmatrix}$$

The dispersion relation has been calculated in chapter two, see e.g. 2.4.3. The coupling of the mode to the boson is given by

$$i\lambda C(\boldsymbol{q}) = \boldsymbol{e}_{\text{soft}}^\dagger \boldsymbol{v}$$

where $\boldsymbol{e}_{\text{soft}}$ is the polarization direction, i.e. the eigenvector of D^{-1} for the eigenvalue $\omega^2(\boldsymbol{q})$. An perturbative approach around the $<1,1,0>$-directions, analogous to the calculation of equation 2.4.2, gives

$$C(\boldsymbol{q}) = q_\parallel + \frac{C_{66} - C_{11}}{C_{12} + C_{66}} \frac{q_\perp^2}{q}$$

$\boldsymbol{q}_\parallel$ again denotes the $<1,1,0>$ direction and $\boldsymbol{q}_\perp$ the corresponding orthogonal component in the x-y-plane such that $(\boldsymbol{q}_\parallel, \boldsymbol{q}_\perp, \boldsymbol{q}_z)$ is a right handed basis. This procedure works for all possible directions of $<1,1,0>$ and leads to the same results since they are equivalent in the tetragonal lattice.

One can see that the $\boldsymbol{q}_z$ contribution vanishes in second order. This resembles the fact that the coupling vector $\boldsymbol{v}$ does not couple to the z-component.

Our aim is to investigate the point where the coupled boson drive the lattice to a critical point. The tuning parameter is again the mass r from the boson propagator.

For the new dispersion relation we calculate the eigenvalues for $G^{-1}(\boldsymbol{q}, 0)$:

$$\omega_\pm(\boldsymbol{q}) = \frac{g_\phi^{-1} + \omega^2(\boldsymbol{q})}{2} \pm \sqrt{\frac{(g_\phi^{-1} - \omega^2(\boldsymbol{q}))^2}{4} + \lambda^2 C^2(\boldsymbol{q})}$$

In the vicinity of $\boldsymbol{q}_\parallel$ they are given by

$$\begin{aligned} &\omega_\pm^2(\boldsymbol{q}) \\ =&\frac{r_0 + E(\boldsymbol{q}) + \frac{C_{11}-C_{12}}{2\rho} q_\parallel^2 + \left(\frac{C_{11}+C_{12}}{2\rho} + \frac{C_{66}}{\rho}\right) q_\perp^2 + \frac{C_{44}}{\rho} q_z^2}{2} \\ \pm& \sqrt{\frac{\left(r_0 + E(\boldsymbol{q}) - \frac{C_{11}-C_{12}}{2\rho} q_\parallel^2 - \left(\frac{C_{11}+C_{12}}{2\rho} + \frac{C_{66}}{\rho}\right) q_\perp^2 - \frac{C_{44}}{\rho} q_z^2\right)^2}{4} + \lambda^2 \left(q_\parallel + \frac{C_{66} - C_{11}}{C_{12} + C_{66}} \frac{q_\perp^2}{q_\parallel}\right)^2} \end{aligned}$$

The lower branch $\omega_-^2(\boldsymbol{q})$ becomes soft when there is a direction $\hat{q}$ with $\omega_-^2(\hat{q}) = 0$. This is equivalent to

$$\begin{aligned} & 0 = \det G^{-1}(\boldsymbol{q}, 0) = g_\phi^{-1}(\boldsymbol{q})\omega^2(\boldsymbol{q}) - \lambda^2 C^2(\boldsymbol{q}) \\ \Leftrightarrow\ & 0 = \big(r_0 + E(\boldsymbol{q})\big)\Big(\frac{C_{11} - C_{12}}{2\rho} q_\parallel^2 + \Big(\frac{C_{11} + C_{12} + 2C_{66}}{2\rho}\Big) q_\perp^2 + \frac{C_{44}}{\rho} q_z^2\Big) - \lambda^2 \Big(q_\parallel + \frac{C_{66} - C_{11}}{C_{12} + C_{66}} \frac{q_\perp^2}{q_\parallel}\Big)^2 \end{aligned}$$

In the low energy regime where $\boldsymbol{q}$ is small, we can keep only the second order terms in q:

$$0 = \Big[r_0 \frac{C_{11} - C_{12}}{2\rho} - \lambda^2\Big] q_\parallel^2 + \Big[r_0 \big(\frac{C_{11} + C_{12} + 2C_{66}}{2\rho}\big) - 2\lambda^2 \frac{C_{66} - C_{11}}{C_{12} + C_{66}}\Big] q_\perp^2 + r_0 \frac{C_{44}}{\rho} q_z^2 - \lambda^2 \frac{C_{66} - C_{11}}{C_{12} + C_{66}} \frac{q_\perp^4}{q_\parallel^2}$$

Assuming $|q_\perp| << |q_\parallel|$ we get the conical equation

$$0 = \Big[r_0 \frac{C_{11} - C_{12}}{2\rho} - \lambda^2\Big] q_\parallel^2 + \Big[r_0 \big(\frac{C_{11} + C_{12} + 2C_{66}}{2\rho} + \big) - 2\lambda^2 \frac{C_{66} - C_{11}}{C_{12} + C_{66}}\Big] q_\perp^2 + r_0 \frac{C_{44}}{\rho} q_z^2$$

Here we see the occurence of a **soft phonon** in $\boldsymbol{q}_\parallel$-direction for

$$\boxed{r_0 = \frac{2\lambda^2 \rho}{C_{11} - C_{12}}}$$

From chapter two we know that a soft phonon is directly related to a symmetry transformation of the lattice. Hence we have found a critical value of the boson mass where the coupled electrons might lead to an instability of the lattice. An important point hereby is that we obtain the soft dispersion only for small momenta. It leads to the conclusion that the lattice transition only occurs for low energies, i.e. low temperatures. The physical reason for this would be that the quantum fluctuations of the critical Fermi liquid are suppressed at high temperatures.
With these basic impressions we will now go over to a more detailed analysis of the thermodynamics of the coupled system. For that we start with the free energy of the system.

4.2.1 Free Energy

The derivation of the free energy was done for the isotropic cubic lattice by [10]. These results are used here to calculate the free energy for the direction dependent system. Appendix B contains the detailed analysis of the sum over the Matsubara frequencies. The result is

$$F(T) - F(0) = -\sum_{\boldsymbol{q}} \Big\{\mathcal{P} \int_0^\infty \frac{dx}{\pi} 2T \Big(\ln\big[2\sinh\frac{x}{2T}\big] - \frac{x}{2T}\Big) Q(x)\Big\}$$

where $Q(x)$ is given by

$$Q(x) = -\frac{\gamma(\hat{q})}{q} \frac{R(x) + E(\boldsymbol{q})}{\big(R(x) + E(\boldsymbol{q})\big)^2 + \big(\frac{\gamma(\hat{q})}{q} x\big)^2} - A(x) \frac{\sigma(x)}{(x - \omega_R(\boldsymbol{q}))^2 + \sigma(x)^2}$$

and

$$\begin{aligned}
R(x,\boldsymbol{q}) &:= r - \frac{\lambda^2}{\rho}\frac{C^2(\boldsymbol{q})}{\omega^2(\boldsymbol{q}) - x^2} \\
A(x,\boldsymbol{q}) &:= \frac{2x\big(\omega^2(\boldsymbol{q}) - \omega_R^2\big)}{(x+\omega_R(\boldsymbol{q}))\big(\omega^2(\boldsymbol{q}) - x^2\big)} \\
\sigma(x,\boldsymbol{q}) &:= \frac{\gamma(\hat{q})}{q}\frac{x\big(\omega^2(\boldsymbol{q}) - x^2\big)}{(x+\omega_R(\boldsymbol{q}))(r+E(\boldsymbol{q}))}
\end{aligned}$$

So we have a free energy consisting of two Lorentz peaks. In the limit $\lambda \to 0$, i.e. when the coupling between the bosons and phonons is absent, the first term simplifies to

$$-\frac{\gamma(\hat{q})}{q}\frac{r+E(\boldsymbol{q})}{\big(r+E(\boldsymbol{q})\big)^2 + \big(\frac{\gamma(\hat{q})}{q}x\big)^2}$$

This is exactly the integrand for the free energy 3.4.2 of the Fermi liquid. So we can identify the first term as the contribution from the Fermi liquid with renormalized parameters.
To recover the phononic free energy in the second term in the limit $\lambda \to 0$ we first rewrite it as

$$\frac{2x^2\frac{\lambda^2}{\rho}C^2(\boldsymbol{q})}{\big(x^2 - \omega_R^2(\boldsymbol{q})\big)^2\big(r+E(\boldsymbol{q})\big)^2 + \big(x\frac{\gamma(\hat{q})}{q}\big)^2\big(\omega^2(\boldsymbol{q}) - x^2\big)^2}$$

We see that this term vanishes in the limit $\lambda \to 0$ for $x \neq \omega(\boldsymbol{q})$. For $x = \omega(\boldsymbol{q})$ the relation $\lim_{\lambda\to 0}\omega_R(\boldsymbol{q}) = \omega(\boldsymbol{q})$ leads to a divergent term. Hence we have a delta peak at the old phonon dispersion. So this term yields the phononic free energy that we have calculated in chapter two.
Another important point in the derivation of the free energy was the appearance of a renormalized dispersion relation

$$\omega_R(\boldsymbol{q}) = \sqrt{\omega^2(\boldsymbol{q}) - \lambda^2\frac{C^2(\boldsymbol{q})}{r_0 + E(\boldsymbol{q})}}$$

Two important limits of the dispersion are

$$\omega_R^2(\boldsymbol{q}) = \begin{cases} \omega^2(\boldsymbol{q}) - \dfrac{\lambda^2}{\rho r}C^2(\boldsymbol{q}) \text{ for } q \ll \sqrt{r} \\ \omega^2(\boldsymbol{q}) - \dfrac{\lambda^2}{\rho}\dfrac{C^2(\boldsymbol{q})}{E(\boldsymbol{q})} \text{ for } q \gg \sqrt{r} \end{cases}$$

So for small momenta we have a dispersion with a new velocity. Especially interesting for us is the $\boldsymbol{q}_{||}$ direction. When we set

$$r \to r_0 = \frac{2\lambda^2\rho}{C_{11} - C_{12}}$$

we get $\omega_R(\boldsymbol{q}_{||}) = 0$. Hence we have dispersion which becomes soft for this value of r. Just as before we then have to take higher order terms into account which come from the expansion of the correction term and from the phonon dispersion itself. In the vicinity of the soft direction the renormalized dispersion has the form

$$\omega_R^2(\boldsymbol{q}) = \frac{C_{11}+C_{12}+2C_{66}}{2\rho} q_\perp^2 + \frac{C_{44}}{\rho} q_z^2 + \Big(v_\parallel^{(4)} + A^2 \frac{\lambda^2}{r_0^2}\Big) q_\parallel^4$$

4.2.2 Specific Heat

With the free energy of the previous section we can now calculate the specific heat of the coupled system via

$$C = -T \frac{\partial^2 F}{\partial T^2}$$

The second derivative of the free energy w.r.t. T is

$$\frac{\partial^2 F}{\partial T^2} = \sum_{\boldsymbol{q}} \left\{ \int_0^\infty \frac{dx}{\pi} \left(\frac{x^2}{2T^3} \sinh^{-2}\left(\frac{x}{2T}\right)\right) Q(x) \right\}$$

Because of the decomposition of the free energy into the electronic and the phononic contributions we are now in the comfortable situation that we can consider the thermodynamics of the two constituents serperately.

4.2.2.1 Electronic Specific Heat

The electronic term of the specific heat can be simplified by the substitution $\omega = \frac{x}{2T}$ to

$$\begin{aligned} &C_{\mathrm{el}}(T) \\ =&\frac{T}{(2\pi)^3} \int_{q\le\Lambda} d^3q \int_0^\infty \frac{d\omega}{\pi} \frac{4\omega^2}{\sinh^2\omega} \frac{\gamma(\hat{q})}{q} \frac{R(2T\omega)+E(\boldsymbol{q})}{\big(R(2T\omega)+E(\boldsymbol{q})\big)^2 + \big(\frac{\gamma(\hat{q})}{q}2T\omega\big)^2} \\ =&\frac{T}{(2\pi)^3} \int_{q\le\Lambda} d^3q \int_0^\infty \frac{d\omega}{\pi} \frac{4\omega^2}{\sinh^2\omega} \frac{\gamma(\hat{q})}{q} \frac{r_0 - \lambda^2 \frac{C^2(\boldsymbol{q})}{\omega^2(\boldsymbol{q})-4T^2\omega^2} + E(\boldsymbol{q})}{\Big(r_0 - \lambda^2 \frac{C^2(\boldsymbol{q})}{\omega^2(\boldsymbol{q})-4T^2\omega^2} + E(\boldsymbol{q})\Big)^2 + \big(\frac{\gamma(\hat{q})}{q}2T\omega\big)^2} \end{aligned}$$

Now we do the substitution $\boldsymbol{q} \to (2T)^{1/3}\boldsymbol{q}$ as we have done for the specific heat of the uncoupled bosons and get

$$\begin{aligned} &C_{\mathrm{el}}(T) \\ &= \frac{T}{(2\pi)^3} \int_{q\le\frac{\Lambda}{(2T)^{1/3}}} d^3q \int_0^\infty \frac{d\omega}{\pi} \frac{4\omega^2}{\sinh^2\omega} \frac{\gamma(\hat{q})}{qE(\boldsymbol{q})} \frac{1 + \frac{1}{(2T)^{2/3}E(\boldsymbol{q})}\Big(r_0 - \lambda^2 \frac{C^2(\boldsymbol{q})}{\omega^2(\boldsymbol{q})-(2T)^{4/3}\omega^2}\Big)}{\Big[1 + \frac{1}{(2T)^{2/3}E(\boldsymbol{q})}\Big(r_0 - \lambda^2 \frac{C^2(\boldsymbol{q})}{\omega^2(\boldsymbol{q})-(2T)^{4/3}\omega^2}\Big)\Big]^2 + \Big[\frac{\omega\gamma(\hat{q})}{qE(\boldsymbol{q})}\Big]^2} \end{aligned} \tag{4.2.1}$$

The central quantity here is

$$r(\boldsymbol{q},\omega) := 1 + \frac{1}{(2T)^{2/3}E(\boldsymbol{q})}\Big(r_0 - \lambda^2 \frac{C^2(\boldsymbol{q})}{\omega^2(\boldsymbol{q})-(2T)^{4/3}\omega^2}\Big) \tag{4.2.2}$$

It can be considered seperately in the three cases

1. $\omega^2(2T)^{4/3} \approx \omega^2(\boldsymbol{q})$
2. $\omega^2(2T)^{4/3} \gg \omega^2(\boldsymbol{q})$
3. $\omega^2(2T)^{4/3} \ll \omega^2(\boldsymbol{q})$

- In the first case $r(\boldsymbol{q},\omega)$ diverges. This leads to a vanishing integrand of the specific heat. Hence this case is irrelevant.
- The second case becomes important when we are in the high temperature regime. The values of ω are restricted to be of the order of 1, because other values are exponentially suppressed. Furthermore we can conclude

  $$r_0 \gg \lambda^2 \frac{C(\boldsymbol{q})}{(2T)^{4/3}\omega^2}$$

  So the contribution of the fraction in the bracket of eq. 4.2.2 to the mass r_0 becomes negligible and we are left with

  $$r(\boldsymbol{q},\omega) = 1 + \frac{r_0}{(2T)^{2/3}E(\boldsymbol{q})}$$

  Inserting this result into the integrand we recover the form of the specific heat we already know from the uncoupled Fermi liquid. This leads us to the conclusion that in the **higher temperature limit we recover the uncoupled system**.
- The third case is important for the low temperature regime. There we can perform the Taylor expansion

  $$\frac{1}{\omega^2(\boldsymbol{q}) - (2T)^{4/3}\omega^2} = \frac{1}{\omega^2(\boldsymbol{q})}\left[1 + \mathcal{O}\left(\left[(2T)^{2/3}\frac{\omega}{\omega(\boldsymbol{q})}\right]^2\right)\right]$$

  So in this approximation we have $r(\boldsymbol{q},\omega) = 1 + \frac{r_0(\hat{q})}{(2T)^{2/3}E(\boldsymbol{q})}$ where

  $$r_0(\hat{q}) := r_0 - \lambda^2 \frac{C^2(\boldsymbol{q})}{\omega^2(\boldsymbol{q})}$$

  is now a function which **only depends on the direction** $\hat{q}$ of $\boldsymbol{q}$. It can be viewed as a direction dependent mass of the bosons. We see

  $$r(\boldsymbol{q},\omega) = \begin{cases} 1 & \text{for } q^2 \gg \dfrac{r_0(\hat{q})}{(2T)^{2/3}e(\hat{q})} \\ \dfrac{r_0(\hat{q})}{(2T)^{2/3}E(\boldsymbol{q})} & \text{for } q^2 \ll \dfrac{r_0(\hat{q})}{(2T)^{2/3}e(\hat{q})} \end{cases}$$

  So the factor $\frac{r_0(\hat{q})}{(2T)^{2/3}e(\hat{q})}$ plays here the role of a parameter that decides which part of $r(\boldsymbol{q},\omega)$ is important.

We have seen that only the third case is relevant for the temperature regime where the coupling can have an effect on the thermodynamics. In the following we will consider this case in more detail. We do this by splitting the momentum integral into the regimes $q \geq \frac{\sqrt{r_0(\hat{q})/e(\hat{q})}}{(2T)^{1/3}}$ and $q \leq \frac{\sqrt{r_0(\hat{q})/e(\hat{q})}}{(2T)^{1/3}}$.

- **First case:** $q \geq \frac{\sqrt{r_0(\hat{q})/e(\hat{q})}}{(2T)^{1/3}}$
  Here we have $r(\boldsymbol{q}, \omega) \approx 1$ and get the following contribution to the specific heat

$$\frac{1}{(2\pi)^4} \int d\Omega \int_0^\infty d\omega \frac{8\omega^2}{\sinh^2 \omega} \int_{\frac{\sqrt{r_0(\hat{q})/e(\hat{q})}}{(2T)^{1/3}}}^{\frac{\Lambda}{(2T)^{1/3}}} dq\, q^2 \frac{\frac{\gamma(\hat{q})}{qE(\boldsymbol{q})}}{1 + \frac{\gamma^2(\hat{q})\omega^2}{q^2 E^2(\boldsymbol{q})}}$$

  Now we use the notation $E(\boldsymbol{q}) = q^2 e(\hat{q})$ to integrate over q. This leads to

$$\begin{aligned}
&\frac{1}{(2\pi)^4} \int d\Omega \int_0^\infty d\omega \frac{8\omega^2}{\sinh^2 \omega} \int_{\frac{\sqrt{r_0(\hat{q})/e(\hat{q})}}{(2T)^{1/3}}}^{\frac{\Lambda}{(2T)^{1/3}}} dq \, \frac{q^5 \frac{\gamma(\hat{q})}{e(\hat{q})}}{q^6 + \frac{\gamma^2(\hat{q})\omega^2}{e^2(\hat{q})}} \\
=&\frac{1}{(2\pi)^4} \int d\Omega \int_0^{\omega_*(\hat{q},T)} d\omega \frac{8\omega^2}{\sinh^2 \omega} \frac{\gamma(\hat{q})}{6e(\hat{q})} \log\left(\frac{\Lambda^6 e^3(\hat{q})}{r_0^3(\hat{q})}\right) \\
&+ \frac{1}{(2\pi)^4} \int d\Omega \int_{\omega_*(\hat{q},T)}^\infty d\omega \frac{8\omega^2}{\sinh^2 \omega} \frac{\gamma(\hat{q})}{6e(\hat{q})} \log\left(\frac{\Lambda^6}{4T^2\omega^2 \frac{\gamma^2(\hat{q})}{e^2(\hat{q})}}\right)
\end{aligned}$$

  with $\omega_*(\boldsymbol{q}, T) = \left(\frac{r_0(\hat{q})}{e(\hat{q})}\right)^{3/2} \frac{e(\hat{q})}{\gamma(\hat{q})} \frac{1}{2T}$.
  In the limit $T \to 0$ we have $\omega_*(\boldsymbol{q}, T) \to \infty$ and we are approximately left with the term

$$\gamma := \frac{1}{(2\pi)^4} \int d\Omega \int_0^\infty d\omega \frac{8\omega^2}{\sinh^2 \omega} \frac{\gamma(\hat{q})}{3e(\hat{q})} \log\left(\frac{\Lambda^3 e^{3/2}(\hat{q})}{r_0^{3/2}(\hat{q})}\right)$$

  which is constant w.r.t. T.
  For large T w.r.t. r_0 we can replace $\omega_*(\boldsymbol{q}, T)$ by 0. Then only the second term survives:

$$\begin{aligned}
&\frac{1}{(2\pi)^4} \int d\Omega \int_0^\infty d\omega \frac{8\omega^2}{\sinh^2 \omega} \frac{\gamma(\hat{q})}{3e(\hat{q})} \log\left(\frac{\Lambda^3}{4T\omega \frac{\gamma(\hat{q})}{e(\hat{q})}}\right) \\
=&\underbrace{\frac{1}{(2\pi)^4} \int d\Omega \int_0^\infty d\omega \frac{8\omega^2}{\sinh^2 \omega} \frac{\gamma(\hat{q})}{3e(\hat{q})} \log\left(\frac{e(\hat{q})}{4\omega\gamma(\hat{q})}\right)}_{=:\nu} \\
&- \underbrace{\frac{1}{(2\pi)^4} \int d\Omega \int_0^\infty d\omega \frac{8\omega}{\sinh^2 \omega} \frac{\gamma(\hat{q})}{3e(\hat{q})}}_{=:\delta} \log \frac{T}{\Lambda^3}
\end{aligned}$$

With $\int_0^\infty d\omega \frac{8\omega^2}{\sinh^2\omega} = \frac{4\pi^2}{3}$, $\Gamma := \int_0^\infty d\omega \frac{8\omega^2}{\sinh^2\omega}\log(4\omega) \approx 13.7644$ and the abbreviation

$$\langle f(\hat q)\rangle_{\gamma/e} := \int d\Omega \frac{\gamma(\hat q)}{e(\hat q)} f(\hat q)$$

we can simplify these terms to

$$\begin{aligned}
\gamma &= \frac{1}{9(2\pi)^2}\left\langle \log \frac{\Lambda^3 e^{3/2}(\hat q)}{r_0^{3/2}(\hat q)} \right\rangle_{\gamma/e} \\
\nu &= -\frac{\Gamma}{3(2\pi)^4}\langle 1\rangle_{\gamma/e} - \frac{1}{9(2\pi)^2}\left\langle \log \frac{\gamma(\hat q)}{e(\hat q)} \right\rangle_{\gamma/e} \\
\delta &= \frac{1}{9(2\pi)^2}\langle 1\rangle_{\gamma/e}
\end{aligned}$$

An important feature of these quantities is that they only depend on the fractions $\frac{\gamma(\hat q)}{e(\hat q)}$ and $\frac{r_0(\hat q)}{e(\hat q)}$ and the momentum cutoff Λ. Hence they do not the depend on the absolute value of the boson propagator. Informations about the phonons are only contained in $r_0(\hat q)$.

- **Second case:** $q \leq \frac{\sqrt{r_0(\hat q)}}{(2T)^{1/3}}$ In the momentum regime we are considering now we have $r(\boldsymbol{q},\omega) = \frac{r_0(\hat q)}{(2T)^{2/3}E(\boldsymbol{q})}$. The resulting contribution to C_{el}/T is

  $$\begin{aligned}
  &\frac{1}{(2\pi)^4}\int d\Omega \int_0^\infty d\omega \frac{8\omega^2}{\sinh^2\omega}\int_0^{\frac{\sqrt{r_0(\hat q)/e(\hat q)}}{(2T)^{1/3}}} dq\, q^2 \frac{\frac{r_0(\hat q)\gamma(\hat q)}{(2T)^{2/3}qE^2(\boldsymbol{q})}}{\frac{r_0^2(\hat q)}{(2T)^{4/3}E^2(\boldsymbol{q})} + \frac{\gamma^2(\hat q)\omega^2}{q^2E^2(\boldsymbol{q})}} \\
  =&\frac{1}{(2\pi)^4}\int d\Omega \int_0^\infty d\omega \frac{8\omega^2}{\sinh^2\omega}\left(\frac{\gamma(\hat q)}{2e(\hat q)} + \frac{\gamma^3(\hat q)}{r_0^3(\hat q)}2\omega^2T^2\log\left[\frac{4\omega^2T^2}{\frac{r_0^3(\hat q)}{e(\hat q)\gamma^2(\hat q)} + 4T^2\omega^2}\right]\right)
  \end{aligned}$$

  The second term is proportional to T^2. Hence this is a subleading term in the temperature regimes we are interested in. The other term resembles a constant contribution to C_{el}/T. The term

  $$\frac{1}{(2\pi)^4}\int d\Omega \int_0^\infty d\omega \frac{8\omega^2}{\sinh^2\omega}\frac{\gamma(\hat q)}{2e(\hat q)} = \frac{1}{6(2\pi)^2}\langle 1\rangle_{\gamma/e}$$

  leads to a T-independent contribution to the specific heat coefficient C_{el}/T. This constant term just shifts the specific heat. So finally we can conclude that this momentum regime doesn't modify the properties of the crossover as long as the crossover temperature is small, i.e. $T_{\text{c,el}} \ll 1$.

The specific heat resulting from these contribution has the following T-dependence

$$\frac{C_{\text{el}}}{T} = \begin{cases} \gamma & \text{for } T \ll T_{\text{c,el}} \\ \nu - \delta\log\frac{T}{\Lambda^3} & \text{for } T \gg T_{\text{c,el}} \end{cases}$$

The value of the crossover temperature $T_{\text{c,el}}$ can be calculated by the equation

$$\gamma = \nu - \delta \log \frac{T_{\text{c,el}}}{\Lambda^3}$$

Solving this for $T_{\text{c,el}}$ leads to

$$\boxed{T_{\text{c,el}} = \underbrace{\exp\big(-\frac{3\Gamma}{4\pi^2}\big)}_{\approx 0.351351} \exp\left(\frac{\Big\langle \log\big(\frac{r_0^{3/2}(\hat{q})}{\gamma(\hat{q})\sqrt{e(\hat{q})}}\big)\Big\rangle_{\gamma/e}}{\langle 1\rangle_{\gamma/e}}\right)}$$

4.2.2.2 Phononic Specific Heat

The **phonon part** of the specific heat is

$$C_{\text{ph}}(T) = \frac{2}{(2\pi)^3}\int_{q\le\Lambda} d^3q \int_0^\infty \frac{dx}{\pi}\frac{x^2/(2T)^2}{\sinh^2\big(x/(2T)\big)} A(x,\boldsymbol{q}) \frac{\sigma(x,\boldsymbol{q})}{(x-\omega_R(\boldsymbol{q}))^2+\sigma^2(x,\boldsymbol{q})}$$

We start again with the substitution $x = 2T\omega$ and get

$$C_{\text{ph}}(T) = \frac{2}{(2\pi)^3}\int_{q\le\Lambda} d^3q \int_0^\infty \frac{d\omega}{\pi}2T\frac{\omega^2}{\sinh^2\omega} A(2T\omega,\boldsymbol{q}) \frac{\sigma(2T\omega,\boldsymbol{q})}{(2T\omega-\omega_R(\boldsymbol{q}))^2+\sigma^2(2T\omega,\boldsymbol{q})}$$

Secondly we substitute $\boldsymbol{q} \to 2T\boldsymbol{q}$ and get

$$C_{\text{ph}}(T) = \frac{2}{(2\pi)^3}(2T)^4\int_{q\le\frac{\Lambda}{2T}} d^3q \int_0^\infty \frac{d\omega}{\pi}\frac{\omega^2}{\sinh^2\omega} A(2T\omega,2T\boldsymbol{q}) \frac{\sigma(2T\omega,2T\boldsymbol{q})}{(2T\omega-\omega_R(2T\boldsymbol{q}))^2+\sigma^2(2T\omega,2T\boldsymbol{q})}$$

The width and the weight of the Lorentz peak are given by

$$\sigma(2T\omega,2T\boldsymbol{q}) = 2T\frac{\gamma(\hat{q})}{q}\frac{\omega(\omega^2(\boldsymbol{q})-\omega^2)}{(\omega+\frac{\omega_R(2T\boldsymbol{q})}{2T})\big(r_0+(2T)^2E(\boldsymbol{q})\big)}$$

$$A(2T\omega,2T\boldsymbol{q}) = \frac{2\omega\Big(\omega^2(\boldsymbol{q})-\big(\frac{\omega_R(2T\boldsymbol{q})}{2T}\big)^2\Big)}{(\omega+\frac{\omega_R(2T\boldsymbol{q})}{2T})\big(\omega^2(\boldsymbol{q})-\omega^2\big)}$$

The new dispersion relation is then given by

$$\omega_R(2T\boldsymbol{q}) = 2T\sqrt{\omega^2(\boldsymbol{q})-\lambda^2\underbrace{\frac{C^2(\boldsymbol{q})}{r_0+(2T)^2E(\boldsymbol{q})}}_{=:d}}$$

We see that the central part which determines the behaviour of the new dispersion w.r.t. T is the rescaled energy of the electrons

$$R := r_0 + (2T)^2E(\boldsymbol{q})$$

Inserting this into the integral leads to

$$C_{\mathrm{ph}}(T) = \frac{2(2T)^3}{(2\pi)^3} \int_{q \leq \frac{\Lambda}{2T}} d^3q \int_0^\infty \frac{d\omega}{\pi} \frac{\omega^2}{\sinh^2 \omega} \frac{2dR\omega\gamma(\hat{q})\frac{\omega}{q}}{R^2\big(\omega^2 - \frac{\omega_R^2(2T\boldsymbol{q})}{(2T)^2}\big)^2 + \big(\gamma(\hat{q})\frac{\omega}{q}\big)^2\big(\omega^2 - \omega(\boldsymbol{q})^2\big)^2} \tag{4.2.3}$$

The numerical analysis of the integrand shows that the fraction obtains a sharp peak as a function of ω for almost all values of $\boldsymbol{q}$ and T. Only for very small momenta and small temperatures the peak becomes thicker. This behaviour can be seen analytically by considering the denominator. In the following we will consider the specific heat 4.2.3 in the cases $T \gg r_0$ and $T \to 0$.

In the limit $T \gg r_0$ we have

$$R = r_0 + (2T)^2 E(\boldsymbol{q}) \approx (2T)^2 E(\boldsymbol{q})$$

The difference between the new and the old dispersion is then given by

$$d = \frac{\lambda^2 C^2(\boldsymbol{q})}{R} \approx \frac{\lambda^2 C^2(\boldsymbol{q})}{(2T)^2 E(\boldsymbol{q})} = \frac{\lambda^2}{(2T)^2} \frac{c(\hat{q})}{e(\hat{q})}$$

We see that d becomes very small since $\lambda \ll 1$ and $T \gg 1$. This means that we can consider the integrand in the limit $d \to 0$. Furthermore we can assume

$$R \gg \gamma(\hat{q})\frac{\omega}{q}$$

although this is not true for $q \to 0$. The reason for that is that the prefactor $\frac{\omega^2}{\sinh^2 \omega}$ suppresses all contributions from $\omega \ll 1$ or $\omega \gg 1$. Thus the integrand vanishes in the limit $\boldsymbol{q} \to 0$.

Now we can rewrite the denominator as

$$\begin{aligned} &R^2\Big(\omega^2 - \frac{\omega_R^2(2T\boldsymbol{q})}{(2T)^2}\Big)^2 + \Big(\gamma(\hat{q})\frac{\omega}{q}\Big)^2\Big(\omega^2 - \frac{\omega_R^2(2T\boldsymbol{q})}{(2T)^2} + d\Big)^2 \\ \approx &\Big(R^2 + \Big(\gamma(\hat{q})\frac{\omega}{q}\Big)^2\Big)\Big(\omega^2 - \frac{\omega_R^2(2T\boldsymbol{q})}{(2T)^2}\Big)^2 + \Big(\gamma(\hat{q})\frac{\omega}{q}\Big)^2 d^2 \end{aligned}$$

Inserting this into the integrand gives us the Lorentz peak

$$\frac{\omega^2}{\sinh^2 \omega} 2R\omega \frac{\gamma(\hat{q})\frac{\omega}{q}d}{\Big(R^2 + \big(\gamma(\hat{q})\frac{\omega}{q}\big)^2\Big)\big(\omega^2 - \frac{\omega_R^2(2T\boldsymbol{q})}{(2T)^2}\big)^2 + \big(\gamma(\hat{q})\frac{\omega}{q}\big)^2 d^2}$$

In the large T limit we have $d \to 0$ and $R \gg \gamma(\hat{q})\frac{\omega}{q}$. The Lorentz peak then becomes a delta peak and we can easily do the ω-integration. The prefactor $2R\omega$ thereby cancels with the factor from the inverse of the derivative of the argument in the delta function.

Finally we recover the ordinary specific heat

$$C_{\mathrm{ph}}(T) = \frac{\pi T^3}{15} \int d\Omega \frac{1}{v^3(\hat{q})}$$

With

$$\left.\frac{\omega_R^2(2T\boldsymbol{q})}{(2T)^2}\right|_{d\to 0} = \omega^2(\boldsymbol{q}) = v_\perp^2 q_\perp^2 + v_\parallel^2 q_\parallel^2 + v_z^2 q_z^2$$

we can write this as

$$\begin{aligned} C_{\text{ph}}(T) =& \frac{2T^3}{\pi^3}\int d^3q \frac{v_\perp^2 q_\perp^2 + v_\parallel^2 q_\parallel^2 + v_z^2 q_z^2}{\sinh^2\sqrt{v_\perp^2 q_\perp^2 + v_\parallel^2 q_\parallel^2 + v_z^2 q_z^2}} \\ =& \frac{2T^3}{\pi^3}\frac{1}{v_\perp v_\parallel v_z}\underbrace{\int d^3q \frac{q_\perp^2 + q_\parallel^2 + q_z^2}{\sinh^2\sqrt{q_\perp^2 + q_\parallel^2 + q_z^2}}}_{=\frac{2\pi^5}{15}} \\ =& T^3\frac{4\pi^2}{15 v_\perp v_\parallel v_z} \end{aligned}$$

This is exactly the same specifc heat as we got by considering an uncoupled phonon mode. The dispersion relation was here proportional to q for all directions.

Now we come to the limit $T \to 0$ where $r_0 + (2T)^2 E(\boldsymbol{q}) \approx r_0$.
Again we consider the equation 4.2.3. Here the lowest order approximation for the dispersion is

$$\frac{\omega_R^2(2T\boldsymbol{q})}{4T^2} = \omega^2(\boldsymbol{q}) - \lambda^2\frac{C^2(\boldsymbol{q})}{r_0}$$

By the choice of r_0 the term in $\omega_R^2(\boldsymbol{q})$ which is proportional to $q_\parallel^2$ vanishes. Thus the new dispersion becomes soft in this direction. Here we expect a modification of the ordinary $C_{\text{ph}} \propto T^3$ law for the specific heat. To describe the dispersion in this direction we now have to take terms proportional to $q_\parallel^4$ into account. The dispersion then looks like

$$\frac{\omega_R^2(2T\boldsymbol{q})}{4T^2} = v_\perp^2 q_\perp^2 + v_z^2 q_z^2 + (2T)^2\Big(\frac{\lambda^2 A^2}{r_0^2} + v_{\parallel,4}^4\Big) q_\parallel^4 + \mathcal{O}(T^3)$$

The A comes form the kinetic energy $E(\boldsymbol{q}) = A^2\big(q_\parallel^2 + q_\perp^2\big) + B^2 q_z^2$ of the electrons. With the relation $r_0 = \frac{\lambda^2}{v_\parallel^2}$ we can write this as

$$\omega_R^2(\boldsymbol{q}) = v_\perp^2 q_\perp^2 + v_z^2 q_z^2 + (2T)^2\Big(\frac{v_\parallel^2 A^2}{r_0} + v_{\parallel,4}^4\Big) q_\parallel^4 + \mathcal{O}(T^3)$$

We see that now the dispersion relation which is soft in the $\boldsymbol{q}_\parallel$ direction is contained in the denominator. The problem is that we cannot assume $\frac{\gamma(\hat{q})}{r_0} \ll 1$ here in general. This would only be satisfied when $\boldsymbol{q}$ is almost directed into $\hat{q}_\parallel$-direction where $\gamma(\hat{q})$ vanishes.
So we start with the substitution $q_\parallel \to \frac{q_\parallel}{\sqrt{2T}}$ to get the renormalized dispersion T-independent:

$$\omega_R^2(\boldsymbol{q}) \to v_\perp^2 q_\perp^2 + v_z^2 q_z^2 + \Big(\frac{v_\parallel^2 A^2}{r_0} + v_{\parallel,4}^4\Big) q_\parallel^4 + \mathcal{O}(T)$$

This leads to

$$
\begin{aligned}
C_{\mathrm{ph}}(T) =& \frac{2(2T)^{2.5}}{(2\pi)^3} \int d^3q \int_0^\infty \frac{d\omega}{\pi} \frac{\omega^2}{\sinh^2 \omega} \times \\
& \times \frac{2\omega \frac{\gamma(\frac{q_\parallel}{\sqrt{2T}}, q_\perp, q_z)}{r_0} \frac{\omega}{\tilde{q}} d}{\left(\omega^2 - \omega_R^2(\boldsymbol{q})\right)^2 + \left(\frac{\gamma(\frac{q_\parallel}{\sqrt{2T}}, q_\perp, q_z)}{r_0} \frac{\omega}{\tilde{q}}\right)^2 \left(\omega^2 - (v_\parallel^2 \frac{q_\parallel^2}{2T} + v_\perp^2 q_\perp^2 + v_z^2 q_z^2)\right)^2}
\end{aligned}
$$

where $\tilde{q} = \sqrt{\frac{1}{2T} q_\parallel^2 + q_\perp^2 + q_z^2}$. The central point here is now that for $q_\parallel \neq 0$ we have

$$
\lim_{T \to 0} \frac{\gamma(\frac{q_\parallel}{\sqrt{2T}}, q_\perp, q_z)}{r_0} \tilde{q} = 0
$$

This means that the **Landau damping vanishes asymptotically for** $T \to 0$. It implies that in the low temperature regime we have a sharp Lorentz peak. The set of momenta where $\frac{q_\parallel}{\sqrt{2T}}$ is small compared to $q_\perp$ and q_z can be ignored in the low temperature limit. The fraction $\frac{\omega}{\tilde{q}}$ can be assumed to be of the order of 1.

Altogether we are again in the situation that we get a very sharp peak at $\omega = \omega_R(\boldsymbol{q})$. The calculations can now be done completely analogous to the peak in the high T case. The result is

$$
C_{\mathrm{ph}}(T) = \frac{\sqrt{2} T^{2.5}}{\pi^3} \int d^3q \frac{\omega_R^2(\boldsymbol{q})}{\sinh^2 \omega_R(\boldsymbol{q})}
$$

Inserting the form of the dispersion relations leads to

$$
\begin{aligned}
C_{\mathrm{ph}}(T) =& \frac{\sqrt{2} T^{2.5}}{\pi^3} \int dq_\perp dq_\parallel dq_z \frac{v_\perp^2 q_\perp^2 + v_z^2 q_z^2 + \left(\frac{v_\parallel^2 A^2}{r_0} + v_{\parallel,4}^4\right) q_\parallel^4}{\sinh^2 \sqrt{v_\perp^2 q_\perp^2 + v_z^2 q_z^2 + \left(\frac{v_\parallel^2 A^2}{r_0} + v_{\parallel,4}^4\right) q_\parallel^4}} \\
=& \frac{\sqrt{2} T^{2.5}}{\pi^3} \frac{4\pi}{v_\perp v_z \left(\frac{v_\parallel^2 A^2}{r_0} + v_{\parallel,4}^4\right)^{1/4}} \int ds dk_\parallel \frac{s}{\sqrt{k_\parallel}} \frac{k_\parallel^2 + s^2}{\sinh^2 \sqrt{k_\parallel^2 + s^2}} \\
=& \frac{\sqrt{2} T^{2.5}}{\pi^3} \frac{8\pi}{v_\perp v_z \left(\frac{v_\parallel^2 A^2}{r_0} + v_{\parallel,4}^4\right)^{1/4}} \int dr \int_0^{\pi/2} d\phi \frac{r \sin\phi}{\sqrt{r \cos\phi}} \frac{r^2}{\sinh^2 r} \\
=& \frac{\sqrt{2} T^{2.5}}{\pi^3} \frac{8\pi}{v_\perp v_z \left(\frac{v_\parallel^2 A^2}{r_0} + v_{\parallel,4}^4\right)^{1/4}} \underbrace{\int_0^{\pi/2} d\phi \frac{\sin\phi}{\sqrt{\cos\phi}}}_{=2} \underbrace{\int_0^\infty dr \frac{r^{7/2}}{\sinh^2 r}}_{= \frac{7/2}{2^{7/2}} 2\Gamma\left(\frac{7}{2}\right) \zeta\left(\frac{7}{2}\right)} \\
=& \underbrace{\frac{\Gamma\left(\frac{7}{2}\right) \zeta\left(\frac{7}{2}\right)}{\pi^2} \frac{7}{2}}_{\approx 1.3279} \frac{1}{v_\perp v_z \left(\frac{v_\parallel^2 A^2}{r_0} + v_{\parallel,4}^4\right)^{1/4}} T^{2.5}
\end{aligned}
$$

Since the critical mass r_0 is very small, the value of $v_{\parallel,4}^4$ is vanishingly small compared to $\frac{v_\parallel^2 A}{r_0}$. We finally end up with the low temperature limit

$$C_{\mathrm{ph}}(T) = \frac{\Gamma\left(7\right)\zeta\left(\frac{7}{2}\right)}{\pi^2}\frac{7}{2}\frac{r_0^{1/4}}{v_\perp v_z\sqrt{v_\parallel A}}T^{2.5}$$

Our **result for the phononic part of the specific heat** is thus

$$C_{\mathrm{ph}}(T) = \begin{cases} \alpha T^{2.5} \text{ for } T \leq T_{\mathrm{c,ph}} \\ \beta T^3 \text{ for } T \geq T_{\mathrm{c,ph}} \end{cases}$$

where

$$\alpha = \frac{\Gamma\left(\frac{7}{2}\right)\zeta\left(\frac{7}{2}\right)}{\pi^2}\frac{7}{2}\frac{r_0^{1/4}}{v_\perp v_z\sqrt{v_\parallel A^2}}, \quad \beta = \frac{4\pi^2}{15 v_\perp v_\parallel v_z}$$

It remains now to calculate a characteristic crossover temperature $T_{\mathrm{c,ph}}$ between the T^3 proportionality of the specific heat in the high temperature regime and the $T^{2.5}$ proportionality in the low temperature regime.
This can be done via the equation

$$\alpha T_{\mathrm{c,ph}}^{2.5} = \beta T_{\mathrm{c,ph}}^3 \quad \Rightarrow \quad \boxed{T_{\mathrm{c,ph}} = \Big(\frac{\alpha}{\beta}\Big)^2 = \Big(\frac{105}{8\pi^4}\Gamma\big(\frac{7}{2}\big)\zeta\big(\frac{7}{2}\big)\Big)^2 v_\parallel \frac{\sqrt{r_0}}{A}}$$

Just as before we get a crossover whose properties only depend on the ratio $\frac{r_0}{A^2}$ and not on the absolute value of the boson propagator. Furthermore we can identify the critical exponents $z = 1$ and $\nu = 1/2$.

4.2.3 Summary

We have seen that the coupling leads to a critical system when the electron mass is given by $r_0 = \frac{2\lambda^2\rho}{C_{11}-C_{12}}$. The resulting specific heat could be split into an electronic part and a phononic part. We were able to recover the logarithmic dropoff of the electronic specific heat for large temperatures. For zero temperature we observed a saturation and recovered the Fermi liquid behaviour. The crossover-temperature $T_{\mathrm{c,el}}$ between these two temperature-dependencies is given by

$$T_{\mathrm{c,el}} = \exp\big(-\frac{3\Gamma}{4\pi^2}\big)\exp\left(\frac{\left\langle \log\frac{r_0^{3/2}(\hat{q})}{\gamma(\hat{q})\sqrt{e(\hat{q})}}\right\rangle_{\gamma/e}}{\langle 1\rangle_{\gamma/e}}\right)$$

The direction-dependence of the new effective boson mass $r_0(\hat{q}) = r_0 - \frac{\lambda^2 C(\boldsymbol{q})^2}{\omega^2(\boldsymbol{q})}$ was a consequence of the coupling of the direction-dependent phonons. Without this dependency we could immediately recover the critical exponents of the uncoupled electrons

$$T_{\mathrm{c}} \propto r_0^{\nu z} \text{ with } \nu = \frac{1}{2},\ z = 3$$

The phononic specific heat obtained the ordinary T^3 proportionality for high temperatures. For low temperatures it was proportional to $T^{2.5}$. This resembles the fact that the renormalized phonon dispersion becomes soft in the $\boldsymbol{q}_{\|}$-direction for low temperatures. A very important fact for the occurence of the $T^{2.5}$ part was that the Landau damping of the electrons vanishes in exactly the same directions as where the phonon mode becomes soft. Otherwise this part would be smeared out.
The crossover-temperature is given by

$$T_{\mathrm{c,ph}} = \left(\frac{105}{8\pi^4}\Gamma\left(\frac{7}{2}\right)\zeta\left(\frac{7}{2}\right)\right)^2 v_{\|}\frac{\sqrt{r_0}}{A}$$

Here we observed the relation

$$T_{\mathrm{c,ph}} \propto r_0^{z\nu}$$

where $\nu = 1/2$ and $z = 1$ are the critical exponents from the bare phonons.
The T-dependence of the complete specific heat of the coupled system can be summarized in the following diagram

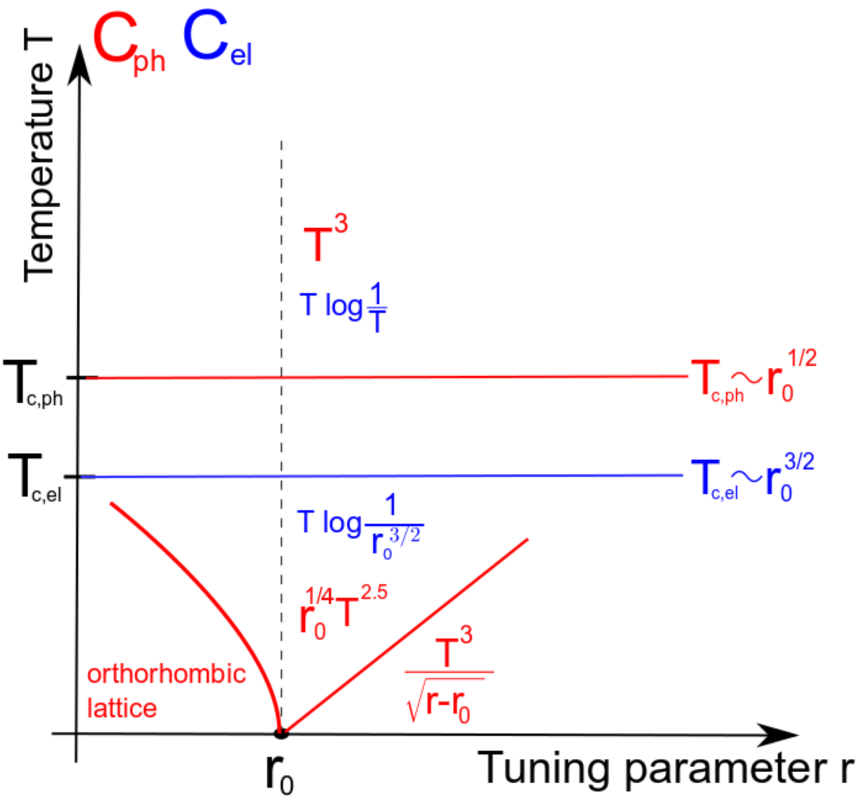

Figure 4.1: This scematic plot views the different crossover of the specific heat of the coupled system. The size of the crossover temperatures w.r.t. each other depends on the paramters of the system. For very small values of r_0 we are always in the case $T_{\mathrm{c,ph}} > T_{\mathrm{c,el}}$ because there we have $r_0^{3/2} \ll \sqrt{r_0}$.

4.2.4 Numerical Validation

In this chapter we check the analytical results for the phase diagram by numerical methods. We do this by calculating the electronic 4.2.1 and the phononic 4.2.3 specific heat via a Monte Carlo integration method for different temperatures T and boson masses r. The full specific heat of the system is given by the sum of these two terms.
The lattice parameters are here chosen to be

$$C_{11} = 19.0,\ C_{12} = 15.0,\ C_{33} = 25.0,\ C_{13} = 4.0,\ C_{44} = 25.0,\ C_{66} = 20.0,\ \rho = 1.0$$

For the bosonic term we choose the cutoff to be $\Lambda = 4000$ and the coupling constant is set to $\lambda = 0.3$.
From the analysis, where we always assumed that the bosonic mass r is tuned to its critical value $r_0 = \frac{2\lambda^2\rho}{C_{11}-C_{12}}$, we get the following parameters:

γ	δ	ν	α	β	$T_{\text{c,el}}$	$T_{\text{c,ph}}$
0.0885	0.0032	0.0035	0.001083	0.061190	0.1314	0.1023

$$C_{\text{ph}}(T) = \begin{cases} \alpha T^{2.5} & \text{for } T \leq T_{\text{c,ph}} \\ \beta T^3 & \text{for } T \geq T_{\text{c,ph}} \end{cases}; \qquad \frac{C_{\text{el}}}{T} = \begin{cases} \gamma & \text{for } T \ll T_{\text{c,el}} \\ \nu - \delta \log \frac{T}{\Lambda^3} & \text{for } T \gg T_{\text{c,el}} \end{cases}$$

Electronic Specific Heat

The comparison of the numerical result for $r = r_0$ is plotted in fig. 4.2. The exact results obtains slightly shifted curve for high T. The reason for this lies in the subleading terms that we have not taken into account because they are irrelevant for the crossover properties.

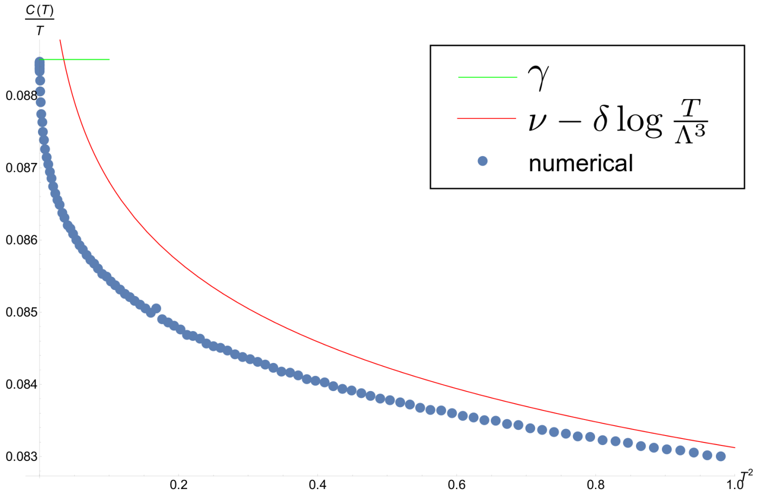

Figure 4.2: Comparison of the analytic result and the numerical results for the electronic part of the specific heat for $\lambda = 0.3$ and $r = r_0$. The limit $\lim_{T\to 0} \frac{C_{\text{el}}}{T} = \gamma$ fits very well to the numerical curve. The high temperature regime obtain a difference between the two results.

The value of δ is very close to the numerical result.
The behaviour of the specific heat can also be calculated for values $r > r_0$. We compare the curves for $r = r_0, r = 2r_0, 2^2 r_0, 2^3 r_0$. The results are plotted in fig. 4.3. There one can see that the specific heat coefficient strongly decreases in the low temperature regime when going to higher values for r. For $T \to 0$ we expect that C_{el}/T is proportional to $\log \frac{1}{r}$. Here we observe, using fig. 4.4, the following deviations differences of the zero temperature limits w.r.t the $r = r_0$ curve. The differences show exactly the behaviour which results from $\frac{C_{\text{el}}}{T} \propto \log \frac{1}{r}$.

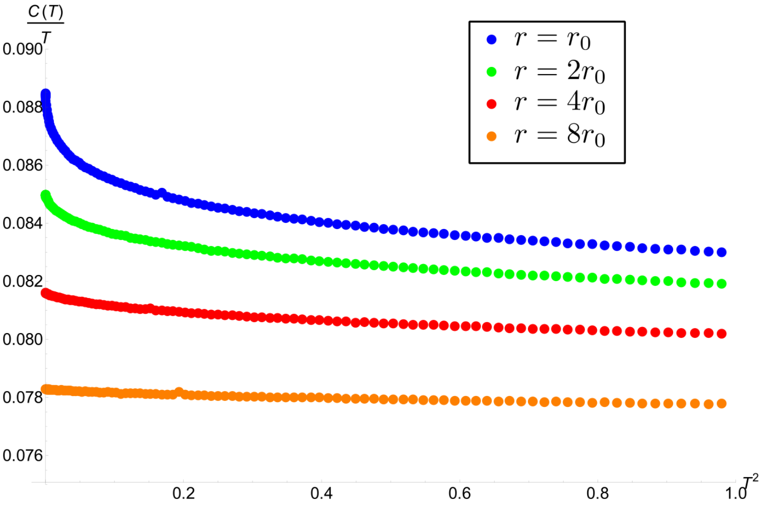

Figure 4.3: Electronic specific heat coefficient plotted against T^2 for different values for the tuning parameter r.

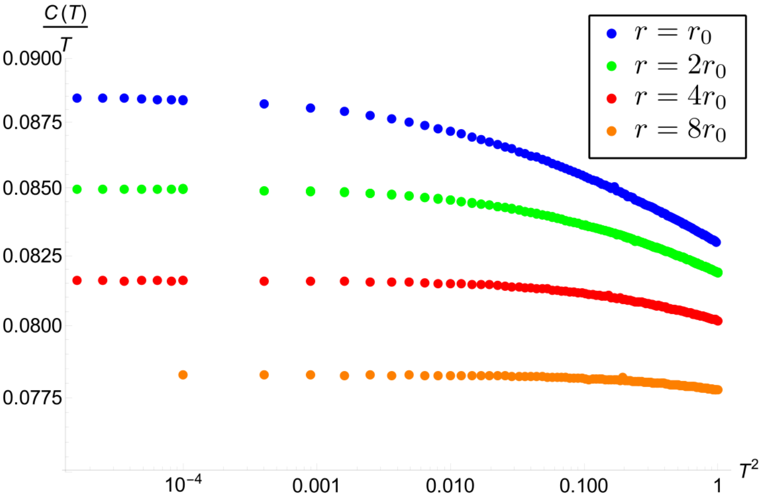

Figure 4.4: Electronic specific heat coefficient plotted against T^2 on logarithmic x-axis for different values for the tuning parameter r. In this plot one can see the behaviour of the curves for $T \to 0$.

	$r = 2r_0$	$r = 4r_0$	$r = 8r_0$
Deviation from γ	0.0033575	0.0067266 $\approx$ 2* 0.0033575	0.0100501 $\approx$ 3*0.0033575

Phononic Specific Heat

For the phononic specific heat we again first check our analysis for $r = r_0$ and then consider its behaviour when we go away from the critical value for the tuning parameter.
The comparison of the numerical curve with the high temperature limit of the specific heat coefficient is plotted in 4.5. There we see that the analytic curve fit very good to the numeric results for high temperatures. For low temperatures we have relatively broad crossover regime where the analytic predictions do not fit to the analytic curves. At very low temperatures the curve fits again very good to the numeric result. Hence the numeric result proof our result that at very low T we have $\frac{C_{\mathrm{ph}}}{T} \propto T^{1.5}$.

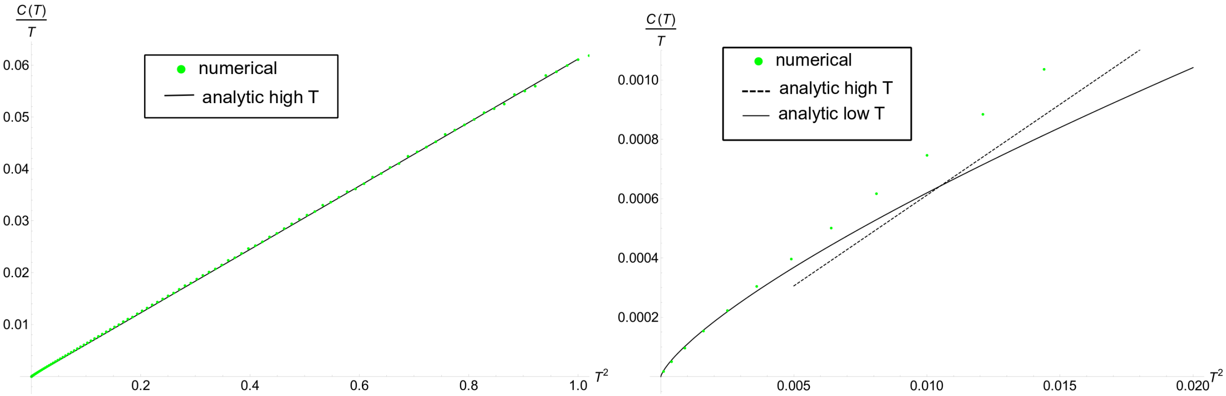

Figure 4.5: Comparison of the analytic result and the numerical results for the phononic part of the specific heat coefficient $\frac{C_{\mathrm{ph}}}{T}$ against T^2 for $\lambda = 0.3$ and $r = r_0$.

As before we now consider the change of the specific heat for values higher values for the tuning parameter r. For this we calculate the phononic specific heat coefficient for $r = r_0, r = 2r_0, r = 4r_0, r = 8r_0$. The results are plotted in fig. 4.6 and fig. 4.7.

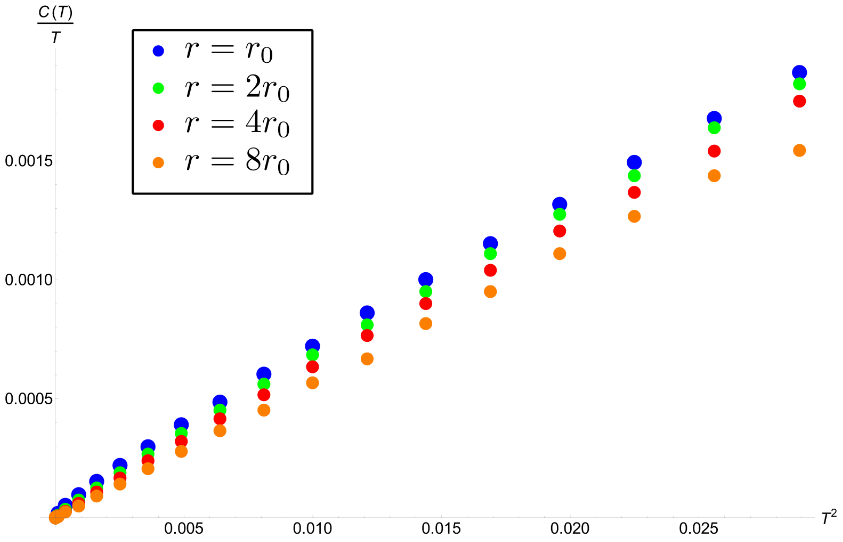

Figure 4.6: Phononic specific heat coefficient plotted against T^2 for different values for the tuning parameter r.

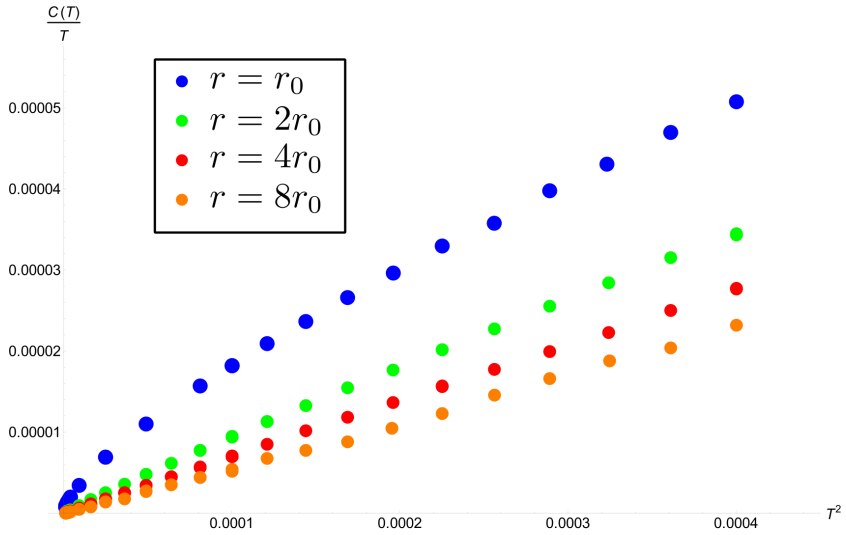

Figure 4.7: Low temperature regime of the phononic specific heat coefficient plotted against T^2 for different values for the tuning parameter r.

There we see that the specific heat decreases for higher r. Especially interesting is the low temperature regime where we observed $\frac{C_{\text{ph}}(T)}{T} \propto T^{1.5}$ for $r = r_0$. For values $r > r_0$ the results show linearly increasing curves i.e. there we have $\frac{C_{\text{ph}}(T)}{T} \propto T^2$. This shows that the phonon mode only becomes soft when we are at the critical value $r = r_0$ for the tuning parameter.

4.3 Fermionic Self Energy

The self energy and the specific heat of a Fermi liquid are closely related quantities. With the self energy one can directly calculate the entropy S, and hence the specific heat of a Fermi liquid, for low temperatures via the equation (from [7], page 169)

$$\frac{S}{V} = \frac{2\pi^2 T}{3}\frac{1}{2\pi}\int \frac{d^3q}{(2\pi)^3} 2\mathrm{Im}\left[G_R^{-1}\frac{\partial G_R}{\partial \varepsilon}\right]_{\varepsilon=0}$$

where $G_R(\boldsymbol{q}, \varepsilon)$ denotes the retarded Green's function of the Fermi liquid including the self energy correction. The calculation of the self energy has been done for many types of nematic transitions, see e.g. [26],[27],[6].

Here we want to check whether the self energy supports our result for the specific heat. For that we consider the first order diagram

$\Sigma^{(1)}\big(\boldsymbol{k}, i\omega_n\big) =$

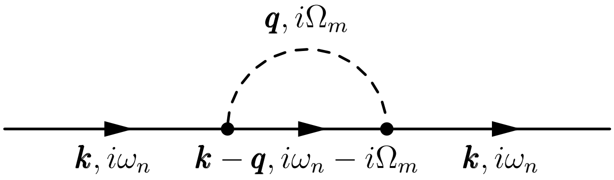

The dashed line denotes the fluctutation bosons which are coupled to the phonons. Again the coupling between the boson and the phonon is the dominating coupling mechanism in the system. Hence the phonons are not directly coupled to the fermions. More details about the effective coupling is given in the next section.

The diagram corresponds to the equation

$$\Sigma^{(1)}\big(\boldsymbol{k}, i\omega_n\big) = \frac{T}{V}\sum_{\Omega_m, \boldsymbol{q}} Q^2\big(\boldsymbol{k} - \frac{\boldsymbol{q}}{2}\big) g_{\mathrm{f}}\big(\boldsymbol{k} - \boldsymbol{q}, i(\omega_n + \Omega_m)\big) G_{\mathrm{b}}(\boldsymbol{q}, i\Omega_m)$$

where $G_{\mathrm{b}}(\boldsymbol{q}, i\Omega_m)$ is the boson component of the propagator G for the coupled boson-phonon system. We know

$$G^{-1}(\boldsymbol{q}, i\Omega_m) = \begin{pmatrix} g_{\mathrm{b}}^{-1}(\boldsymbol{q}, i\Omega_m) & i\lambda C(\boldsymbol{q}) \\ -i\lambda C(\boldsymbol{q}) & g_{\mathrm{ph}}^{-1}(\boldsymbol{q}, i\Omega_m) \end{pmatrix}$$

Inverting this 2x2 matrix leads to the boson propagator

$$G_{\mathrm{b}}(\boldsymbol{q}, i\Omega_m) = \frac{g_{\mathrm{ph}}^{-1}(\boldsymbol{q}, i\Omega_m)}{g_{\mathrm{ph}}^{-1}(\boldsymbol{q}, i\Omega_m) g_{\mathrm{b}}^{-1}(\boldsymbol{q}, i\Omega_m) - \lambda^2 C^2(\boldsymbol{q})}$$

Inserting $g_{\mathrm{ph}}^{-1}(\boldsymbol{q}, i\Omega_m) = \rho\omega(\boldsymbol{q})^2 + \rho\Omega_m^2$ and $g_{\mathrm{b}}^{-1}(\boldsymbol{q}, i\Omega_m) = r + E(\boldsymbol{q}) + \gamma(\hat{q})\frac{|\Omega_m|}{q}$ gives

$$\begin{aligned} G_{\mathrm{b}}(\boldsymbol{q}, i\Omega_m) =& \frac{\omega(\boldsymbol{q})^2 + \Omega_m^2}{(\omega(\boldsymbol{q})^2 + \Omega_m^2)(r + E(\boldsymbol{q}) + \gamma(\hat{q})\frac{|\Omega_m|}{q}) - \frac{\lambda^2}{\rho}C^2(\boldsymbol{q})} \\ =& \frac{1}{E(\boldsymbol{q}) + \gamma(\hat{q})\frac{|\Omega_m|}{q} + r - \frac{\lambda^2}{\rho}\frac{C^2(\boldsymbol{q})}{\omega(\boldsymbol{q})^2 + \Omega_m^2}} \end{aligned}$$

Instead of evaluating the sum over the frequencies, we first consider the integral over the direction of $\boldsymbol{q}$. We can approximate $\varepsilon_{\boldsymbol{k}-\boldsymbol{q}} \approx -v_F \boldsymbol{q}\cdot\hat{k} = -v_F q \hat{q}_k$. Inserting this gives

$$\Sigma\big(\boldsymbol{k}, i\omega_n\big) = \frac{TQ^2\big(\boldsymbol{k}\big)}{(2\pi)^3 v_F} \int d^3q \sum_{\Omega_m} \frac{1}{i\frac{\omega_n-\Omega_m}{v_F q} - \hat{q}_k} G_{\mathrm{b}}(\boldsymbol{q}, i\Omega_m)$$

The fraction can be approximated by $-i\pi\mathrm{sign}\big(\omega_n - \Omega_m\big)\delta(\hat{q}_k)$, i.e. the dominating terms come from the momenta $\boldsymbol{q}$ which are perpendicular to $\boldsymbol{k}$.

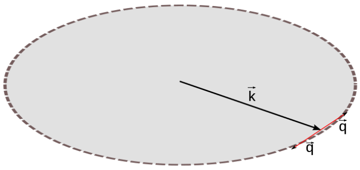

Figure 4.8: The vector $\boldsymbol{k}+\boldsymbol{q}$ has to be at the Fermi surface. For more complex forms of the surface we get other restrictions for the relation between $\boldsymbol{k}$ and $\boldsymbol{q}$.

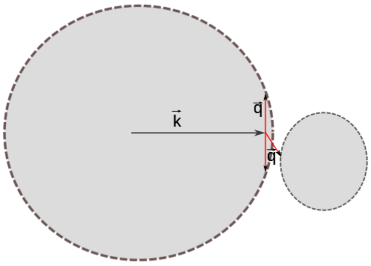

Figure 4.9: The vector $\boldsymbol{k}+\boldsymbol{q}$ has to be at the Fermi surface. The Fermi sphere leads in first order to $\boldsymbol{q} \perp \boldsymbol{k}$. For more complex surfaces, such as pockets (small circle), we get additional possibilities for $\boldsymbol{q}$

This orthogonality of $\boldsymbol{k}$ and $\boldsymbol{q}$ plays an important role in the final result of the self energy. Physically this can be understood as a result of the Pauli blocking on the one side and the Fermi statistics on the other side.
An important point for these relations is that the Fermi surface is a sphere. In practice this surface is deformed by strain, see fig. 4.8. A strong coupling of the electrons to the underlying lattice leads to surface shape, which can be very sensitive to strain. Furthermore there are cases where one has more than one connected Fermi sphere, see fig. 4.9. If these pockets are present we get more complex conditions for the relation between $\boldsymbol{k}$ and $\boldsymbol{q}$.
The quadrupolar mode vanishes for $|k_x| = |k_y|$. But this equality is exactly the condition for $\boldsymbol{k}$ such that the roots of the Landau damping prefactor $\gamma(\hat{q})$, see 3.2.1 lie in the plane perpendicular to $\boldsymbol{k}$. It implies that these roots are not seen in this approximation for the self energy. So in the following we can assume that $\gamma(\hat{q})$ is finite.
The self energy now has the form

$$\Sigma\big(\boldsymbol{k}, i\omega_n\big) = \frac{-iTQ^2\big(\boldsymbol{k}\big)}{2(2\pi)^2 v_F} \int_{\boldsymbol{q}\perp\boldsymbol{k}} d^2q \sum_{\Omega_m} \mathrm{sign}\big(\omega_n - \Omega_m\big) G_{\mathrm{b}}(\boldsymbol{q}, i\Omega_m)$$

The boson propagator is even in Ω_m. So the sign prefactor cancels all contribution from the terms with $|\Omega_m| > |\omega_n|$. In the end we are interested in the self energy as a function of ω. For that it is sufficient to perform the calculations in the zero temperature limit. This has the advantage that one can replace the sum by an integral $\sum_{\Omega_m} \to \frac{\beta}{2\pi}\int d\Omega$.

$$\Sigma\big(\boldsymbol{k}, i\omega_n\big) = \frac{-iQ^2\big(\boldsymbol{k}\big)\mathrm{sign}(\omega_n)}{(2\pi)^3 v_F} \int_0^{|\omega_n|} d\Omega \int_{\boldsymbol{q}\perp\boldsymbol{k}} d^2q G_{\mathrm{b}}(\boldsymbol{q}, i\Omega)$$

The integral over the momentum can be split into an integral over the absolute value and the direction of $\boldsymbol{q}$ in the plane perpendicular to $\boldsymbol{k}$.
An analytical integration is now possible in the limits of small and large frequency ω_n:

- **First case:** $\gamma_{\max}|\omega_n|^{3/2} \ll r(\hat{q})$
  At very large q the kinetic energy of the bosons is always the dominating term. For small q the situation is more complicated. Therefore we split the momenta at $q_c = \frac{|\omega_n|}{\omega(\hat{q})}$. In the $q < q_c$ regime the influence of the coupled phonons is tiny and hence can be ignored. Moreover we can ignore the Landau damping term. In the $q > q_c$ regime we recover the effective direction dependent mass $r(\hat{q})$ as the relevant term. This leads to the following splitting of the integral

$$\begin{aligned}&\int_0^{|\omega_n|} d\Omega \int_0^{q_c} dq \frac{q}{E(\boldsymbol{q}) + r_0} + \int_0^{|\omega_n|} d\Omega \int_{q_c}^{\Lambda} dq \frac{q}{E(\boldsymbol{q}) + r(\hat{q})} \\ =&\int_0^{|\omega_n|} d\Omega \frac{1}{2e(\hat{q})} \left[\log \frac{|\omega_n|^2 e(\hat{q}) + r_0}{r_0} + \log \frac{\Lambda^2}{|\omega_n|^2 + r(\hat{q})/e(\hat{q})} \right] \\ =&\frac{|\omega_n|}{2e(\hat{q})} \left[\log \frac{|\omega_n|^2 e(\hat{q}) + r_0}{r_0} + \log \frac{\Lambda^2}{|\omega_n|^2 + r(\hat{q})/e(\hat{q})} \right]\end{aligned}$$

  The cutoff Λ is very large. Hence the dominating term is given by

$$\frac{|\omega_n|}{2e(\hat{q})} \log \frac{\Lambda^2}{r(\hat{q})/e(\hat{q})}$$

- **Second case:** $\gamma_{\min}|\omega_n|^{3/2} \gg r(\hat{q})$
  The difference is that now the Landau damping term is dominating in the small momenta regime. This leads to

$$\begin{aligned}&\int_0^{|\omega_n|} d\Omega \int_0^{\Lambda} \frac{q}{E(\boldsymbol{q}) + \gamma(\hat{q})\frac{\Omega}{q}} \approx \int_0^{|\omega_n|} d\Omega \log \frac{e(\hat{q})\Lambda^3}{\gamma(\hat{q})\Omega} \\ =& |\omega_n| \left(1 + \log \frac{e(\hat{q})\Lambda^3}{\gamma(\hat{q})\omega_n} \right) \approx |\omega_n| \log \frac{e(\hat{q})\Lambda^3}{\gamma(\hat{q})\omega_n}\end{aligned}$$

A comparison of the two limits leads to the self energy of the form

$$\Sigma(\boldsymbol{k}, i\omega_n) = \frac{-iQ^2(\boldsymbol{k})}{2(2\pi)^2 v_F} \omega_n \begin{cases} \log\left(\frac{\Lambda^3 e(\hat{q})}{\bar{\gamma}|\omega_n|}\right) & \text{for } |\omega_n| \gg \frac{\bar{r}^{3/2}}{\bar{\gamma}} \\ \log\left(\frac{\Lambda^2 e(\hat{q})}{\bar{r}}\right) & \text{for } |\omega_n| \ll \frac{\bar{r}^{3/2}}{\bar{\gamma}} \end{cases}$$

The averaged values $\bar{r}$ and $\bar{\gamma}$ are defined as

$$\int_{\hat{q}\perp\boldsymbol{k}} d\hat{q}\, \ln\big(\gamma(\hat{q})\big) = \ln(\bar{\gamma}), \quad \int_{\hat{q}\perp\boldsymbol{k}} d\hat{q}\, \ln\big(r(\hat{q})\big) = \ln(\bar{r})$$

where $r(\hat{q}) = r_0 - \lambda^2 \frac{C^2(\boldsymbol{q})}{\omega^2(\boldsymbol{q})}$ is again the direction dependent mass. This averaging is allowed here, because $\gamma(\hat{q})$ and $r(\hat{q})$ only vanish in the $\left[\boldsymbol{q}_{\|}\right]$ directions. But these directions are only contained in the plane perpendicular to $\boldsymbol{k}$, when $Q(\boldsymbol{k}) = k_x^2 - k_y^2$ vanishes.

Finally we end up with a self energy which is quite similar to the specific heat of the bosonic modes. The major effect of the coupled phonons is a modified value for the crossover point between the high and the low frequency limit of the self energy. This is a consequence of the approximations we made.

A more detailed calculation of the self energy in its analytically continued form $\omega_n \to \omega + i\delta^+$ for the Fermi liquid due to phonon coupling can be found in [7]. The phonons lead to an imaginary part of the self energy which is in lowest order proportional to ω^3, i.e. $\mathrm{Im}\Sigma(\boldsymbol{k}, \omega) \propto \omega^3$. The real part of the self energy obtains a term linear in ω for small ω and furthermore a term proportional to $\omega^3 \log \omega$. So the identification of the phononic term is very difficult since we have more than one term with ω^3.

4.4 Effective Electron-Phonon Coupling

The common approach to describe the free electron to phonon interaction is to consider the coupling between these two fields directly. The typical form of the interaction term in the effective action is

$$\sum_{\boldsymbol{k},\boldsymbol{q}} g_\alpha(\boldsymbol{k},\boldsymbol{k}')\psi^\dagger(\boldsymbol{k})\psi(\boldsymbol{k}')\big(u_\alpha^\dagger(-\boldsymbol{q})+u_\alpha(\boldsymbol{q})\big)$$

where $\boldsymbol{q}=\boldsymbol{k}-\boldsymbol{k}'$ and $g_\alpha(\boldsymbol{k},\boldsymbol{k}')$ denotes the coupling amplitude.
We are in a slightly different situation since we have a quadrupolar interaction between the electrons. We constructed an effective interaction by coupling the bosons originating from the Hubbard-Stratonovich transformation ϕ to phonons. These bosons constitute the quadrupolar fluctuations of the Fermi surface and were defined as

$$\phi_{ij}=\psi^\dagger Q_{ij}\psi$$

Now we compare our results to the ordinary coupling. We want to know whether the coupling is enhanced in the vicintiy of the critical point of the system. For that we integrate out the bosonic mode ϕ.

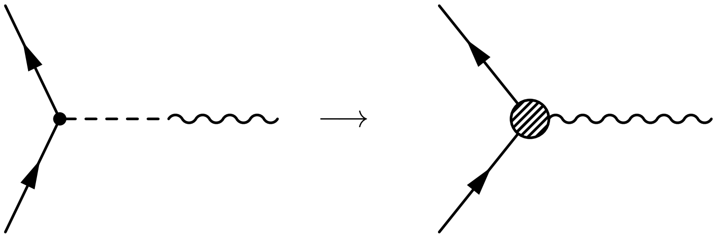

The action of the full system is given by

$$S[\psi^\dagger,\psi,\phi,u^\dagger,u]=\int d^3x d\tau\Big\{\psi^\dagger g_{\mathrm{f}}^{-1}\psi+\phi g_{\mathrm{b}}^{-1}\phi+u^\dagger g_{\mathrm{ph}}^{-1}u-\phi\big(\Psi^\dagger Q\Psi\big)$$
$$+\phi\big(-i\lambda C(\boldsymbol{q})\big)u+u^\dagger\big(i\lambda C(\boldsymbol{q})\big)\phi\Big\}$$

The effective action of the electron-phonon system can now be calculated by integrating out the bosons in the partition sum

$$Z=\int\mathcal{D}[\psi^\dagger,\psi,u^\dagger,u]\int\mathcal{D}\phi\exp\big(-S[\psi^\dagger,\psi,\phi,u^\dagger,u]\big)$$

Since we consider a linear coupling this integral can be evaluated exactly and leads to

$$S_{\mathrm{eff}}[\psi^\dagger,\psi,u^\dagger,u]=\int d^3x d\tau\Big\{\psi^\dagger g_{\mathrm{f}}^{-1}\psi+u^\dagger\big(g_{\mathrm{ph}}^{-1}-\lambda^2C^2(\boldsymbol{q})g_{\mathrm{b}}\big)u$$
$$+\frac{i\lambda C(\boldsymbol{q})}{2}g_{\mathrm{b}}(u^\dagger-u)\big(\psi^\dagger Q\psi\big)+\frac{1}{4}\big(\psi^\dagger Q\psi\big)g_{\mathrm{b}}\big(\psi^\dagger Q\psi\big)\Big\}$$

Here one can now read of the effective fermion-phonon coupling amplitude

$$\frac{\lambda C(\boldsymbol{q})}{r_0+E(\boldsymbol{q})+\gamma(\hat{q})\frac{|\Omega_m|}{q}}$$

The critical value of the tuning parameter is given by $r_0 = \frac{2\lambda^2\rho}{C_{11}-C_{12}} \propto \lambda^2$.
This result has an interesting consequence for the limit $\Omega = 0, \boldsymbol{q} \to 0$. There the effective coupling amplitude reduces to

$$\frac{\lambda C(\boldsymbol{q})}{r_0} \propto \frac{1}{\lambda}$$

This means that there we have an enhanced coupling due to the fact that λ is small.

Chapter 5

Summary

In this thesis we considered the effects of electron-phonon interaction in metals in three dimensions at very low temperatures. Thereby we restricted ourselves to samples where the electrons could be modeled by a Fermi liquid with quadrupolar interaction term. These are interesting because they have a nematic quantum critical point, see [6], [21], [5]. We are interested in the effects of the fluctuations of the Fermi liquid in the vicinity of this point for the sample.

We started with a general discussion of the elasticity of crystals. Thereby we first gave an introduction into the classical elasticity theory. Then we modified the quantities of this theory such that we can apply it to crystals. The central quantities which determine the elastic properties of crystals are the entries of the elastic modulus tensor $C_{\alpha\beta}$. To get information about the stability of crystals we had to decompose the possible strain directions into the eigenvectors of $C_{\alpha\beta}$. The eigenvalues indicate the stability of the crystal w.r.t strain along the corresponding eigenvector. A vanishing eigenvalue indicates an instable lattice. With the knowledge of the relation between the eigenvalues and the stability we were then able to construct a Landau theory for the strain. With this we could determine the properties of lattice transformations, such as the order of the transformation. Moreover we observed the appearance of soft phonons. These are acoustic phonon modes whose velocity is going to zero for some directions. Finally we calculated the free energy and the specific heat of stable crystals as well as for crystal at a lattice transformation point. The most important observation thereby was that the soft phonon modes lead to a modification of the typical law $C(T) \propto T^3$. So phonon modes with discrete soft directions lead to specific heat which is proportional to $T^{2.5}$. These modifications are especially interesting for the experimental analyzation of lattice transformations.

In the third chapter we considered a Fermi liquid with quadrupolar interaction as a model for the electrons. The key point in the analysis of the interaction term was the introduction of bosonic fields via a Hubbard-Stratonovich transformation. Each quadrupolar component corresponds to a different bosonic fields. Physically these fields can be considered as deformations of the Fermi sphere of quadrupolar shape. We derived an effective action for the complete Fermi liquid in terms of the bosonic fields. In the following we then focused on the dynamics of a isolated mode $\phi_{x^2-y^2}$. This mode is because of its symmetries the best candidate for inducing the tetragonal to orthorhombic lattice transition. We observed the appearance of a quantum critical point, indicated by a vanishing effective mass r, for certain parameters of the system. Furthermore this mode obtained a Landau damping which vanishes in the $<1,1,0>$ directions. These are exactly the same directions as the soft directions of the soft phonon mode in the tetragonal to orthorhombic transition. This fact plays an important role for the coupled system.

The temperature dependence of specific heat at the quantum critical point $r = 0$ turned out be of the form $T \log 1/T$. So the typical Fermi liquid property $C(T) \propto T$, which can be found e.g. in [7], page 169, is modified. Such a modification is called non-Fermi liquid behaviour.

In the fourth chapter we finally considered the full system of the crystal lattice and the electrons. The action of the two constituents are known from the previous chapters. Here we then constructed an effective interaction term. The crucial point thereby was that the coupling terms have to satisfy the lattice symmetries. In the lowest order contribution most of the coupling terms between the different phonon modes and the bosons are forbidden. In the tetragonal lattice that we considered, only the bosons $\phi_{x^2-y^2}$ could be coupled linearly to the phonon mode that becomes soft at the transformation into an orthorhombic lattice. So at low temperatures we have this dominant phonon mode which is strongly coupled to the bosonic field that we already considered in chapter three. For the sake of simplicity we ignored in the following the coupling to the other subleading phonon modes as well as to the other bosons. Thus we end up with an effective system of a coupled phonon-boson pair and miscellaneous decoupled constituents whose properties are well known from the previous chapters.

The strong boson-phonon coupling leads to a hybridization of the constituents. So the identification of a renormalized phonon mode and Fermi liquid is in general very difficult. To solve this problem we used the results from [10] for the free energy of this system in the isotropic case. There the free energy could be split into two terms which could be identified as an electronic and a phononic contribution. We got the analogue results for the non-isotropic system. In the analysis of these two terms we observed a renormalized dispersion relation for the phonons. For small energies this new dispersion obtained soft directions when the bosonic mass r is tuned to a small but finite critical value $r_0 > 0$. This lead us to the conclusion that at this point the fluctuations in the Fermi liquid induce a instability of the crystal. The bosonic mass played thereby the role of an order parameter. So at this point we expect a symmetry transformation of the lattice. As before we derived the thermodynamical properties of the system at the critical point via the specific heat. There we were able to analyze the contributions from the Fermi liquid and the phonons separately. The Fermi liquid obtained for large temperatures the $T \log T$ behaviour we already know form the uncoupled case. In the limit $T \to 0$ we got a finite value for C/T, i.e. there the critical fluctuations are suppressed and we recovered the Fermi liquid behaviour. The critical parameters for this crossover are $z = 3$ and $\nu = 1/2$. The phononic part obtained a $T^{2.5}$ proportionality for small T and a T^3 proportionality for large T. This crossover indicates the appearance of the soft dispersion and a transition of the tetragonal into an orthorhombic lattice. The critical parameters of this crossover are $z = 2$ and $\nu = 1/2$. Since we are in three dimensions, we are above the upper critical dimension $d_+ = 4$.

These analytic results were then confirmed by a numerical calculation of the specific heat. Large differences only occured in the vicinty of the crossover temperatures. Otherwise we observed only small deviations originating from subleading terms.

With the knowledge about the thermodynamics of the full system we then considered the effects of this hybridization of the two system. The lowest order contribution to the fermionic self energy $\Sigma(\boldsymbol{q}, \omega_n)$ at zero temperature turned out to be linear in ω_n when this frequency is small. For large frequencies it was of form $\omega_n \log(C/|\omega_n|)$. This result in accordance with the electronic specific heat we have calculated before. From the phonons we expect terms proportional to ω_n^3 and $\omega_n^{2.5}$. The extraction of these terms is in general very complicated because one gets a mixture of phononic and Fermi liquid contributions. These calculations are not done here because they would go beyond the scope of this thesis. In the last section we calculated the effective fermion-phonon vertex for our system. The consideration of its effects for physical mechanisms, such as sound absorption in the crystal, would be a topic for future work.

Deutsche Zusammenfassung

In dieser Arbeit wird der Einfluss der Elektronen-Gitter-Wechselwirkung von bestimmten Metallen in drei Dimensionen bei niedrigen Temperaturen untersucht. Diese Metalle zeichnen sich dadurch aus, dass die effektive Elektronen-Elektronen-Wechselwirkung durch eine quadrupolare Kopplung beschrieben werden kann. Das Standardmodell zur Beschreibung von Elektronen in Metallen ist das Fermiflüssigkeitenmodell. In Kombination mit der quadrupolaren Wechselwirkung sagt dieses Modell einen quantenkritischen Punkt des Systems vorraus, siehe [6], [21], [5]. An diesem Punkt treten starke Fluktuationen auf, deren Einfluss auf das gekoppelte Gitter wir untersuchen wollen.

Wir beginnen mit einer Einführung in die Elastizitätstheorie für Kristalle. Dabei wird zunächst die klassische Elastizitätstheorie von makroskopischen Objekten beschrieben, um anschließend die grundlegenden Konzepte dieser Theorie auf Kristalle anzuwenden. Die zentrale Größe, welche die elastischen Eigenschaften der Kristalle bestimmt, ist dabei der Elastizitätstensor $C_{\alpha\beta}$. Anhand dieses Tensors können wir die Stabilität von Kristallen beschreiben und die Eigenschaften von Gittertransformationen bestimmen. Einer der wesentlichsten Effekte bei den Gittertransformationen ist das Auftreten von weichen akustischen Phononmoden. Als weiche Phononmoden bezeichnet man Phononen, deren Geschwindigkeit für bestimmte Richtungen gegen Null geht. Sie modifizieren das typische Verhalten $C_{\text{ph}}(T) \propto T^3$ der spezifischen Wärme zu $C_{\text{ph}}(T) \propto T^{2.5}$. Dies liefert uns ein experimentell überprüfbares Resultat für das Auftreten einer weichen Phononmode.

Im dritten Kapitel werden die Eigenschaften der Fermiflüssigkeit in der Nähe des quantenkritischen Punktes behandelt. Die quadrupolare Wechselwirkung kann durch bosonische Quasiteilchen beschrieben werden, welche anschaulich eine Deformation der Fermikugel darstellen. Zu jeder unabhängigen quadrupolaren Komponente existiert ein entsprechendes Boson. Die Eigenschaften der Fermiflüssigkeit lassen sich dann anhand einer effektiven Wirkung für diese Felder beschreiben. Diese leiten wir für den Fall eines dominierenden Feldes $\phi_{x^2-y^2}$ her. Dabei können wir zum Einen das Auftreten des quantenkritischen Punktes reproduzieren. Desweiteren beobachten wir einen Landau-Dämpfungsterm, welcher entlang der Richtungen $<1,1,0>$ verschwindet. Die spezifische Wärme der Fermiflüssigkeit zeigt beim kritschen Punkt ein $T \log 1/T$ Verhalten.

Im zentralen vierten Kapitel betrachten wir das gesamte gekoppelte System. Dabei beschränken wir uns exemplarisch auf einen Kristall mit tetragonaler Gittersymmetrie. Aufgrund der Gittersymmetrien und der Symmetrien der Bosonen ist die Kopplung zwischen bestimmten Kombinationen aus Phononmoden und Bosonen bevorzugt. Unser System lässt sich damit auf eine dominierende Phonon-Boson-Kopplung reduzieren, währendessen die restlichen Beiträge als annähernd frei behandelt werden können.

Dieses System analysieren wir dann anhand der freien Energie und beobachten eine Renormalisierung der Parameter der Fermiflüssigkeit und der Phononmode. Eine entscheidener Punkt dabei ist, dass die Phononen für einen bestimmten Wert der effektiven Bosonmasse r und für niedrige Energien weich werden. Dies führt zu dem Schluss, dass die Quantenfluktuationen der Fermiflüssigkeit bei niedrigen Temperaturen einen Phasenübergang des Gitters induzieren. In der phononischen spezifischen Wärme spiegelt sich dies in einem Übergang von $C_{\mathrm{ph}}(T) \propto T^3$ zu $C_{\mathrm{ph}}(T) \propto T^{2.5}$ für $r = r_0$ bei niedrigen Temperaturen wider. Die kritischen Parameter für diesen Übergang sind $z = 1$ und $\nu = 1/2$. Für die Fermiflüssigkeit führt die Kopplung zu einer Unterdrückung des $T \log 1/T$ Verhaltens bei niedrigen Temperaturen. Dort erhalten wir das übliche Verhalten $C_{\mathrm{el}}(T) \propto T$ für Fermiflüssigkeiten. Bei diesem Übergang lauten die kritischen Parameter $z = 3$ und $\nu = 1/2$. Die analytischen Resultate konnten durch eine numerische Berechnung der spezifischen Wärme bestätigt werden. Anschließend berechnen wir noch die fermionische Selbstenergie für das gekoppelte System. Der elektronische Anteil der spezifischen Wärme kann dabei reproduziert werden. Für den phononischen Anteil muss eine komplexe Kombination aus Beiträgen der Diagramme erster und höherer Ordnung analysiert werden. Die Aufgabe würde den Rahmen dieser Arbeit sprengen und wird deshalb hier nicht durchgeführt.

Den Abschluss bildet die Berechnung der effektiven Kopplung im Fermion-Phonon System. Dazu müssen die bosonischen Felder ausintegriert werden. Die Analyse der physikalischen Effekte der resultierenden Kopplung ist eine mögliche Aufgabe für zukünftige Arbeiten.

Appendix A

Dispersion Relations of the Acoustic Phonons

To get the dispersions we have to calculate the eigenvalues of $D_{jk}(\boldsymbol{q}) = q_i C_{ijkl} q_l$. These are determined by the equation

$$0 = \det\left[D(\boldsymbol{q}) - \omega\mathbb{1}\right] = -\omega^3 + a(\boldsymbol{q})\omega^2 - b(\boldsymbol{q})\omega + c(\boldsymbol{q})$$

where

$$\begin{aligned}
a(\boldsymbol{q}) &= D_{11} + D_{22} + D_{33} \\
b(\boldsymbol{q}) &= -D_{12}D_{12} + D_{11}D_{22} - D_{13}D_{13} - D_{23}D_{23} + D_{11}D_{33} + D_{22}D_{33} \\
c(\boldsymbol{q}) &= -D_{13}D_{22}D_{13} + D_{12}D_{23}D_{13} + D_{13}D_{12}D_{23} - D_{11}D_{23}D_{23} - D_{12}D_{12}D_{33} + D_{11}D_{22}D_{33}
\end{aligned}$$

This equation can now be solved by Cardano's method and leads to

$$\omega_1 = -\sqrt{-\frac{4}{3}p} \cdot \cos\left(\frac{1}{3}\arccos\left(-\frac{q}{2}\sqrt{-\frac{27}{p^3}}\right) + \frac{\pi}{3}\right) \tag{A.0.1}$$

$$\omega_2 = \sqrt{-\frac{4}{3}p} \cdot \cos\left(\frac{1}{3}\arccos\left(-\frac{q}{2}\sqrt{-\frac{27}{p^3}}\right)\right) \tag{A.0.2}$$

$$\omega_3 = -\sqrt{-\frac{4}{3}p} \cdot \cos\left(\frac{1}{3}\arccos\left(-\frac{q}{2}\sqrt{-\frac{27}{p^3}}\right) - \frac{\pi}{3}\right) \tag{A.0.3}$$

with $p = b - \frac{a^3}{3}$, $\quad q = ba - c - \frac{2a^3}{27}$.
In general one can now calculate the dispersion for all kinds of lattices. Though in practise we will only consider the dispersion in local approximations whenever it is possible.

Appendix B

Phononic Free Energy

The free energy is given by

$$F = -\frac{T}{V}\sum_{\alpha=1}^{3}\Big\{\sum_{\boldsymbol{q},\Omega_m}\ln\left[\rho\Omega_m^2 + \rho\omega_\alpha^2(\boldsymbol{q})\right]\Big\}$$

Since all three terms have the same structure, it is sufficient to consider only one phonon mode.

To ensure the convergence of the complex integrals that will occur in the following calculations, we have to take an additional factor $e^{-i\varepsilon\Omega_m}$ with $\varepsilon \to 0^+$ in account. This factor occurs naturally in the general derivation of the Matsubara representation and doesn't change the result, see e.g. [23] page 171.

We start with the summation over the bosonic frequencies Ω_m. With the complex function

$$g(z) = \beta n_B(z) = \frac{\beta}{e^{\beta z} - 1}$$

the sum can be rewritten as the complex integral

$$F_\alpha = -\frac{T}{V}\sum_{\boldsymbol{q}}\oint_{\mathcal{C}}\frac{dz}{2\pi i}g(z)\,\ln\left[\rho\omega_\alpha^2(\boldsymbol{q}) - \rho z^2\right]e^{z\varepsilon}$$

In the complex plane we have to take care of the branch cut of the logarithm which is given by the equations

$$\begin{aligned} 0 &= \mathrm{Im}\Big(\omega_\alpha^2(\boldsymbol{q}) - z^2\Big) = -2xy \\ 0 &> \mathrm{Re}\Big(\omega_\alpha^2(\boldsymbol{q}) - z^2\Big) = \omega_\alpha^2(\boldsymbol{q}) + y^2 - x^2 \end{aligned}$$

where $z =: x + iy$. Hence we have $y = 0$ and $|x| > \omega_\alpha(\boldsymbol{q})$ at the branch cut.

The contour can now be deformed as plotted in B.1. The integrals along the half circles vanish for infinitely large radius. For the integration along the real axis we can use that g

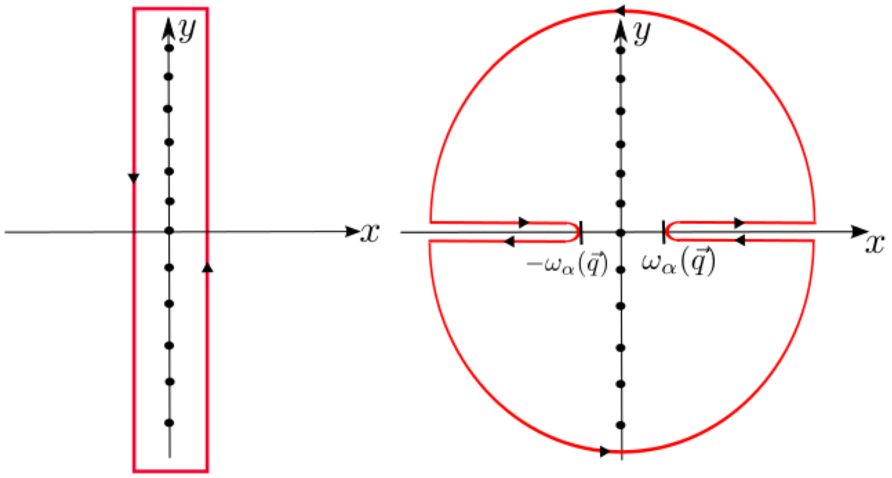

Figure B.1: Deformation of the initial integration path (left) to the new path (right).

is continuous around the real axis, i.e. $\lim_{\delta\to 0^+} g(x+i\delta) = g(x+i\delta) = g(x)$ to get

$$\begin{aligned}F_\alpha =& -\frac{T}{V}\sum_{\boldsymbol{q}}\Big\{\int_{-\infty}^{-\omega_\alpha(\boldsymbol{q})} - \int_{\omega_\alpha(\boldsymbol{q})}^{\infty}\Big\}\frac{dx}{2\pi i}\,g(x)\Big(\ln\big[\rho\big(\omega_\alpha^2(\boldsymbol{q}) - x^2 - 2i\delta x\big)\big] - \ln\big[\rho\big(\omega_\alpha^2(\boldsymbol{q}) - x^2 + 2i\delta x\big)\big]\Big)\\ =&\frac{T}{V}\sum_{\boldsymbol{q}}\Big\{\int_{-\infty}^{-\omega_\alpha(\boldsymbol{q})} - \int_{\omega_\alpha(\boldsymbol{q})}^{\infty}\Big\}\frac{dx}{\pi}\,g(x)\left(\arctan\left(\frac{2\delta x}{\omega_\alpha^2(\boldsymbol{q}) - x^2}\right) + \pi\right)\end{aligned}$$

Now we project the integral over the negative x-axis to the positive axis by the substitution $x \to -x$. Thereby we can use that the Fermi function has the property

$$g(-x) = -g(x) - \beta$$

Furthermore we can consider the integral in the limit $\delta \to 0^+$ where

$$\lim_{\delta\to 0^+} \arctan\left(\frac{2\delta x}{\omega_\alpha^2(\boldsymbol{q}) - x^2}\right) = 0$$

This leads to

$$F_\alpha = \frac{T}{V}\sum_{\boldsymbol{q}}\int_{\omega_\alpha(\boldsymbol{q})}^{\infty} dx\,\beta - 2\frac{T}{V}\sum_{\boldsymbol{q}}\int_{\omega_\alpha(\boldsymbol{q})}^{\infty} dx\,g(x)$$

The temperature is canceled out in the first term and gives us a temperature independent contribution. This can be interpreted as the phononic analogue to the zero point fluctuations of the harmonic oscillator. Hence this term can be written as $F(0)$. So we finally get

$$F_\alpha = F_\alpha(0) - \frac{2T}{V}\sum_{\boldsymbol{q}}\int_{\omega_\alpha(\boldsymbol{q})}^{\infty} dx\,g(x) = F_\alpha(0) + \frac{2}{V}\sum_{\boldsymbol{q}}\Big(T\ln\big[2\sinh\big(\frac{\omega_\alpha(\boldsymbol{q})}{2T}\big)\big] - \frac{\omega_\alpha(\boldsymbol{q})}{2}\Big)$$

Appendix C

Quadrupolar Polarization

Polarization for $\Omega_n > 0$

We are only interested in the lowest order contribution w.r.t. q since the momentum $\boldsymbol{q}$ of the boson is much smaller than the Fermi momentum. To get the corresponding terms we can ignore $\boldsymbol{q}$-dependence of Q. The dynamic part of the polarization then has the form

$$\Pi(\boldsymbol{q}, i\Omega_n) = -\frac{T}{V}\sum_{\boldsymbol{k},\omega_n} Q(\boldsymbol{k})Q(\boldsymbol{k})g_{\mathrm{f}}(\boldsymbol{k}+\frac{\boldsymbol{q}}{2}, i\omega_n + i\Omega_n)g_{\mathrm{f}}(\boldsymbol{k}-\frac{\boldsymbol{q}}{2}, i\omega_n)$$

where $g_{\mathrm{f}}^{-1}(\boldsymbol{k},\omega_n) = i\omega_n - \varepsilon(\boldsymbol{k})$ is the free electron propagator and $\varepsilon(\boldsymbol{k}) = \frac{\boldsymbol{k}^2 - k_F^2}{2m}$. The sum over the fermionic Matsubara frequencies can be written as the complex integral

$$\Pi(\boldsymbol{q}, i\Omega_n) = -\frac{1}{V}\sum_{\boldsymbol{k}} \oint_{\mathcal{C}_1} \frac{dz}{2\pi i} n_F(z) \frac{Q(\boldsymbol{k})Q(\boldsymbol{k})}{(z + i\Omega_n - \varepsilon(\boldsymbol{k}+\frac{\boldsymbol{q}}{2}))(z - \varepsilon(\boldsymbol{k}-\frac{\boldsymbol{q}}{2}))}$$

$n_F(z) = (\exp(\beta z)+1)^{-1}$ denotes the Fermi function over the complex plane.
Now one deformes the path $\mathcal{C}_1$ to the path $\mathcal{C}_2$, as plotted in fig. C.1, without changing the integral. The circle of $\mathcal{C}_2$ which lies at infinity does not contribute to the integral. For the small circles around the poles

$$z_1 = \varepsilon(\boldsymbol{k}+\frac{\boldsymbol{q}}{2}) - i\Omega_n \text{ and } z_2 = \varepsilon(\boldsymbol{k}-\frac{\boldsymbol{q}}{2})$$

one can again use the residuum theorem.

$$\begin{aligned}
\Pi(\boldsymbol{q}, i\Omega_n) =& -\frac{1}{V}\sum_{\boldsymbol{k}} \mathrm{Res}\left(n_F(z)\frac{Q^2(\boldsymbol{k})}{(z - \varepsilon(\boldsymbol{k}-\frac{\boldsymbol{q}}{2}))}, z_1\right) + \mathrm{Res}\left(n_F(z)\frac{Q^2(\boldsymbol{k})}{(z + i\Omega_n - \varepsilon(\boldsymbol{k}+\frac{\boldsymbol{q}}{2}))}, z_2\right)\\
=& -\frac{1}{V}\sum_{\boldsymbol{k}} Q^2(\boldsymbol{k})\left(\frac{n_F(\varepsilon(\boldsymbol{k}+\frac{\boldsymbol{q}}{2}) - i\Omega_n)}{\varepsilon(\boldsymbol{k}+\frac{\boldsymbol{q}}{2}) - \varepsilon(\boldsymbol{k}-\frac{\boldsymbol{q}}{2}) - i\Omega_n} - \frac{n_F(\varepsilon(\boldsymbol{k}-\frac{\boldsymbol{q}}{2}))}{\varepsilon(\boldsymbol{k}+\frac{\boldsymbol{q}}{2}) - \varepsilon(\boldsymbol{k}-\frac{\boldsymbol{q}}{2}) - i\Omega_n}\right)\\
=& \frac{1}{V}\sum_{\boldsymbol{k}} Q^2(\boldsymbol{k})\frac{n_F(\varepsilon(\boldsymbol{k}+\frac{\boldsymbol{q}}{2}) - n_F(\varepsilon(\boldsymbol{k}-\frac{\boldsymbol{q}}{2}))}{i\Omega_n - \left(\varepsilon(\boldsymbol{k}+\frac{\boldsymbol{q}}{2}) - \varepsilon(\boldsymbol{k}-\frac{\boldsymbol{q}}{2})\right)}\\
=& \frac{1}{V}\sum_{\boldsymbol{k}} Q^2(\boldsymbol{k})\frac{n_F(\varepsilon(\boldsymbol{k}+\frac{\boldsymbol{q}}{2}) - n_F(\varepsilon(\boldsymbol{k}-\frac{\boldsymbol{q}}{2}))}{i\Omega_n - \frac{1}{m}\boldsymbol{k}\cdot\boldsymbol{q}}
\end{aligned}$$

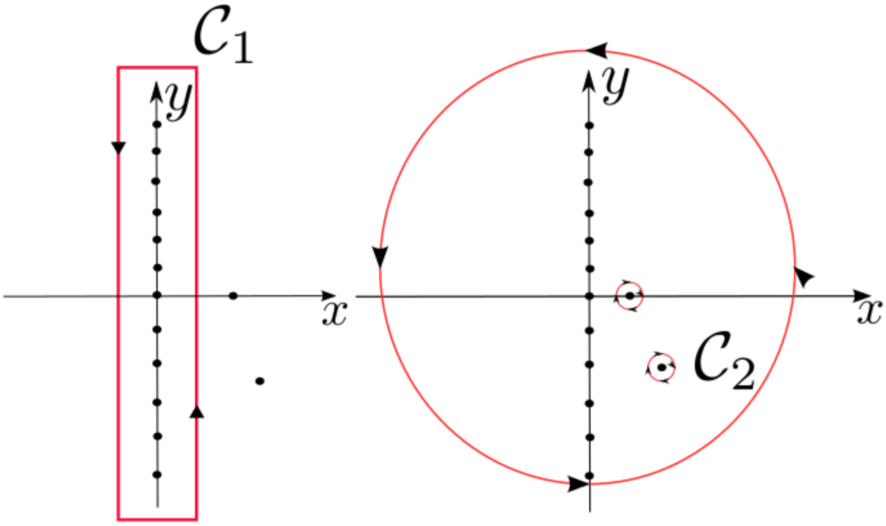

Figure C.1: Deformation of the integration path. The circle at infinity has no contribution to the integral.

We are interested in the low temperature regime. Therefore we can make the approximation

$$n_F(\varepsilon(\boldsymbol{k} \pm \frac{\boldsymbol{q}}{2})) \approx \Theta(\varepsilon(\boldsymbol{k})) + \boldsymbol{q} \cdot \frac{\partial \varepsilon(\boldsymbol{k} \pm \frac{\boldsymbol{q}}{2})}{\partial \boldsymbol{q}}|_{\boldsymbol{q}=0} \delta(\varepsilon_{\boldsymbol{k}}) = \Theta(\varepsilon(\boldsymbol{k})) \pm \boldsymbol{q} \cdot \frac{\boldsymbol{k}}{4m} \delta(\varepsilon_{\boldsymbol{k}})$$

which implies

$$n_F(\varepsilon(\boldsymbol{k} + \frac{\boldsymbol{q}}{2})) - n_F(\varepsilon(\boldsymbol{k} - \frac{\boldsymbol{q}}{2})) \approx \frac{\boldsymbol{q} \cdot \boldsymbol{k}}{2m} \delta\big(\varepsilon(\boldsymbol{k})\big)$$

Together which the approximation $\sum_{\boldsymbol{k}} \approx \frac{V}{(2\pi)^3} \int d^3k$ we get

$$\boxed{\Pi(\boldsymbol{q}, i\Omega_n) = \frac{1}{(2\pi)^3} \int d^3k \, Q^2(\boldsymbol{k}) \frac{\boldsymbol{q} \cdot \boldsymbol{k}}{2m} \frac{1}{i\Omega_n - \boldsymbol{k} \cdot \boldsymbol{q}/m} \delta(\varepsilon_{\boldsymbol{k}})}$$

The remaining task is now to evaluate the integral over the momentum. With

$$\varepsilon_{\boldsymbol{k}} = 0 \Leftrightarrow \frac{\boldsymbol{k}^2}{2m} - \frac{k_F^2}{2m} = 0 \Leftrightarrow |\boldsymbol{k}| = k_F$$

follows

$$\Pi(\boldsymbol{q}, i\Omega_n) = \frac{m k_F}{(2\pi)^3} \int_{S_{k_F}} d^2\Omega \, Q^2(\boldsymbol{k}) \frac{q k_F \hat{q} \cdot \hat{k}}{2 i\Omega_n m - 2 k_F q \hat{q} \cdot \hat{k}}$$

where S_{k_F} is the sphere around the origin with radius k_F. Here we are interested in the dynamical part $\delta\Pi(\boldsymbol{q}, i\Omega_n)$ of the polarization. Hence we make the decomposition

$$\frac{\boldsymbol{q} \cdot \boldsymbol{k}}{i\Omega_n m - \boldsymbol{k} \cdot \boldsymbol{q}} = -1 + \frac{i\Omega_n m}{i\Omega_n m - \boldsymbol{k} \cdot \boldsymbol{q}}$$

and consider in the following only the second term:

$$\delta\Pi(\boldsymbol{q}, i\Omega_n) = \Pi(\boldsymbol{q}, i\Omega_n) - \Pi(\boldsymbol{q}, 0) = i\frac{mk_F}{2(2\pi)^3}\frac{\Omega_n}{v_F q}\int_{S_{k_F}} d^2k \frac{Q^2(\boldsymbol{k})}{i\frac{\Omega_n}{v_F q} - \hat{k}\cdot\hat{q}}$$

The denominator only depends on the angle between $\boldsymbol{k}$ and $\boldsymbol{q}$. We will now rotate our coordinate system such that $\boldsymbol{q}$ points into the z-direction. This has the advantage that the denominator will transform into a simple form.
The rotation $\boldsymbol{k} \to D\boldsymbol{k}$ is defined via the matrix

$$D = \begin{pmatrix} \cos(\Theta_q)\cos(\varphi_q) & \sin(\varphi_q)\cos(\Theta_q) & -\sin(\Theta_q) \\ -\sin(\varphi_q) & \cos(\varphi_q) & 0 \\ \sin(\Theta_q)\cos(\varphi_q) & \sin(\Theta_q)\sin(\varphi_q) & \cos(\Theta_q) \end{pmatrix}$$

It maps $\boldsymbol{q} = q\begin{pmatrix} \sin(\Theta_q)\cos(\varphi_q) \\ \sin(\Theta_q)\sin(\varphi_q) \\ \cos(\Theta_q) \end{pmatrix}$ to the z-axis. The polarization then has the form

$$\delta\Pi(\boldsymbol{q}, i\Omega_n) = i\frac{mk_F}{2(2\pi)^3}\frac{\Omega_n}{v_F q}\int_{S_{k_F}(0)} d^2k \frac{Q^2(D^{-1}\boldsymbol{k})}{i\frac{\Omega_n}{v_F q} - \cos(\Theta)}$$

where Θ is the angle between $\boldsymbol{k}$ and the z-axis.
Now we can use $\frac{\Omega_n}{v_F q} << 1$. This implies that the leading contributions come from the directions where $\cos\Theta = 0$.
So the first order contribution in $\frac{\Omega_n}{v_F q}$ can be calculated by the relation

$$\lim_{\delta\to 0^+}\frac{1}{x + i\delta} = -i\pi\delta(x) + \mathcal{P}\frac{1}{x}$$

for the Θ-integral. Doing so we get:

$$\begin{aligned}
&\delta\Pi(\boldsymbol{q}, i\Omega_n) \\
&= \frac{3mk_F}{4(2\pi)^2}\frac{\Omega_n}{v_F q}\mathrm{sign}(\Omega_n)\int_0^{2\pi} d\varphi \left\{ \cos(2\varphi_q)[\cos^2(\Theta_q)\cos^2(\varphi) - \sin^2(\varphi)] + \sin(2\varphi)\cos(\Theta_q)\sin(2\varphi_q)\right\}^2 \\
&= \frac{mk_F}{4(2\pi)^2}\frac{|\Omega_n|}{v_F q}\frac{3\pi}{64}\big(41 + 9\cos(4\varphi_q) + 4(5 - 3\cos(4\varphi_q))cos(2\Theta_q) + 6\cos^2(2\varphi_q)\cos(4\Theta_q)\big) \\
&= \frac{3mk_F}{1024\pi}\frac{|\Omega_n|}{v_F q}\big(41 + 9\cos(4\varphi_q) + 4(5 - 3\cos(4\varphi_q))\cos(2\Theta_q) + 6\cos^2(2\varphi_q)\cos(4\Theta_q)\big)
\end{aligned}$$

We summarize the remaining direction dependence in the function

$$\gamma(\varphi_q, \Theta_q) = \frac{3}{1024\pi}\big(41 + 9\cos(4\varphi_q) + 4(5 - 3\cos(4\varphi_q))\cos(2\Theta_q) + 6\cos^2(2\varphi_q)\cos(4\Theta_q)\big)$$

We see that this vanishes for

$$\varphi_q \in \{\pi/4,\ 3\pi/4,\ 5\pi/4,\ 7\pi/4\}, \quad \Theta_q = \pi/2$$

In these cases we have to take the second order term in $\frac{\Omega_n}{v_F q}$ into account. For that we go back to the formula

$$\delta\Pi(\boldsymbol{q}, i\Omega_n) = i\frac{mk_F}{2(2\pi)^3}\frac{\Omega_n}{v_F q}\int_{S_{k_F}(0)} d^2k \frac{Q_x^2(D^{-1}\boldsymbol{k})}{i\frac{\Omega_n}{v_F q} - \cos(\Theta)}$$

Instead of directly using Dirac's identity, we replace the integral $\int_{-1}^{1} d(\cos\Theta)$ by its residuum at $z = i\Omega_n/(v_F q)$. This is an approximation because the contribution of the integral along the unit circle in the lower half plane is set to 0. The reason why this approximation is allowed lies in the fact that $i\frac{\Omega_n}{v_F q}$ lies very close at the real axis. Thus we get the second order term by setting $\cos\Theta = \frac{i\Omega_n}{v_F q}$, neglecting the first order and multiply the result by $i\pi\mathrm{sign}(\Omega_n)$:

$$\begin{aligned}
&\delta\Pi(\boldsymbol{q}, i\Omega_n)\\
=&-i\pi\frac{mk_F\mathrm{sign}\big(\Omega_n\big)}{2(2\pi)^3}\frac{\Omega_n^2}{v_F^2 q^2}\int_0^{2\pi} d\varphi\times\\
&\times\Bigg\{4\big[(\cos\Theta_q\cos\varphi_q\cos\varphi - \sin\varphi_q\sin\varphi)^2 - (\cos\Theta_q\sin\varphi_q\cos\varphi + \cos\varphi_q\sin\varphi)^2\big]\\
&\big[\sin\Theta_q\cos\varphi_q(\cos\Theta_q\cos\varphi_q\cos\varphi - \sin\varphi_q\sin\varphi)\\
&-\sin\Theta_q\sin\varphi_q(\sin\varphi_q\cos\Theta_q\cos\varphi + \cos\varphi_q\sin\varphi)\big]\Bigg\}\\
=&0
\end{aligned}$$

Thus the second order vanishes for all angles of $\boldsymbol{q}$ and we have to do the same procedure for the **third order**. There we get

$$\begin{aligned}
&\delta\Pi(\boldsymbol{q}, i\Omega_n)\\
=&-\pi\frac{mk_F}{2(2\pi)^3}\left(\frac{|\Omega_n|}{v_F q}\right)^3\frac{\pi}{32}\left[13 + 36\cos(2\Theta_q) + 15\cos(4\Theta_q) + 120\cos(4\varphi_q)\sin^4\Theta_q\right]
\end{aligned}$$

We see that the **third order of $\delta\Pi(\boldsymbol{q}, i\Omega_n)$ never vanishes**!

Polarization for $\Omega_n = 0$

For the static part of the polarization we have to take care of the $\boldsymbol{q}$-dependence of the quadrupolar projections. It is given by

$$\Pi(\boldsymbol{q}, 0) = \frac{T}{V}\lim_{\Omega\to 0}\sum_{\boldsymbol{k},\omega_n} Q(\boldsymbol{k})Q(\boldsymbol{k}+\boldsymbol{q})\frac{1}{i\omega_n - \varepsilon_{\boldsymbol{k}}}\frac{1}{i\omega_n + i\Omega - \varepsilon_{\boldsymbol{k}+\boldsymbol{q}}}$$

The standard procedure for the Matsubara summation leads to

$$\begin{aligned}
\Pi(\boldsymbol{q}, 0) =& \frac{1}{V}\lim_{\Omega\to 0}\sum_{\boldsymbol{k}}\frac{n_f(\xi_{\boldsymbol{k}}) - n_f(\xi_{\boldsymbol{k}+\boldsymbol{q}})}{i\Omega - \big(\varepsilon_{\boldsymbol{k}+\boldsymbol{q}} - \varepsilon_{\boldsymbol{k}}\big)}Q(\boldsymbol{k})Q(\boldsymbol{k}+\boldsymbol{q})\\
=&\lim_{\Omega\to 0}\int\frac{d^3k}{(2\pi)^3}\frac{n_f(\xi_{\boldsymbol{k}}) - n_f(\xi_{\boldsymbol{k}+\boldsymbol{q}})}{i\Omega - \big(\varepsilon_{\boldsymbol{k}+\boldsymbol{q}} - \varepsilon_{\boldsymbol{k}}\big)}Q(\boldsymbol{k})Q(\boldsymbol{k}+\boldsymbol{q})
\end{aligned}$$

Now we can use the Dirac identity

$$\lim_{\delta\to 0^+} \frac{1}{x+i\delta} = -i\pi\delta(x) + \mathcal{P}\Big(\frac{1}{x}\Big)$$

The contribution of the delta distribution vanishes and we are left with the principal value of

$$\Pi(\boldsymbol{q},0) = \int \frac{d^3k}{(2\pi)^3} \frac{n_f(\xi_{\boldsymbol{k}}) - n_f(\xi_{\boldsymbol{k}+\boldsymbol{q}})}{\varepsilon_{\boldsymbol{k}} - \varepsilon_{\boldsymbol{k}+\boldsymbol{q}}} Q(\boldsymbol{k})Q(\boldsymbol{k}+\boldsymbol{q})$$

Next we split the terms of the two fermi functions and shift the integration of one term to get the same argument in the function.

$$\begin{aligned}\Pi(\boldsymbol{q},0) =& \Bigg[\int \frac{d^3k}{(2\pi)^3} \frac{n_f(\varepsilon_{\boldsymbol{k}})}{\varepsilon_{\boldsymbol{k}} - \varepsilon_{\boldsymbol{k}+\boldsymbol{q}}} Q_\parallel(\boldsymbol{k})Q_\parallel(\boldsymbol{k}+\boldsymbol{q}) - \int \frac{d^3k}{(2\pi)^3} \frac{n_f(\varepsilon_{\boldsymbol{k}+\boldsymbol{q}})}{\varepsilon_{\boldsymbol{k}} - \varepsilon_{\boldsymbol{k}+\boldsymbol{q}}} Q_\parallel(\boldsymbol{k})Q_\parallel(\boldsymbol{k}+\boldsymbol{q})\Bigg] \\ =& \Bigg[\int \frac{d^3k}{(2\pi)^3} \frac{n_f(\varepsilon_{\boldsymbol{k}})}{\varepsilon_{\boldsymbol{k}} - \varepsilon_{\boldsymbol{k}+\boldsymbol{q}}} Q_\parallel(\boldsymbol{k})Q_\parallel(\boldsymbol{k}+\boldsymbol{q}) - \int \frac{d^3k}{(2\pi)^3} \frac{n_f(\varepsilon_{\boldsymbol{k}})}{\varepsilon_{\boldsymbol{k}-\boldsymbol{q}} - \varepsilon_{\boldsymbol{k}}} Q(\boldsymbol{k}-\boldsymbol{q})Q(\boldsymbol{k})\Bigg]\end{aligned}$$

Now substitiuting $\boldsymbol{k} \to -\boldsymbol{k}$ in the second term leads to

$$\begin{aligned}\Pi(\boldsymbol{q},0) =& \Bigg[\int \frac{d^3k}{(2\pi)^3} \frac{n_f(\varepsilon_{\boldsymbol{k}})}{\varepsilon_{\boldsymbol{k}} - \varepsilon_{\boldsymbol{k}+\boldsymbol{q}}} Q(\boldsymbol{k})Q(\boldsymbol{k}+\boldsymbol{q}) - \int \frac{d^3k}{(2\pi)^3} \frac{n_f(\varepsilon_{-\boldsymbol{k}})}{\varepsilon_{-\boldsymbol{k}-\boldsymbol{q}} - \varepsilon_{-\boldsymbol{k}}} Q(-\boldsymbol{k}-\boldsymbol{q})Q(-\boldsymbol{k})\Bigg] \\ =& \Bigg[\int \frac{d^3k}{(2\pi)^3} \frac{n_f(\varepsilon_{\boldsymbol{k}})}{\varepsilon_{\boldsymbol{k}} - \varepsilon_{\boldsymbol{k}+\boldsymbol{q}}} Q(\boldsymbol{k})Q(\boldsymbol{k}+\boldsymbol{q}) - \int \frac{d^3k}{(2\pi)^3} \frac{n_f(\varepsilon_{\boldsymbol{k}})}{\varepsilon_{\boldsymbol{k}+\boldsymbol{q}} - \varepsilon_{\boldsymbol{k}}} Q(\boldsymbol{k}+\boldsymbol{q})Q(\boldsymbol{k})\Bigg] \\ =& \int \frac{d^3k}{(2\pi)^3} \frac{n_f(\varepsilon_{\boldsymbol{k}})}{\varepsilon_{\boldsymbol{k}} - \varepsilon_{\boldsymbol{k}+\boldsymbol{q}}} Q(\boldsymbol{k})Q(\boldsymbol{k}+\boldsymbol{q})\end{aligned}$$

where we used that $\varepsilon_{\boldsymbol{k}}$ and $Q(\boldsymbol{k})$ are even.
We can again rotate our coordinate system such that $\boldsymbol{q}$ is parallel to the $z-$axis via the rotation matrix D. Thereby we can use that ε is invariant under rotations.

$$\begin{aligned}\Pi(\boldsymbol{q},0) =& \frac{2}{k_F^4} \int \frac{d^3k}{(2\pi)^3} \frac{n_f(\varepsilon_{\boldsymbol{k}})}{\varepsilon_{\boldsymbol{k}} - \varepsilon_{\boldsymbol{k}+\boldsymbol{q}}} \boldsymbol{k}^T \big(D\hat{Q}D^{-1}\big)\boldsymbol{k}\,(\boldsymbol{k}+\boldsymbol{q})^T \underbrace{\big(D\hat{Q}D^{-1}\big)}_{=\tilde{Q}}(\boldsymbol{k}+\boldsymbol{q}) \\ =& \frac{2}{k_F^4} \int \frac{d^3k}{(2\pi)^3} \frac{n_f(\varepsilon_{\boldsymbol{k}})}{\varepsilon_{\boldsymbol{k}} - \varepsilon_{\boldsymbol{k}+\boldsymbol{q}}} \boldsymbol{k}^T\tilde{Q}\boldsymbol{k}\,(\boldsymbol{k}+\boldsymbol{q})^T\tilde{Q}(\boldsymbol{k}+\boldsymbol{q}) \\ =& -\frac{4m}{k_F^4 q} \int \frac{d^3k}{(2\pi)^3} \frac{n_f(\varepsilon_{\boldsymbol{k}})}{2k_z+q} \boldsymbol{k}^T\tilde{Q}\boldsymbol{k}\,(\boldsymbol{k}+\boldsymbol{q})^T\tilde{Q}(\boldsymbol{k}+\boldsymbol{q})\end{aligned}$$

In cylindrical coordinates $\boldsymbol{k} = \big(r\cos\varphi, r\sin\varphi, k_z\big)^T$ this reads as

$$\begin{aligned}\Pi(\boldsymbol{q},0) = \frac{-4m}{k_F^4 q} \int \frac{d^3k}{(2\pi)^3} \frac{n_f(\varepsilon_{\boldsymbol{k}})}{2k_z+q} \big(r\cos\varphi, r\sin\varphi, k_z\big)\tilde{Q} \begin{pmatrix} r\cos\varphi \\ r\sin\varphi \\ k_z \end{pmatrix} \times \\ \times \big(r\cos\varphi, r\sin\varphi, k_z+q\big)\tilde{Q} \begin{pmatrix} r\cos\varphi \\ r\sin\varphi \\ k_z+q \end{pmatrix}\end{aligned}$$

This integration can now be carried out in the low temperature regime where the Fermi function is approximately given by the Heaviside function.

$$\Pi(\boldsymbol{q}, 0) = -\frac{2mk_F}{45\pi^2} + \frac{mk_F\big(2 - \cos(2\theta_q)\big)}{54\pi^2}\frac{q^2}{k_F^2} + \mathcal{O}\Big(\frac{q^4}{k_F^4}\Big)$$

Here we have now a constant mass term and a kinetic term which is proportional to q^2. The direction dependence of the kinetic term is determined by the positon of $\boldsymbol{q}$ w.r.t. the z-axis. Hence we can write this term in the form

$$A^2(q_x^2 + q_y^2) + B^2 q_z^2$$

A comparison of the two forms, using $\cos(2\theta_q) = \cos^2\theta_q - \sin^2\theta_q$, implies

$$A^2 = \frac{mk_F}{18\pi^2}\frac{1}{k_F^2},\ B^2 = \frac{mk_F}{54\pi^2}\frac{1}{k_F^2}$$

Appendix D

Free Energy of the Coupled System

The following calculations are adopted from [10]. There the free energy was derived for an isotropic system. So the difference is that here the Landau damping and the dispersion are direction dependent.
The free energy is given by the relation $F = -\frac{T}{V}\ln Z$. Inserting the partition sum leads to

$$F = \frac{T}{V}\sum_{\boldsymbol{q},\Omega_m} \ln\left[\Big(r + E(\boldsymbol{q}) + \frac{\gamma(\hat{q})}{q}|\Omega_m|\Big)\Big(\rho\omega^2(\boldsymbol{q}) + \rho\Omega_m^2\Big) - \lambda^2 C^2(\boldsymbol{q})\Big)^2\right]$$

Now we perform the Matsubara sum. Again we split the sum into positive and negative Matsubara frequencies to avoid the absolute value.

$$F(T) = F(0) + 2T\sum_{\boldsymbol{q},\Omega_m>0} \ln\left[\Big(r + E(\boldsymbol{q}) + \frac{\gamma(\hat{q})}{q}\Omega_m\Big)\Big(\rho\omega^2(\boldsymbol{q}) + \rho\Omega_m^2\Big) - \lambda^2 C^2(\boldsymbol{q})\right]$$

This sum can again be transformed into a complex integral

$$F(T) - F(0) = \sum_{\boldsymbol{q}} \int \frac{dz}{2\pi i}\Big(\coth\frac{z}{2T} - 1\Big) \ln\Bigg[\underbrace{\Big(r + E(\boldsymbol{q}) - i\frac{\gamma(\hat{q})}{q}z\Big)\Big(\rho\omega^2(\boldsymbol{q}) - \rho z^2\Big) - \lambda^2 C^2(\boldsymbol{q})}_{=:f(\boldsymbol{q},z)}\Bigg]$$

With $z := x + iy$ we can read of the imaginary and real part of the argument of ln:

$$\begin{aligned}
\mathrm{Im}[f] &= -x\rho\Big(2y\Big(r + E(\boldsymbol{q}) + \frac{\gamma(\hat{q})}{q}y\Big) + \frac{\gamma(\hat{q})}{q}\Big(\omega^2(\boldsymbol{q}) + y^2 - x^2\Big)\Big)\\
\mathrm{Re}[f] &= \Big(r + E(\boldsymbol{q}) + \frac{\gamma(\hat{q})}{q}y\Big)\rho\Big(\omega^2(\boldsymbol{q}) + y^2 - x^2\Big) - 2\rho y x^2 - \lambda^2 C^2(\boldsymbol{q})
\end{aligned}$$

The branch cut of the logarithm is given by

$$\mathrm{Im}[f] = 0 \quad \text{and} \quad \mathrm{Re}[f] < 0$$

The first equation is fulfilled for

$$x = 0 \quad \text{or} \quad 2y\Big(r + E(\boldsymbol{q}) + \frac{\gamma(\hat{q})}{q}y\Big) + \frac{\gamma(\hat{q})}{q}\Big(\omega^2(\boldsymbol{q}) + y^2 - x^2\Big) = 0$$

For the case $x = 0$ the second equation implies $y < 0$. So we can ignore this case since we consider the regime $y \geq 0$.
In the other case we have

$$y(x) = -\frac{q}{3}\frac{r + E(\boldsymbol{q})}{\gamma(\hat{q})} + \sqrt{\frac{q^2}{9}\frac{(r + E(\boldsymbol{q}))^2}{\gamma^2(\boldsymbol{q})} + \frac{x^2 - \omega^2(\boldsymbol{q})}{3}}$$

This solution becomes relevant when $y(x)$ becomes positive, i.e. for $|x| \geq \omega(\boldsymbol{q})$.
Inserting this into the real part one can show, that $\mathrm{Re} < 0$ is fulfilled for large q. This is given in our problem, thus

$$z(x) = x + iy(x) \quad \text{for} \quad |x| \geq \omega(\boldsymbol{q})$$

describes the branch cut of the logarithm.
Now we can deform the integration curve analogously to the calculations in [10] and finally get

$$\begin{aligned} F(T) - F(0) =& \sum_{\boldsymbol{q}} \Big(\int_0^{\omega(\boldsymbol{q})} + \int_{\omega(\boldsymbol{q})}^{\infty} \Big) \frac{dx}{\pi} \Big(\coth\frac{z}{2T} - 1 \Big) \mathrm{Im}\big[\ln[f(\boldsymbol{q}, x)] \big] \\ &+ \int_a \frac{dz}{\pi} \Big(\coth\frac{z}{2T} - 1 \Big) \mathrm{Im}\big[\ln[f(\boldsymbol{q}, z^+)] \big] \\ &+ \int_b \frac{dz}{\pi} \Big(\coth\frac{-z}{2T} - 1 \Big) \mathrm{Im}\big[\ln[f(\boldsymbol{q}, -z^-)] \big] \end{aligned}$$

In the integrals along $\mathcal{C}_\pm$ we are closely under and above the branch cut. By definition the real part of $f(\boldsymbol{q}, z^\pm)$ is always negative and the imaginary part is infinitesimally small. Hence we have

$$\begin{aligned} \mathrm{Im}\big[\ln[f(\boldsymbol{q}, z^+)] \big] &= \arctan\Big(\frac{-\delta}{\mathrm{Re}[f(\boldsymbol{q}, z^+)]} \Big) - \pi \\ \mathrm{Im}\big[\ln[f(\boldsymbol{q}, -z^-)] \big] &= \arctan\Big(\frac{\delta}{\mathrm{Re}[f(\boldsymbol{q}, z^+)]} \Big) + \pi \end{aligned}$$

In both cases we have a continuous integrand. Hence we can take the limit $\delta \to 0$ and set $\mathrm{Im}\big[\ln[f(\boldsymbol{q}, \pm z^\pm)] \big] = \mp\pi$. The integration is now easily carried out and yields

$$4T\Big(\log\sinh\frac{\omega(\boldsymbol{q})}{2T} - \frac{\omega(\boldsymbol{q})}{2T} \Big)$$

The free energy is now simplified to

$$\begin{aligned} F(T) - F(0) =& \sum_{\boldsymbol{q}} \Big(\int_0^{\omega(\boldsymbol{q})} + \int_{\omega(\boldsymbol{q})}^{\infty} \Big) \frac{dx}{\pi} \Big(\coth\frac{z}{2T} - 1 \Big) \mathrm{Im}\big[\ln[f(\boldsymbol{q}, x)] \big] \\ &+ 4T\Big(\log\sinh\frac{\omega(\boldsymbol{q})}{2T} - \frac{\omega(\boldsymbol{q})}{2T} \Big) \end{aligned}$$

For the integration along the real axis we have

$$\begin{aligned}\mathrm{Im}[f(\boldsymbol{q},x)] &= -\frac{\gamma(\hat{q})}{q}x\rho\big(\omega^2(\boldsymbol{q})-x^2\big)\\ \mathrm{Re}[f(\boldsymbol{q},x)] &= \rho\big(r+E(\boldsymbol{q})\big)\big(\omega^2(\boldsymbol{q})-x^2\big)-\lambda^2C^2(\boldsymbol{q})\end{aligned}$$

We see that $\mathrm{Re}[f(\boldsymbol{q},x)]$ has a sign change at

$$x=\omega_R(\boldsymbol{q}) := \sqrt{\omega^2(\boldsymbol{q})-\lambda^2\frac{C^2(\boldsymbol{q})/\rho}{r+E(\boldsymbol{q})}}$$

The imaginary part of the logarithm is then given by

$$\mathrm{Im}\big[\ln[f(\boldsymbol{q},x)]\big] = \arctan\left[\frac{-\frac{\gamma(\hat{q})}{q}x\big(\omega^2(\boldsymbol{q})-x^2\big)}{\big(r+E(\boldsymbol{q})\big)\big(\omega^2(\boldsymbol{q})-x^2\big)-\frac{\lambda^2}{\rho}C^2(\boldsymbol{q})}\right]+\begin{cases}0,\ x<\omega_R(\boldsymbol{q})\\ -\pi,\ \omega_R(\boldsymbol{q})<x<\omega(\boldsymbol{q})\\ \pi,\ x>\omega(\boldsymbol{q})\end{cases}$$

At the point $x=\omega_R(\boldsymbol{q})$ the argument diverges to $-\infty$. The free energy has no pole or discontinutity at this point because $\arctan(-\infty)=-\frac{\pi}{2}$ is finite. At $x=\omega(\boldsymbol{q})$ the argument crosses the branch cut of the logarithm. This leads to a discontinutity at this point.
A partial integration of the remaining integral leads to

$$F(T)-F(0) = -\sum_{\boldsymbol{q}}\left\{\mathcal{P}\int_0^\infty\frac{dx}{\pi}2T\Big(\ln\big[2\sinh\frac{x}{2T}\big]-\frac{x}{2T}\Big)Q(x)\right\}$$

The boundary terms originating from the discontinutity at $x=\omega(\boldsymbol{q})$ exactly cancel out with the contribution from the integrals along the branch cuts. The function $Q(\boldsymbol{q},x)$ denotes the derivative

$$\begin{aligned}Q(\boldsymbol{q},x) =&\partial_x\left(\arctan\left[\frac{-\frac{\gamma(\hat{q})}{q}x\big(\omega^2(\boldsymbol{q})-x^2\big)}{\big(r+E(\boldsymbol{q})\big)\big(\omega^2(\boldsymbol{q})-x^2\big)-\frac{\lambda^2}{\rho}C^2(\boldsymbol{q})}\right]\right)\\ =&-\frac{\frac{\gamma(\hat{q})}{q}\big(r-\frac{\lambda^2}{\rho}\frac{C^2(\boldsymbol{q})}{\omega^2(\boldsymbol{q})-x^2}+E(\boldsymbol{q})\big)}{\big(r-\frac{\lambda^2}{\rho}\frac{C^2(\boldsymbol{q})}{\omega^2(\boldsymbol{q})-x^2}+E(\boldsymbol{q})\big)^2+\big(\frac{\gamma(\hat{q})}{q}x\big)^2}\\ &-\frac{2\frac{\gamma(\hat{q})}{q}x^2\frac{\lambda^2}{\rho}C^2(\boldsymbol{q})}{\big(r+E(\boldsymbol{q})\big)^2\big(\omega^2(\boldsymbol{q})-x^2-\frac{\lambda^2}{\rho}C^2(\boldsymbol{q})\big)^2+\big(\frac{\gamma(\hat{q})}{q}x\big)^2\big(\omega^2(\boldsymbol{q})-x^2\big)^2}\\ =&-\frac{\gamma(\hat{q})}{q}\frac{R(x)+E(\boldsymbol{q})}{\big(R(x)+E(\boldsymbol{q})\big)^2+\big(\frac{\gamma(\hat{q})}{q}x\big)^2}-A(x)\frac{\sigma(x)}{(x-\omega_R(\boldsymbol{q}))^2+\sigma(x)^2}\end{aligned}$$

and

$$\begin{aligned}R(x,\boldsymbol{q}) &:= r-\frac{\lambda^2}{\rho}\frac{C^2(\boldsymbol{q})}{\omega^2(\boldsymbol{q})-x^2}\\ A(x,\boldsymbol{q}) &:= \frac{2x\big(\omega^2(\boldsymbol{q})-\omega_R^2\big)}{(x+\omega_R(\boldsymbol{q}))\big(\omega^2(\boldsymbol{q})-x^2\big)}\\ \sigma(x,\boldsymbol{q}) &:= \frac{\gamma(\hat{q})}{q}\frac{x\big(\omega^2(\boldsymbol{q})-x^2\big)}{(x+\omega_R(\boldsymbol{q}))(r+E(\boldsymbol{q}))}\end{aligned}$$

Bibliography

[1] H. K. Onnes, "The resistance of pure mercury at helium temperatures," *Commun. Phys. Lab. Univ. Leiden*, vol. 12, pp. 120+, 1911.

[2] V. Oganesyan, S. A. Kivelson, and E. Fradkin, "Quantum theory of a nematic fermi fluid," *Phys. Rev. B*, vol. 64, p. 195109, Oct 2001.

[3] Xia Jing, Eisenstein J. P., Pfeiffer L. N., and West K. W., "Evidence for a fractionally quantized Hall state with anisotropic longitudinal transport," *Nat. Phys.*, vol. 7, pp. 845–848, nov 2011. 10.1038/nphys2118.

[4] S. A. Kivelson, E. Fradkin, and V. J. Emery, "Electronic liquid-crystal phases of a doped Mott insulator," *Nat. Phys.*, vol. 393, pp. 550–553, June 1998.

[5] M. Zacharias, "The quadrupolar pomeranschuk instability: Interplay of multiple critical modes with different dynamics," 2009.

[6] M. Zacharias, P. Wölfle, and M. Garst, "Multiscale quantum criticality: Pomeranchuk instability in isotropic metals," *Phys. Rev. B*, vol. 80, p. 165116, Oct. 2009.

[7] A. Abrikosov, L. Gorkov, I. Dzyaloshinski, and R. Silverman, *Methods of Quantum Field Theory in Statistical Physics.* Dover Books on Physics, Dover Publications, 2012.

[8] L. Landau, L. Pitaevskii, A. Kosevich, and E. Lifshitz, *Theory of Elasticity.* No. Bd. 7, Elsevier Science, 2012.

[9] A. Ghatak and L. Kothari, *An introduction to lattice dynamics.* Addison-Wesley, 1972.

[10] M. Zacharias, "Mott Transition and Quantum Critical Metamagnetism on Compressible Lattices," 2013.

[11] R. Cowley, "Acoustic phonon instabilities and structural phase transitions," *Phys. Rev. B*, vol. 13, pp. 4877–4885, Jun 1976.

[12] M. Zacharias, I. Paul, and M. Garst, "Quantum critical elasticity," *ArXiv e-prints*, Nov. 2014.

[13] N. Nagasawa, T. Onimaru, K. T. Matsumoto, K. Umeo, and T. Takabatake, "Non-magnetic Γ 3 doublet ground state in a caged compound PrRh 2 Zn 20," *Journal of Physics: Conference Series*, vol. 391, no. 1, p. 012051, 2012.

[14] T. Hitomi and Y. Yanase, "Electric Octupole Order in Bilayer Ruthenate $Sr_3Ru_2O_7$," *Journal of the Physical Society of Japan*, vol. 83, p. 114704, Nov. 2014.

[15] S. A. Grigera, P. Gegenwart, R. A. Borzi, F. Weickert, A. J. Schofield, R. S. Perry, T. Tayama, T. Sakakibara, Y. Maeno, A. G. Green, and A. P. Mackenzie, "Disorder-sensitive phase formation linked to metamagnetic quantum criticality," *Science*, vol. 306, no. 5699, pp. 1154–1157, 2004.

[16] Wysocki Aleksander L., Belashchenko Kirill D., and Antropov Vladimir P., "Consistent model of magnetism in ferropnictides," *Nat Phys*, vol. 7, pp. 485–489, jun 2011. 10.1038/nphys1933.

[17] Yi Ming, Lu Donghui, Chu Jiun-Haw, Analytis James G, Sorini Adam P, Kemper Alexander F, Moritz Brian, Mo Sung-Kwan, Moore Rob G, Hashimoto Makoto, Lee Wei-Sheng, Hussain Zahid, Devereaux Thomas P, Fisher Ian R, and Shen Zhi-Xun, "Symmetry-breaking orbital anisotropy observed for detwinned Ba(Fe(1-x)Co(x))(2)As(2) above the spin density wave transition," *Proceedings of the National Academy of Sciences of the United States of America*, vol. 108, pp. 6878–6883, apr 2011.

[18] L. W. Harriger, H. Q. Luo, M. S. Liu, C. Frost, J. P. Hu, M. R. Norman, and P. Dai, "Nematic spin fluid in the tetragonal phase of $BaFe_2As_2$," *PhysRevB*, vol. 84, p. 054544, Aug. 2011.

[19] Kasahara S., Shi H. J., Hashimoto K., Tonegawa S., Mizukami Y., Shibauchi T., Sugimoto K., Fukuda T., Terashima T., Nevidomskyy Andriy H., and Matsuda Y., "Electronic nematicity above the structural and superconducting transition in BaFe2(As1-xPx)2," *Nature*, vol. 486, pp. 382–385, jun 2012. 10.1038/nature11178.

[20] Frandsen Benjamin A., Bozin Emil S., Hu Hefei, Zhu Yimei, Nozaki Yasumasa, Kageyama Hiroshi, Uemura Yasutomo J., Yin Wei-Guo, and Billinge Simon J. L., "Intra-unit-cell nematic charge order in the titanium-oxypnictide family of superconductors," *Nat Commun*, vol. 5, dec 2014.

[21] M. Garst and A. V. Chubukov, "Electron self-energy near a nematic quantum critical point," *Phys. Rev. B*, vol. 81, p. 235105, Jun 2010.

[22] K. Hattori and H. Tsunetsugu, "Antiferro Quadrupole Orders in Non-Kramers Doublet Systems," *Journal of the Physical Society of Japan*, vol. 83, p. 034709, Mar. 2014.

[23] A. Altland and B. Simons, *Condensed Matter Field Theory.* Cambridge University Press, 2010.

[24] M. Vojta, "Quantum phase transitions," *Reports on Progress in Physics*, vol. 66, pp. 2069–2110, Dec. 2003.

[25] S. Sachdev, *Quantum Phase Transitions.* Troisième Cycle de la Physique, Cambridge University Press, 2011.

[26] D. G. Barci, A. Mendoza-Coto, and D. A. Stariolo, "Nematic phase in stripe-forming systems within the self-consistent screening approximation," *Phys.Rev.E*, vol. 88, p. 062140, Dec. 2013.

[27] R. Mahajan, D. M. Ramirez, S. Kachru, and S. Raghu, "Quantum critical metals in d=3+1 dimensions," *Phys.Rev.E*, vol. 88, p. 115116, Sept. 2013.

Danksagung

Ich möchte mich bei PD Markus Garst für die sehr gute Betreuung während der Masterarbeit bedanken. Die zahlreichen Diskussionen und seine Geduld bei der Beantwortung meiner Fragen haben mir sehr geholfen.
Auch Prof. Achim Rosch möchte ich für die Möglichkeit danken, die Masterarbeit in seiner Arbeitsgruppe zu schreiben. Seine anschaulichen physikalischen Erklärungen haben mir beim Verständnis meines Themas sehr geholfen.
Mein besonderer Dank gilt auch Dr. Kazumasa Hattori für die interessanten Gepräche während seiner Zeit in Köln.
Desweiteren möchte ich Robert Bamler für die Hilfe bei der Monte-Carlo-Intergration sowie Jan Müller für die Lösung meiner vielen Probleme mit mathematica danken.
Schlussendlich möchte ich mich noch bei meiner Familie und ganz besonders bei meiner Freundin bedanken, die mich während des letzten Jahres auch in schwierigen Momenten immer unterstützt haben.

Eigenständigkeitserklärung

"'Hiermit versichere ich, dass ich die vorliegende Arbeit selbstständig verfasst und nur die angegebenen Quellen und Hilfsmittel verwendet habe."'

Köln, den 13.01.2015

(Christopher Max)